Capturing Stormwater Nitrate and Phosphate with Sorptive Filter Media

A Dissertation
SUBMITTED TO THE FACULTY OF
UNIVERSITY OF MINNESOTA
BY

Andrew Jacob Erickson

IN PARTIAL FULFILLMENT OF THE REQUIREMENTS
FOR THE DEGREE OF
DOCTOR OF PHILOSOPHY

Dr. John S. Gulliver and Dr. William A. Arnold

July 2017

Acknowledgements

The author thanks Professors John Gulliver and William Arnold for agreeing to be my advisors. Their guidance, patience, and wisdom is invaluable. The author also thanks Professors Ray Hozalski and Bruce Wilson for agreeing to be on my committee. Their assistance with these and other projects is greatly appreciated. The author thanks Professor Pete Weiss, who has been a valued mentor. The author also thanks Professor Paul Capel for being a substitute member for my oral prelim exam and also providing timely laboratory space to conduct the experiments.

The author thanks St. Anthony Falls Laboratory staff and students for their support and assistance, including Lanre Adekola, Laina Breidenbach, James Crist, Dick Christopher, Peter Corkery, Chris Ellis, Ben Erickson, Rob Gabrielson, Anne Haws, David Liddell, Jeff Marr, Raphael Martins, Chris Milliren, Joel Morgan, Poornima Natarajan, Ugonna Ojiaku, Tyler Olsen, Lisa Ostlund, James (Phi) Pham, Jenni Snyder, Elliot Spronk, Seth Strelow, James Tucker, Anthony Vecchi, Nathan Warner, and others. The author also thanks Cecilie Brekke and Mikal Bredal, whose assistance with research is greatly appreciated. The author thanks Professor Jian Peng (University of Saskatchewan) for his helpful insight and advice.

The author thanks the funding agencies that provided financial support for the projects reflected herein: Local Road Research Board of Minnesota, Minnesota Pollution Control Agency, and the United States Environmental Protection Agency Federal Clean Water Act Section 319 grant program. Specifically, Greg Johnson and David Wall at the Minnesota Pollution Control Agency served as project managers, and their assistance is greatly appreciated.

The author thanks businesses that donated commercial products for our experiments, including Connelly GPM, Inc., Norit Americas, and Carbon Resources, Inc. The author also thanks individuals and organizations for partnering with the University of Minnesota to complete this research: Ross Bintner, Pete Young, and the City of Prior Lake, Minnesota; Joe Jacobs, Dan Nadeau, Alicia O'Hare, Kerry Saxton, and summer support staff with the Wright Soil and Water Conservation District.

The author thanks volunteer industry professionals to become members of the Technical Advisory Panel for projects associated with this research. The author thanks the anonymous reviewers for reviewing and providing comments on the manuscripts describing this research.

Dedication

To my mom, who simply loved me. I miss her dearly.

To my dad, who showed me the value of hard work.

To Lana and my kids, who make me a better husband and father every day.

To Julie and Alan, and Gina and Rob, who love me the way we are called to love.

To my family, whose prayers and support have carried me through it all.

Abstract

Soluble phosphate and nitrate are more bioavailable than particulate forms. These nutrients result in eutrophication in both freshwater (typically phosphate-limited) and marine (typically nitrate-limited) systems. In addition, nitrate poses a public health risk at elevated concentrations in drinking water. This research shows that sand filters mixed with 5% iron filings captured, on average, 88% of the influent phosphate in laboratory experiments. Neither incorporation of iron filings into a sand filter nor capture of phosphate had a significant effect on the hydraulic conductivity. Pond-perimeter applications of iron enhanced sand filtration (IESF) with up to 10.7% iron by weight achieved between 29% and 91% phosphate reduction for five events within the first year of operation. After five years, however, a different pond perimeter IESF retained on average 26% of the influent phosphate over three rainy seasons. Retention was best for larger filtered volume events, but negative removal was observed for events with smaller filtered volume and low influent phosphate concentration. Non-routine maintenance improved the hydraulic performance of the pond perimeter IESF and, after a rinsing event, also improved phosphate retention rates to an average of 45%. An IESF was installed to treat agricultural tile drainage and found to reduce total phosphorus loads by 42% to 95% with a flow-weighted mean reduction of 66.3% ± 6.7% ($\alpha = 0.05$) for 20 events in 2016. The phosphate load reduction varied from 9% to 87% with a flow-weighted mean reduction of 63.9% ± 7.7% ($\alpha = 0.05$) for 31 events in 2015 and 2016. This research also shows that nitrate is captured abiotically by granular activated carbon (GAC) in laboratory experiments designed to mimic urban and agricultural stormwater runoff. The short contact time and inorganic characteristics of the influent synthetic stormwater suggest that the nitrate was captured by ion exchange, but (bi)carbonate may have competed with nitrate for capture by GAC. Abiotic capture of nitrate requires less stormwater storage volume and less residence time to remove nitrate compared to denitrification, and thus GAC could be used to design smaller treatment practices for nitrate removal.

Table of Contents

List of Tables

List of Figures

Chapter 1: Introduction

Urbanization increases the amount of impervious land surfaces such as roads, parking lots, and rooftops, which results in less infiltration of rainfall and more surface runoff. This nonpoint source stormwater runoff is typically conveyed to and through storm sewers, often carrying pollutants (e.g., sediments, nutrients, and metals) to receiving water bodies, resulting in water quality impairments (U.S. EPA 2000). Eutrophication in lakes and rivers is exacerbated by excess nutrients as evidenced by nuisance algae blooms (U.S. EPA 1999). Dissolved phosphorus, which in stormwater is usually in the form of phosphate (PO_4^{3-}) (Stumm and Morgan 1981), is typically the limiting nutrient for plant growth in temperate freshwater systems (Schindler 1997). In such systems, the addition of phosphate leads to eutrophication, which is undesirable due to the corresponding negative environmental impacts such as low dissolved oxygen, fish kills and less biotic diversity, and increased turbidity.

Stormwater is a major contributor of phosphorus load from sources such as fertilizer, vegetation, and detergents (U.S. EPA 1999, APHA 1998). In agricultural watersheds, phosphorus sources include fertilizers, manure, and atmospheric deposition (Ruddy *et al*. 2006). A pollutant such as phosphorus can either exist in soluble phase (e.g., molecule) or in particulate phase (e.g., sand grain or detritus). The total concentration is the sum of the soluble concentration and particulate concentration, where the soluble portion is defined as that measured after filtering with a pore size smaller than 0.45 μm (APHA 1998). Stormwater runoff from highways and urban areas, on average, has 30 – 45% soluble and 55 – 75% particulate phosphorus (Kayhanian *et al.* 2007, Pitt *et al.* 2005), but the soluble fraction ranges from 3 – 100% (Erickson *et al.* 2007). In addition, phosphate comprises 90% of dissolved phosphorus (Kayhanian *et al.* 2007) and phosphate exhibits a greater bioavailability than particulate phosphorus (Sharpley *et al.* 1992), which means that capturing only particulate forms may not significantly reduce phosphate bioavailability or eutrophication in freshwater lakes and rivers.

Nitrate (NO_3^-) in another primary nutrient and has water quality limits to reduce biological overproduction (eutrophication) in marine environments, such as the hypoxic

zone in the Gulf of Mexico near the mouth of the Mississippi River in the United States (U.S. EPA 2007). In addition, nitrate causes methemoglobinemia (U.S. EPA 2012) in human infants when drinking water with a concentration > 10 mg NO_3^--N/L is consumed by the mother (breast milk) or baby. Sources of nitrate in urban runoff include fertilizers, plant debris, and animal waste (U.S. EPA 1999). Kayhanian *et al.* (2007) analyzed the results from 34 highway water quality stations and a total of 634 storms to determine that nitrate and total Kjeldahl nitrogen (TKN) concentrations increased with increasing antecedent dry period and traffic counts and decreased with an increase in storm rainfall and seasonal cumulative rainfall. Nitrate concentration in runoff from agricultural fields is also variable, but it is generally higher than that from highways (Stuntebeck *et al.*, 2011) due to chemical fertilizers.

Removing nitrogen from impacted waters requires an understanding of biotic and abiotic nitrogen cycling. Nitrogen cycling in the environment is dominated by biologically mediated redox processes (Brezonik and Arnold 2011). Nitrification is the chemoautotrophic oxidation of ammonium (NH^+) to nitrite (NO^-) through *Nitrosomanas* and to nitrate (NO_3^-) through *Nitrobacter* (Stumm and Morgan 1981). Denitrification is the anaerobic biodegradation of nitrate to nitrogen gas (N_2) by bacterial species such as *Pseudomonas* and *Clostridium* (Smil 2000). Such processes are commonly used to remove nitrogen from wastewater, but the short residence time and limited water storage volume provided by stormwater treatment practices are often not sufficient to allow adequate removal of nitrate by denitrification alone, unless significant design changes are incorporated (Kim *et al.* 2003, Hsieh and Davis 2005).

Typical stormwater control measures (SCMs, sometimes called best management practices or BMPs) such as detention basins, rain gardens, wet ponds, etc. do little to remove the phosphate or nitrate fraction. Thus, stormwater professionals need enhanced stormwater treatment practices to effectively protect and improve water quality. This research expands the depth of knowledge for two advanced stormwater treatment practices; iron enhanced sand filtration for capturing phosphate and granular activated carbon for capturing nitrate abiotically.

Chapter 2 introduces iron enhanced sand filtration (IESF), which comprises iron filings mixed with sand and is tested for phosphate removal from synthetic stormwater. Results indicate that sand mixed with 5% iron filings captures an average of 88% phosphate for at least 200 m of treated depth, which is significantly greater than a sand filter without iron filings. Neither incorporation of iron filings into a sand filter nor capture of phosphate onto iron filings in column experiments had a significant effect on the hydraulic conductivity of the filter at mixtures of 5% or less iron by weight. Field applications with up to 10.7% iron were operated over 1 year without detrimental effects upon hydraulic conductivity. A model is applied and fit to column studies to predict the field performance of iron-enhanced sand filters. The model predictions are verified through the predicted performance of the filters in removing phosphate in field applications. Practical applications of the technology, both existing and proposed, are presented in this chapter so stormwater managers can begin implementation.

Chapter 3 presents results from field monitoring and maintenance of two iron enhanced sand filters (IESFs) over one to three years. The first, a traditional IESF in an agricultural watershed, retained over 64% of the influent phosphate load during one year of monitoring while the second, a pond perimeter IESF in a developing suburban watershed, retained 26% over three years. All events measured at the traditional IESF exhibited positive removal of phosphate (i.e., effluent loads < influent loads) while half of the events (14 out of 28) at the pond perimeter IESF were found to have negative removal (i.e., effluent loads > influent loads). Events with negative removal tended to be smaller events with low influent phosphate concentrations (3.7 – 39.4 μg/L). Non-routine maintenance improved the hydraulic performance of the pond perimeter IESF and, after a rinsing event, also improved phosphate retention rates to an average of 45%. It is believed that there are at least two reasons for this difference in performance between the two IESFs: First, the traditional IESF was treating runoff from drain tiles with a low particulate phosphorus concentration, while the pond-perimeter IESF had a degrading mat of filamentous algae transported onto the surface, creating a source of phosphate that was not quantified. Second, the pond perimeter IESF had treated a relatively large volume of water for its size, resulting in substantial flow-through in the filter within 5 years of operations.

This is greater than anticipated for an IESF, and may have partially caused the reduction in performance.

Chapter 4 expands on Chapter 3 by presenting two full years of monitoring data at the traditional IESF treating agricultural runoff, for both total phosphorus and phosphate. Overall, for natural rainfall events that were monitored between June and November 2015 and again in 2016, the IESF captured 66% ± 7% ($\alpha = 0.05$) of the influent total phosphorus mass (n = 21) and 64% ± 8% ($\alpha = 0.05$) of the influent phosphate mass (n = 33). Removal of total phosphorus and phosphate was approximately uniform for large and small rainfall events and varied from 42% to 95% for total phosphorus and 9% to 87% for phosphate. The IESF treated 290 m of treated depth since installation, and results indicate that performance may be decreasing due to exhaustion of sorption media. Routine and non-routine maintenance was performed throughout the project to ensure adequate flow through the IESF and adequate performance. Detailed results, maintenance activities, design and operating & maintenance recommendations, and lessons learned are given within this chapter.

Finally, Chapter 5 presents research that quantifies abiotic nitrate removal of two granular activated carbons (GACs) and illustrates use of GACs in stormwater treatment practices. The short contact time and inorganic characteristics of the influent synthetic stormwater suggest that the nitrate is captured by ion exchange, but (bi)carbonate may compete with nitrate for capture by GAC. Current stormwater treatment practices rely on denitrification to capture nitrate in stormwater treatment practices, requiring storage of captured stormwater, anaerobic conditions, and enough residence time for the bacteria to convert nitrate to nitrogen gas. Compared with removal of nitrate by denitrification, abiotic capture during rainfall events requires less stormwater storage volume and less residence time to remove nitrate because it accumulates on the media as stormwater passes through the filter. This suggests that nitrate can be removed from stormwater with less storage and smaller treatment practices.

This research is the culmination of several research projects and tasks varying from relatively simple laboratory bench-top batch tests to extensive full-scale field monitoring studies of pollutant removal performance. The four chapters described above each

correspond to a peer-reviewed journal publication, which was written by the lead author for the publications and this dissertation (Andrew J. Erickson). The publications were written with assistance by the co-authors, and the research was completed with assistance from several individuals as described below.

A version of Chapter 2, "Capturing Phosphates with Iron Enhanced Sand Filtration," was published in Water Research in 2012 (Erickson *et al.* 2012). Permission was obtained from Elsevier to reproduce the publication in this dissertation. It is co-authored by John S. Gulliver and Peter T. Weiss, who both provided input on the research itself and on the text of the publication. In addition, St. Anthony Falls staff assisted with experiments and data collection as follows: James Crist, Dick Christopher, and Ben Erickson: preparation for field testing and collection of field samples and data for field applications of pond-perimeter trenches; and Joel Morgan: collection of samples and data for laboratory column experiments.

A version of Chapter 3, "Monitoring and Maintenance of Phosphate Adsorbing Filters," has been accepted for publication in the Journal of Environmental Engineering, Special Issue: Environment and Sustainable Systems: A Global Overview (Erickson *et al.* 2017b). It is co-authored by Peter T. Weiss and John S. Gulliver, who both provided input on the research itself and on the text of the publication. In addition, St. Anthony Falls staff assisted with experiments and data collection as follows: Dick Christopher, Chris Ellis, Ben Erickson, Rob Gabrielson, Chris Milliren, James (Phi) Pham, Nathan Warner: preparation and maintenance of field equipment of both the pond-perimeter IESF trenches and surface IESF treating agricultural runoff; Peter Corkery, David Liddell, Raphael Martins, Poornima Natarajan, Tyler Olsen, Seth Strelow, Anthony Vecchi: collection of data, and collection and analysis of samples on both the pond-perimeter IESF trenches and surface IESF treating agricultural runoff.

A version of Chapter 4, "Phosphate Removal from Agricultural Tile Drainage with Iron Enhanced Sand," has been submitted for publication in Water: Special Issue: Additives in Stormwater Filters for Enhanced Pollutant Removal (Erickson *et al.* 2017a). It is co-authored by John S. Gulliver and Peter T. Weiss, who both provided input on the research itself and on the text of the publication. In addition, St. Anthony Falls staff assisted

with experiments and data collection as follows: Dick Christopher, Chris Ellis, Ben Erickson, Rob Gabrielson, Chris Milliren: preparation and maintenance of field equipment for the surface IESF treating agricultural runoff; Peter Corkery, David Liddell, Raphael Martins, Poornima Natarajan, Tyler Olsen, Seth Strelow: collection of data, and collection and analysis of samples for the surface IESF treating agricultural runoff.

A version of Chapter 5, "Abiotic Capture of Stormwater Nitrates with Granular Activated Carbon," was published in the Journal of Environmental Engineering Science in 2016 (Erickson *et al.* 2016). Permission was obtained from Mary Ann Liebert to reproduce the publication in this dissertation. It is co-authored by John S. Gulliver, William A. Arnold, Cecilie Brekke, and Mikal Bredal. John S. Gulliver and William A. Arnold provided input on the research itself and on the text of the publication. Cecilie Brekke conducted batch experiments under my direct supervision and with my assistance; her effort is represented by her MSc thesis: Brekke, C. (2012): Sorption of nitrates to activated carbon. MSc thesis. University of Stavanger. Mikal Bredal assisted with column experiments; his effort is represented by his MSc thesis: Bredal, M. (2013). Column studies on nitrate removal by activated carbon. MSc thesis. University of Stavanger. Professor Jian Peng (University of Saskatchewan) provided insight and advice on the experiments and interpretation of the results. In addition, St. Anthony Falls staff assisted with experiments and data collection as follows: Dick Christopher, Ben Erickson, James Tucker: preparation of the column experiments and repair of a shaker table; Lanre Adekola, Laina Breidenbach, Anne Haws, David Liddell, Ugonna Ojiaku, Elliot Spronk, Anthony Vecchi: collection of data, and collection and analysis of samples for batch and column experiments.

Chapter 2: Capturing Phosphate with Iron Enhanced Sand Filtration[1]

Abstract: Most treatment practices for urban runoff capture pollutants such as phosphorus by either settling or filtration while dissolved phosphorus, typically as phosphate, is untreated. Dissolved phosphorus, however, represents an average 45% of total phosphorus in stormwater runoff and can be more than 95%. In this study, a new stormwater treatment technology to capture phosphate, called the Minnesota Filter, is introduced. The filter comprises iron filings mixed with sand and is tested for phosphate removal from synthetic stormwater. Results indicate that sand mixed with 5% iron filings captures an average of 88% phosphate for at least 200 m of treated depth, which is significantly greater than a sand filter without iron filings. Neither incorporation of iron filings into a sand filter nor capture of phosphate onto iron filings in column experiments had a significant effect on the hydraulic conductivity of the filter at mixtures of 5% or less iron by weight. Field applications with up to 10.7% iron were operated over 1 year without detrimental effects upon hydraulic conductivity. A model is applied and fit to column studies to predict the field performance of iron-enhanced sand filters. The model predictions are verified through the predicted performance of the filters in removing phosphate in field applications. Practical applications of the technology, both existing and proposed, are presented so stormwater managers can begin implementation.

1 Introduction

Eutrophication in lakes and rivers can be exacerbated by excess nutrients as evidenced by nuisance algae blooms (U.S. EPA, 1999). Dissolved phosphorus is the limiting nutrient in most temperate freshwater systems (Aldridge and Ganf, 2003; Schindler, 1977) and primarily exists in the form of phosphate ($H_XPO_4^{X-3}$, Stumm and

[1] A version of this chapter was published in Water Research in 2012 as Erickson, A.J., Gulliver, J.S. and Weiss, P.T. (2012). "Capturing phosphates with iron enhanced sand filtration." Water Research 46(9), 3032-3042. Permission was obtained from Elsevier to reproduce the publication in this dissertation.

Morgan, 1981). Sources of phosphate in urban stormwater include lawn fertilizers, leaf litter, grass clippings, unfertilized soils, detergents, and rainfall, among others (U.S. EPA, 1999; APHA, 1998).

A recent study of nationwide monitoring data (Pitt *et al.* 2005) reports that the median values of total phosphorus and phosphate are 0.27 and 0.12 mg PO_4^{3-} -P/L, respectively, indicating that a typical fraction of dissolved to total phosphorus can be expected to be approximately 44%. Erickson *et al.* (2007), however, found that it is not uncommon for phosphate to be over 90% of the total load. Total Maximum Daily Load (TMDL) studies have required total phosphorus load reductions from stormwater sources of greater than fifty percent (50%) (U.S. EPA 2007b). Therefore, to achieve these load reductions, both particulate and dissolved fractions of total phosphorus must be captured. In addition, phosphate exhibits a greater bioavailability than particulate phosphorus (Sharpley *et al.* 1992), which means that capturing only particulate forms may not significantly reduce phosphate bioavailability or eutrophication in freshwater lakes and rivers.

Physical processes such as filtration and sedimentation capture particulate phosphorus in most stormwater treatment practices, but very few practices have a mechanism that consistently captures phosphate over the life-cycle of a treatment practice (Erickson *et al.* 2007). Results from Erickson *et al.* (2007) indicate that phosphate is strongly bound to iron in a stormwater filtration system and any iron-bound phosphate present in the effluent is not bioavailable. The median value for pH in stormwater is 7.4 ± 0.11 (coefficient of variation) (Pitt *et al.* 2005) and in this range, the primary capture mechanism for phosphate with iron is adsorption (Stumm and Morgan 1981). As iron oxidizes to form rust, phosphate binds to these iron oxides by surface adsorption. For a full description of chemical sorption of phosphate and iron, see Erickson *et al.* (2007) and Erickson (2005). Ferrous-based materials have been shown to also capture other pollutants including As, Cd, Cr, Cu, Ni, Pb, and Zn (Genc-Fuhrman *et al.* 2008, Wu and Zhou 2009, Namasivayam and Ranganathan 1995).

Local units of government need a cost-effective tool that can significantly reduce phosphate concentrations in stormwater and sorption to iron-based materials is one viable

mechanism. Steel wool and iron-based media filters have been shown to capture a significant amount of phosphate (Erickson *et al.* 2007, Rosenquist *et al.* 2010). Iron filings (ground cast iron) are an alternative to steel wool that can be obtained with a size distribution similar to that of sand. At the time of writing, iron filings are less expensive than steel wool per unit weight primarily because iron filings require less manufacturing to produce. Therefore, iron filings have been chosen for several applications of iron enhanced sand filtration in Minnesota, USA. This chapter will investigate the phosphate sorption capabilities of iron filings, apply a physically-based model to column study data, examine results from field applications, and use the model to predict performance in field applications.

2 Methods

Column studies were performed on mixes of iron filings and C 33 (ASTM 2002) sand. Synthetic stormwater runoff with a variable phosphate concentration passed through the columns while the flow rate was measured and effluent samples were collected and analyzed for phosphate concentration. In addition, field testing of iron enhanced filtration practices was conducted to verify laboratory experiments.

2.1 Column Experiments

Ten vertical, gravity fed, columns were constructed from clear acrylic pipe as shown in Figure 1. A valve at the base of the supply reservoir allowed for sample collection prior to treatment (influent) and a spout at the bottom of each column allowed for sample collection after treatment (effluent). Filter media (iron and sand) was mixed to a total mass of 1600 g at weight ratios of 5% (3 columns), 2% (3 columns), 0.3% (3 columns), and 0% (1 column) and poured into the columns. The columns were then dry consolidated to remove excess pore spaces. Connelly-GPM (http://www.connellygpm.com/) donated the iron filings for these experiments. The particle size distribution for the iron filings and the standard (ASTM 2002) for fine aggregate used in most stormwater filtration systems (Claytor and Schueler 1996) is shown in Table 1. The iron filings used in this study were

composed of 87 – 93% metallic iron, 2.85 – 3.23% total carbon, 1.0 – 1.85% silicon, 0.14 – 0.60% manganese, 0.067 – 0.107% sulfur, 0.000 – 0.132% phosphorus, and less than 0.935% of other trace elements (Connelly GPM Inc. 2009).

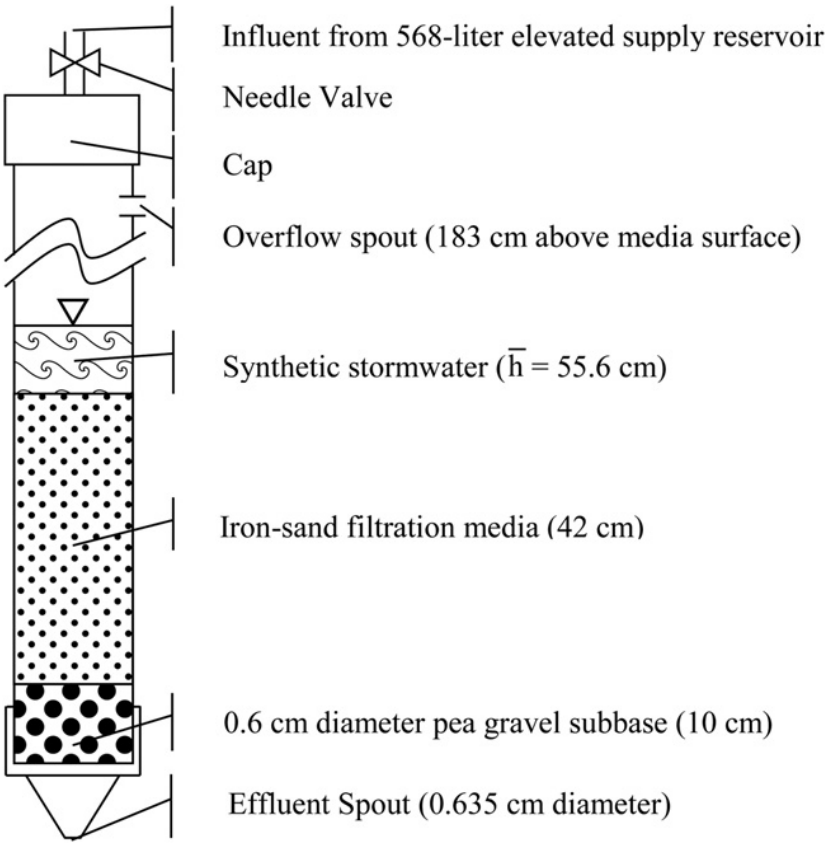

Figure 1. Column (inside diameter = 5.08 cm) experiment diagram (not to scale).

Table 1. Particle size distribution for iron filings and standard fine aggregate (ASTM 2002) used in most stormwater filtration systems.

Sieve opening (mm)	Iron filings percent smaller	Fine aggregate percent smaller
9.5	100%	100%
4.75	100%	95 – 100%
2.36	95 – 100%	80 – 100%
1.18	75 – 90%	50 – 85%
0.60	25 – 45%	25 – 60%
0.30	0 – 10%	5 – 30%
0.15	0 – 5%	0 – 10%

In order to mimic the variability found in natural stormwater runoff, the synthetic stormwater was composed of municipal drinking water (mean pH = 9.1, mean alkalinity = 40 mg/L) (City of Minneapolis 2011) mixed with potassium phosphate (KH_2PO_4) to various phosphate concentrations between 0.233 and 0.531 mg PO_4^{3-} -P/L with a flow-volume-weighted mean concentration of 0.340 mg PO_4^{3-} -P/L. One objective of these experiments was to determine to what extent, if any, the retention of phosphate and the formation of iron oxides affected the hydraulic conductivity of the filter media; therefore synthetic stormwater was chosen instead of natural stormwater to reduce the interference of other constituents (e.g., suspended sediment, etc.) found in natural stormwater.

The columns were operated similar to a sand filter used to treat stormwater runoff. The flow from the reservoir was turned on at time zero and the columns were allowed to fill to the level at which the free outfall was set (mean water depth = 55.6 cm). After influent, effluent, and overflow flow rates equilibrated, volumetric flow rate and head (water depth) were measured and effluent samples were collected at various intervals. Influent samples were collected periodically to verify adequate mixing in the supply reservoir. Laboratory-simulated runoff events lasted between 1.93 and 6.88 h, after which the columns were allowed to drain and dry for 4 – 290 h.

2.2 Field Sites

The City of Prior Lake, Minnesota installed two iron enhanced sand filtration (called the "Minnesota Filter") trenches along the perimeter of a wet detention basin in Prior Lake, MN in January and February 2010. The trenches were designed to be below the normal water level created by the outlet structure of the wet detention basin (see Figure 2). During rainfall events, stormwater flows into the wet detention basin, increasing the water level such that stormwater begins to flow over the surface of the trenches and into the media. The stormwater flows through the mix of iron and sand, through a layer of pea gravel, and into a perforated pipe under-drain where it is captured and conveyed to the outlet structure of the wet detention basin. For small rainfall events, where the pond water surface does not rise to the level of the overflow structure, all of the stormwater is filtered by the trenches to capture phosphate. For large rainfall events the water level in the wet

detention basin overflows the outlet structure and a portion of the stormwater runoff bypasses the trenches. When the water level drops below the weir, the remaining stormwater is filtered by the trenches to capture phosphate.

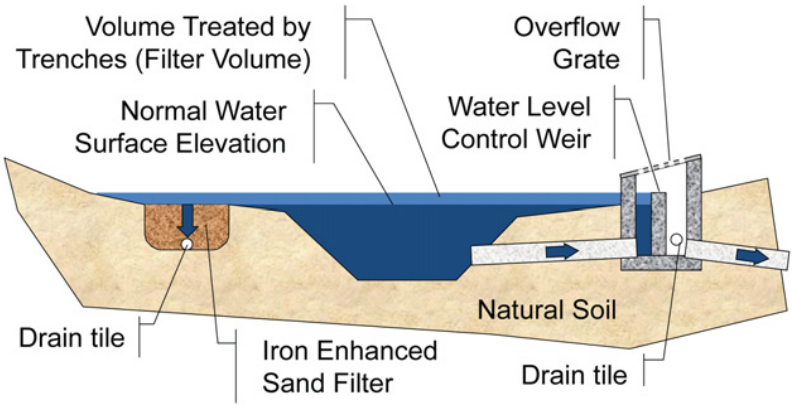

Figure 2. Schematic of an iron enhanced trench installed around the perimeter of a wet detention basin in Prior Lake, MN.

The two trenches in this study were installed with approximately 7.2% and 10.7% by weight iron filings. The trenches are each approximately 12 m long, 1.5 m wide, and 0.6 m deep. The drainage area for the wet detention basin is approximately 6.2 ha in size and composed of suburban residential land use. Most sand filters and infiltration trenches are designed such that the surface area of the practice is approximately 2 – 3% of the impervious watershed (Weiss *et al.* 2007). The trenches installed in Prior Lake were specifically designed for experimental purposes and purposely undersized such that the filter surface area is approximately 0.24% of the impervious watershed. The wet detention basin can capture approximately 0.4 m of water depth or 1300 m^3 on top of the pond before overflow occurs.

2.3 Field Methods

Two types of tests were used to measure the phosphate capture performance of the iron enhanced trenches: synthetic runoff testing and natural runoff testing. Synthetic runoff testing consists of fitting flow control values to a local fire hydrant to supply synthetic runoff (no pollutants were added). The fire hydrant was turned on and the synthetic

stormwater was allowed to flow down the street via the gutter to a catch basin directly upstream of the treatment practice. As synthetic stormwater entered the practice, the water level increased such that stormwater within the basin began to flow into the iron enhanced trenches. The flow rate of stormwater leaving the trenches was measured and samples were collected as described below. The fire hydrant was allowed to flow for approximately 1 h such that a significant volume of synthetic stormwater was added to the treatment practice. Flow rates were measured and samples were collected for approximately 8 h as stormwater flowed through the trenches.

Natural runoff testing consists of allowing natural rainfall events to fill the treatment practice with stormwater which increased the water level such that the stormwater would flow into the trenches. The flow rate of stormwater leaving the trenches was measured and samples were collected (as described below) for approximately 8 h as natural stormwater flowed through the trenches.

2.3.1 Flow Rate

The flow rate of stormwater was measured at the outlet of the under-drain systems using one of two V-notch weirs (called green and orange). The weirs were calibrated by measuring the time required to fill a known volume of water throughout the range of possible water depths, resulting in a stage-discharge relationship. The stage-discharge relationship and calibration parameters for the two weirs used in this study are given in Equation (1) (Chow 1959). The confidence for Equation (1) is ± 0.377 L/min ($p = 0.95$, $n = 6$, range = 6.20 – 102.4 L/min) and ± 0.486 L/min ($p = 0.95$, $n = 10$, range = 2.89 – 58.5 L/min) for the green and orange weirs, respectively.

$$Q = C_0 \frac{8}{15} C_d \tan\left(\frac{\theta}{2}\right)\sqrt{2g}(h)^{5/2} \quad (1)$$

where:

Q = Flow rate (L per min)

C_0 = unit conversion factor for m^3/s to L/min (C_0 = 60,000)

C_d = discharge coefficient (C_d = 0.831 for green weir, C_d = 0.876 for orange weir)

θ = weir angle (θ = 1.39 radians (79.6°) for green weir, θ = 0.526 radians (30.1°) for orange weir)

g = gravitational acceleration (g = 9.81 m/s)

h = depth of water flowing over the weir (m)

The weirs were placed in the outlet structure below the under-drains such that the outflow from each under-drain filled one of the containers for the weirs. The water then overflowed the weir and the water level, which was measured to the nearest 3.2 mm, was recorded at regular intervals. The flow rate was then calculated using Equation (1).

2.3.2 Phosphate Sampling and Analysis

Samples were collected in two locations for each trench: within the wet detention basin near the surface of the iron enhanced trench (influent sample) and from the under-drain system (effluent sample). Stormwater samples were collected, stored, and transported to the St. Anthony Falls Laboratory to be analyzed for phosphate concentration.

2.4 Analytical Methods

Samples were analyzed for phosphate according to standard methods section 4500-P Section E (ascorbic acid) in Standard Methods (APHA 1998) with a minimum detection limit of 0.01 mg PO_4^{3-} -P/L.

2.5 Calculation Methods

Saturated hydraulic conductivity values in the columns were calculated using Darcy's Law, rearranged as given in Equation (2). Flow rate was measured volumetrically (mean volume = 47 mL) from the outflow of the columns, and water depth above the media surface was measured whenever a sample was collected (approximately 2.5 h between measurements, 115 measurements total for each column). Media depth was constant with time but varied between columns and was measured periodically throughout the experiments. Column cross-sectional area was constant for all columns.

$$k = \frac{Q_i d_j}{A_c \left(h_i + d_j \right)} \tag{2}$$

where:

k = Saturated hydraulic conductivity (cm/s)

Q_i = Flow rate for i^{th} measurement (cm^3/s)

d_j = Depth of filtration media for j^{th} column (cm)

A_c = Cross-sectional area of the columns (cm^2)

h_i = Depth of water above media surface for i^{th} measurement (cm)

A flow-volume weighted average was computed by summing the product of each measurement's value and its corresponding flow volume and dividing this sum by the total flow volume, as given by Equation (3). When Equation (3) is used to compute the flow-volume weighted concentration of a substance in stormwater runoff, the value of C is commonly referred to as the event mean concentration (EMC). This method makes measurements from a larger portion of the total flow-volume more important and measurements from smaller portions of the total flow volume less important.

$$\bar{C} = \frac{\sum_i C_i V_i}{\sum_i V_i} \tag{3}$$

where:

C = Flow-volume weighted average characteristic (e.g., concentration, hydraulic loading rate, etc.)

C_i = Characteristic for i^{th} measurement

V_i = Flow volume for i^{th} measurement (mL)

The contact time between the synthetic stormwater and the iron-sand media was estimated using the measurements of volumetric flow rate, the volume of the column, and an estimated porosity for each column, as given by Equation (4).

$$t_{contact} = \frac{A_c d_m \eta}{Q} \tag{4}$$

where:

$t_{contact}$ = Contact time between synthetic stormwater and iron-sand media (s)

A_c = Cross-sectional area of the columns (cm^2)

d_m = Depth of iron-sand media (cm)

η = Porosity of the iron-sand media

Q = Volumetric flow rate (mL/s)

To calculate the contact time with only the iron, the estimated ratio of the iron surface area to the total surface area was multiplied by the total contact time with the iron-sand media. Assuming spherical particles, the surface area for each size fraction within the particle size distribution for both sand and iron was estimated with Equation (5). The total surface areas for each size fraction were then summed to determine the total surface area and the surface area ratio of iron was calculated for each column as the ratio of the iron surface area to the total surface area. Contact time with iron as shown in Table 2 was calculated as the product of the contact time with the iron-sand media and the surface area ratio of iron to the total surface area.

$$SA_{total} = SA_p\, n = SA_p\, MF\, \frac{M_{total}}{M_p} = \frac{3\, MF\, M_{total}}{\rho_w\, s\, r_p} \tag{5}$$

where:

SA_{total} = Total surface area for all particles of a given size (cm^2)

SA_p = Surface area of a single particle of given size (cm^2) = $4\ \pi\ r_p^2$

r_p = Radius of particle for a given size (cm)

n = Number of particles

MF = Mass fraction of particles of a given size

M_{total} = Total mass of particles (g)

M_p = Mass of a single particle of given size (g) = $\rho_w\, s\, V$

ρ_w = Density of water (g/cm^3), assumed $\rho_w = 1\ g/cm^3$

s = Specific gravity of particles, assumed $s = 2.65$ for sand, $s = 7.8$ for iron

V = Volume of a single particle of given size (cm^3) = $(4\ \pi\ r_p^3)/3$

Table 2. Summary of hydraulic measurements in columns (flow-volume weighted average ± 95% confidence interval, n = 115).

Column Designator	Percent Iron Filings (%)	Total Treated Depth (m)	Hydraulic Loading Rate (m/hr)	Hydraulic conductivity (cm/sec)	Contact time with iron-sand media (sec)	Contact time with iron (sec)
A	5%	189	1.61 ± 0.11	0.0185 ± 0.001	315 ± 27.8	1.73 ± 0.15
B	5%	147	1.38 ± 0.11	0.0172 ± 0.001	440 ± 51.5	2.42 ± 0.28
C	5%	182	1.76 ± 0.15	0.0215 ± 0.002	354 ± 50.7	1.95 ± 0.28
D	2%	220	1.72 ± 0.09	0.0194 ± 0.001	249 ± 12.2	0.53 ± 0.03
E	2%	203	1.54 ± 0.06	0.0186 ± 0.001	296 ± 11.2	0.63 ± 0.02
F	2%	208	1.56 ± 0.05	0.0191 ± 0.001	288 ± 10.0	0.62 ± 0.02
G	0.3%	185	1.34 ± 0.01	0.0170 ± 0.0001	338 ± 2.6	0.11 ± 0.001
H	0.3%	206	1.49 ± 0.01	0.0188 ± 0.0002	299 ± 2.5	0.09 ± 0.001
I	0.3	208	1.51 ± 0.01	0.0196 ± 0.0001	310 ± 2.2	0.10 ± 0.001
J	0	187	1.36 ± 0.01	0.0175 ± 0.0002	339 ± 3.2	0

To calculate percent exceedance, all data for a parameter (e.g., effluent concentration) were sorted independently for each mix (5%, 2%, 0.3%, and 0% iron) from largest to smallest and a rank, in ascending order, was assigned to each value. The percent

exceedance was then calculated as the ratio of the rank to the total number of samples collected from each mix. For example, after the effluent concentration data for 5% iron filings (95% sand) columns was sorted in descending order, a data point with a value of 0.036 mg PO_4^{3-} -P/L was assigned the rank of 168. The total number of samples collected from the 5% iron-sand columns is 336 and therefore the percent exceedance for this data point is 50% (100% x 168 / 336).

3 Column Experiment Results

Design guidelines for sand filtration systems recommend a hydraulic conductivity of 0.0013 cm/s or greater (Claytor and Schueler 1996). As shown in Table 2, the flow-volume-weighted average hydraulic conductivity for all of the columns is at least ten times larger than the recommended design value of 0.0013 cm/s. The average hydraulic conductivity for 100% sand is also more than ten times larger than the design value but is similar to the average hydraulic conductivity of the iron-sand columns. According to these results, the hydraulic conductivity does not appear to be affected by the addition of iron filings or the sorption of phosphate to iron filings at iron filing concentrations up to 5% by weight.

Table 2 shows that the estimated contact time between the synthetic stormwater and the iron-sand media varied from 249 to 440 s (4.15 – 7.3 min), with an average for all columns of approximately 318 s (5.3 min). This corresponds to a hydraulic loading rate (ratio of volumetric flow rate to cross-sectional area) of 1.34 – 1.76 m/h. The contact time with only iron varied from approximately 0.10 s for 0.3% iron filings up to 1.73 – 2.42 s for the columns mixed with 5% iron. This analysis reveals that only a few seconds are available to achieve phosphate capture by iron filings.

The effluent concentration for all samples collected from the columns with 5%, 2%, 0.3%, and 0% iron mixed with sand has been plotted as a function of percent exceedance in Figure 3. The effluent phosphate concentration from the column mixed with 100% sand is similar to the influent concentration which indicates that little phosphate is captured by 100% sand.

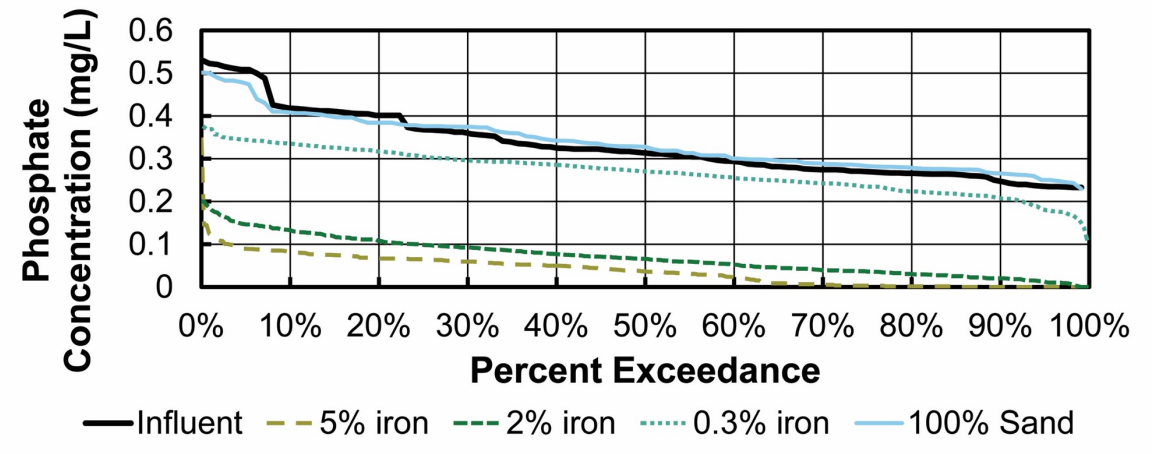

Figure 3. Phosphate concentration as a function of percent exceedance for all Data: Influent (n = 112), 5% (n = 336), 2% (n = 336), 0.3% (n = 336), and 0% iron enhanced sand.

The median (i.e., 50% exceedance) influent concentration is approximately 0.313 mg PO_4^{3-} -P/L and the median effluent concentrations from the 5%, 2%, 0.3%, and 0% iron-sand columns are 0.036, 0.066, 0.271, and 0.328 mg PO_4^{3-} -P/L, respectively. Both the 5% and 2% iron-sand columns retained a substantial amount of phosphate. Of the samples collected from the 5% iron-sand columns (n = 336), approximately 36.6% would be considered an oligotrophic (< 0.01 mg PO_4^{3-} -P/L) in-lake concentration. Approximately 7.7% would be considered mesotrophic (0.01 – 0.03 mg PO_4^{3-} -P/L), 52.7% would be considered eutrophic (0.03 – 0.1 mg PO_4^{3-} -P/L), and only 3% would be considered a hypereutrophic (> 0.1 mg PO_4^{3-} -P/L) in-lake concentration. It is apparent when comparing these values that mixing iron filings with sand significantly increases the amount of phosphate that can be captured by filtration media.

While Figure 3 provides an indication of phosphate capture performance by iron enhanced filtration media, total capture capacity (i.e., longevity) is of equal importance. The cumulative phosphate mass retained within the filter media is shown in Figure 4 as a function of treated depth. Depth treated is the total volume of water passed through the column divided by the cross-sectional area of the column. Treated depth for a field application of sand filtration (existing or proposed) can be similarly estimated given the estimated runoff volume and the sand filter surface (plan) area.

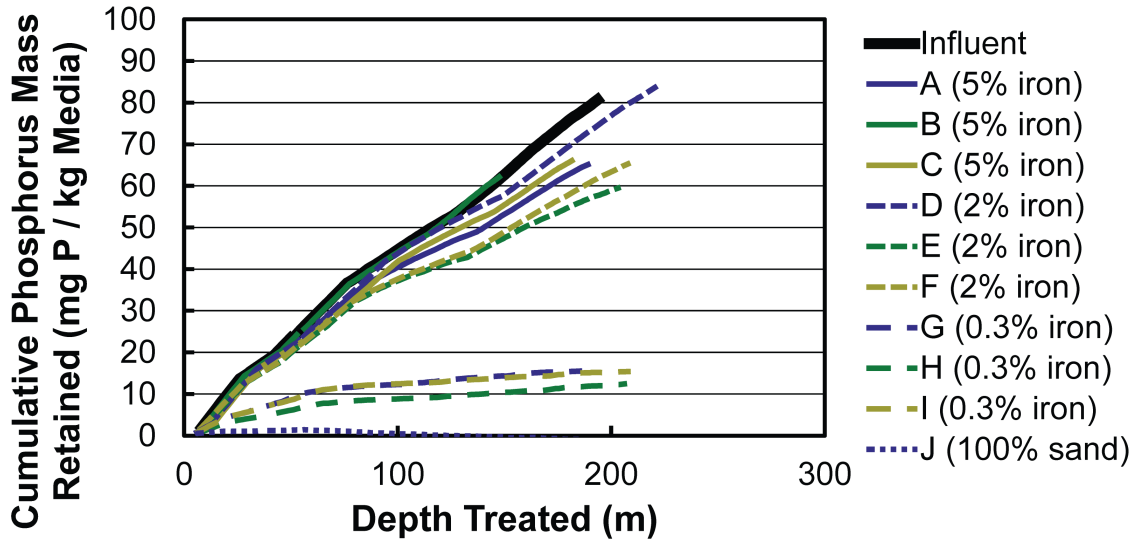

Figure 4. Cumulative phosphate mass retained (mg P/kg Sand and Iron Media) by 5%, 2%, 0.3% iron and 100% sand columns.

Plotting cumulative phosphate mass retained as a function of treated depth can illustrate both the performance and the capacity for a filter media to capture phosphate. The slope of the cumulative phosphate mass retained is an indication of the phosphate capture performance. When the slope of the cumulative phosphate mass retained is identical to the slope of the cumulative influent phosphate mass, all of the influent phosphate mass is captured (i.e., 100% retention). Any positive slope indicates that phosphate is captured within the filter media, with a steep slope indicating more phosphate has been captured compared to a horizontal slope (no phosphate capture) or a negative slope (phosphate release).

The slope of the cumulative phosphate mass retained decreases as the phosphate capture efficiency decreases, which may be an indication that the potential sorption capacity is becoming saturated with phosphate. When the slope becomes horizontal (i.e., 0% retention), the phosphate sorption capacity is likely exhausted and the cumulative phosphate mass retained can be assumed to be equal to the total sorption capacity.

As shown in Figure 4, the 100% sand captures little, if any, phosphate as indicated by the nearly horizontal slope. Furthermore, the 100% sand column has little capacity for

capturing phosphate as indicated by the near zero cumulative phosphate retained. This corresponds well with the interpretations made from Figure 3 above.

The iron enhanced columns with 0.3% iron filings initially captured phosphate, as indicated by the positive slope. The slope of the cumulative phosphate mass retained, however, is significantly less than the slope of the cumulative influent phosphate mass, which indicates that a relatively small fraction of the influent phosphate is captured. Also, after approximately 60 m of treated depth the capacity for phosphate retention is nearly exhausted as indicated by the near horizontal slope.

Initially, the slope of the cumulative phosphate mass retained for the 2% and 5% iron filings columns is similar to the slope of the cumulative influent phosphate mass, which indicates that most of the influent phosphate is captured within the 2% and 5% iron filings columns (~100% retention). After approximately 100 m of treated depth, however, the phosphate retention of the 2% iron filings columns decreases as indicated by a decrease in the slope of the cumulative phosphate mass retained. This is an indication that the phosphate retention performance decreases as sorption sites are being used in the 2% iron filing columns. After 100 m of treated depth the slope of the cumulative mass retained for the 5% iron filings columns is more positive (i.e., steeper) than the slope of the 2% iron filings columns, indicating that the 5% iron filings captures more phosphate after 100 m of treated depth. Both slopes of the cumulative phosphate mass retained are still positive, however, so sorption capacity of the iron filings is not reached in the 2% and 5% iron filing columns during the experiments.

The flow-volume weighted average hydraulic conductivity, contact time, normalized effluent concentration, total effluent phosphate mass per mass of influent mass, and mass of phosphate captured per mass of iron for mixes of 5%, 2%, 0.3% and 0% iron with C33 sand are listed in Table 3. It is apparent from Table 3 that the hydraulic conductivity is not affected for these ratios by mixing iron with sand because the average hydraulic conductivity is approximately the same for 5%, 2%, 0.3%, and 0% iron columns.

Table 3. Flow-volume weighted average values for hydraulic conductivity, contact time with iron, normalized effluent concentration; and total values for effluent phosphate mass per total influent phosphate mass and mass of phosphate captured per mass of iron filings ("-" = Not applicable).

Percent Iron Filings (%) =	**5%**	**2%**	**0.3%**	**0%**
Flow-volume weighted average hydraulic conductivity (cm/sec)	0.019	0.019	0.018	0.017
Flow-volume weighted average contact time with iron (sec)	2.002	0.593	0.099	339[a]
Flow-volume weighted average normalized effluent concentration	0.126	0.222	0.841	1.025
Total effluent phosphate mass per total influent phosphate mass	0.118	0.210	0.824	1.014
Total mass of phosphate captured per gram iron filings (mg P per g Fe)	1.29	3.47	4.81	-

[a] = *Contact time with sand*

The total effluent phosphate mass per total influent phosphate mass (Table 3) is a measure of the overall performance for the iron-sand media. Values close to zero indicate that very little of the influent phosphate is present in the effluent because it is captured by the iron-sand media. Conversely, values close to unity indicate that most of the influent phosphate passes through the iron-sand media and is discharged as effluent. Values larger than unity indicate that more phosphate is present in the effluent than in the influent as a result of phosphate release from the media, as demonstrated by the 0% iron filings (100% sand) columns. Approximately 12% of the influent phosphate passed through the media with 5% iron filings. By comparison, approximately 82% of the influent mass passed through the media with only 0.3% iron filings. It is apparent from these findings that increasing the amount of iron filings will also increase the amount of phosphate that is captured. As indicated by the values in Table 3, iron-sand media will capture more phosphate than a conventional sand filter that does not contain iron filings.

Figure 4 indicates that the 0.3% iron-sand media columns are nearly exhausted (as described above) at treated depths of 50 m or more. The mass of phosphate captured per mass iron filings (Table 3) for the columns with 0.3% iron filings after 200 m of treated depth is approximately 4.8 mg P per g Fe. Because the column is nearly exhausted, the total capacity for a sand filter with 0.3% iron filings is expected to be approximately 4.8

mg of phosphate per gram of iron filings. Assuming the sorption capacity of iron filings is independent of iron mass, the sorption capacity of a sand filter mixed at any ratio is expected to be approximately 4.8 mg P per mg Fe. After 200 m of treated depth, the mass of phosphate captured in the columns with 5% and 2% iron filings is 1.29 and 3.47 mg P per mg Fe, respectively, which is expected because the columns with 5% and 2% iron filing are not near exhaustion.

4 Model

A mathematical model, as given by Equation (6) (Erickson *et al.* 2007, Erickson 2005), was applied to understand phosphate retention on iron as a function of contact time, total mass of phosphate retained, and influent concentration. The model can be used to estimate phosphate retention by field applications of iron enhanced sand filtration and may also be used to design facilities by using estimates of the model parameters.

$$\frac{C_{out}}{C_{in}} = 1 - \left(\beta_0 e^{-\beta_1 \sum M}\right)\left(1 - e^{-\beta_2 t_{contact}}\right) \tag{6}$$

where:

C_{in} = Influent concentration (mg/L)

C_{out} = Effluent concentration (mg/L)

β_0 = Coefficient related to the phosphate retention capacity of iron

β_1 = Coefficient related to the rate at which C_{out} approaches C_{in} (g Fe/g P)

$\sum M$ = Instantaneous sum of phosphate mass retained (g P/g Fe)

β_2 = Coefficient related to the phosphate sorption rate constant (1/s)

$t_{contact}$ = Contact time between phosphate and iron (s)

Sum of mass retained (∑M) is used for simplicity because the reactions governing the phosphate retention by iron are numerous and complex. Rosenquist *et al.* (2010) have found that phosphate capture can be related to sum of mass retained. Phosphate retention capacity decreases as phosphate is captured by iron but increases as iron rusts. To avoid the complexity of these two diverging mechanisms, a single variable (∑M) is used to

describe the net result of both. This process illustrates why iron filings are ideally suited for use in stormwater treatment because the intermittent dry and wet periods allow the iron to rust and create more sorption sites between runoff events.

The first term of Equation (6), ($\beta_0 e^{-\beta 1 \Sigma M}$), is the phosphate retention capacity of iron where β_0 is related to the mass of iron available for phosphate adsorption: $\beta_0 \sim 0$ indicates little or no potential for phosphate removal ($C_{out}/C_{in} \sim 1$) and $\beta_0 = 1$ indicates that the potential phosphate removal is 100% ($C_{out}/C_{in} \sim 0$). β_0 is therefore constrained to be less than or equal to 1 for all columns and held constant for columns with the same mass of iron because the capacity should be a function of iron mass.

β_1 relates to the rate at which the equilibrium concentration (C^*) approaches C_{in} and is affected by rusting (retention capacity increases) and phosphate adsorption (retention capacity decreases). Normalized effluent phosphate concentration was found to be less than unity ($C_{out}/C_{in} < 1$) for all columns enhanced with iron (see Figure 5 – Figure 7). From Equation (6) and $C^* = C_{in}(1 - \beta_0 e^{-\beta 1 \Sigma M})$ (Erickson *et al.* 2007) it can be concluded that C^* is less than C_{in} throughout the experiments. Therefore β_1 was constrained to be ≥ 0 but allowed to vary between each column because these studies did not individually quantify rusting or adsorption. A value of $\beta_1 = 0$ indicates that retention capacity has not decreased due to phosphate adsorption.

The second term of Equation (6), ($1 - e^{-\beta 2 t contact}$), is a value between zero and unity that represents the rate at which the interaction between phosphate and iron approaches equilibrium. β_2 represents the product of the rate constant and the specific surface area. The specific surface area is an intensive property of the iron filing media. The packing and shape of the iron filings will determine the specific surface area. Thus, β_2 is a different non-negative constant for each column.

The model predicted normalized effluent concentration is shown in Figure 5 – Figure 7 for 0.3%, 2%, and 5% iron-sand columns. Standard error between model-predicted values and measured values of normalized effluent concentration was minimized to solve for the coefficients (β_0, β_1, β_2) for mixes of iron filings and sand. The total standard error for nine mixes of iron and sand is 0.0735 (n = 1008, data-weighted average) and the

best-fit model coefficients (β_0, β_1, β_2) are listed in Table 4. The accuracy of the model is illustrated in Figure 5 – Figure 7.

Table 4. Best-fit model coefficients for iron filing sand columns. Constraints: β_0 is equal for 5% iron-sand columns and ≤ 1; β_0 is equal for 2% iron-sand columns and ≤ 1; and β_0 is equal for 0.3% iron-sand column sand ≤ 1; $\beta_1 \geq 0$; β_2 is equal for all columns and ≥ 0.

Percent Iron Filings (%) =	**5%**	**2%**	**0.3%**
β_0 (all replicates)	0.984	0.945	0.611
β_1 (g Fe/g P) (1st replicate)	236.4	17.9	340.8
β_1 (g Fe/g P) (2nd replicate)	0	180.5	599.1
β_1 (g Fe/g P) (3rd replicate)	169.9	120.0	370.3
Final $e^{-\beta 1 \Sigma M}$ (1st replicate)	0.735	0.928	0.172
Final $e^{-\beta 1 \Sigma M}$ (2nd replicate)	1.000	0.585	0.084
Final $e^{-\beta 1 \Sigma M}$ (3rd replicate)	0.799	0.676	0.150
β_2 (1/s) (all replicates)	54.6	54.6	54.6

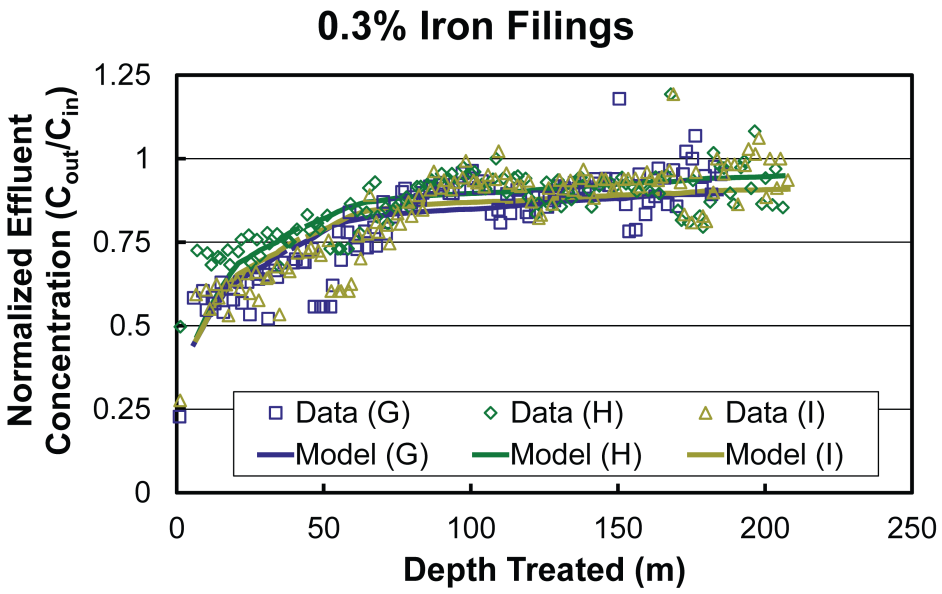

Figure 5. Effluent phosphate concentration normalized to the influent concentration (flow-weighted mean = 0.340 mg PO_4^{3-} -P/L, range = 0.233 to 0.531 mg PO_4^{3-} -P/L) and model prediction for 0.3% iron filings.

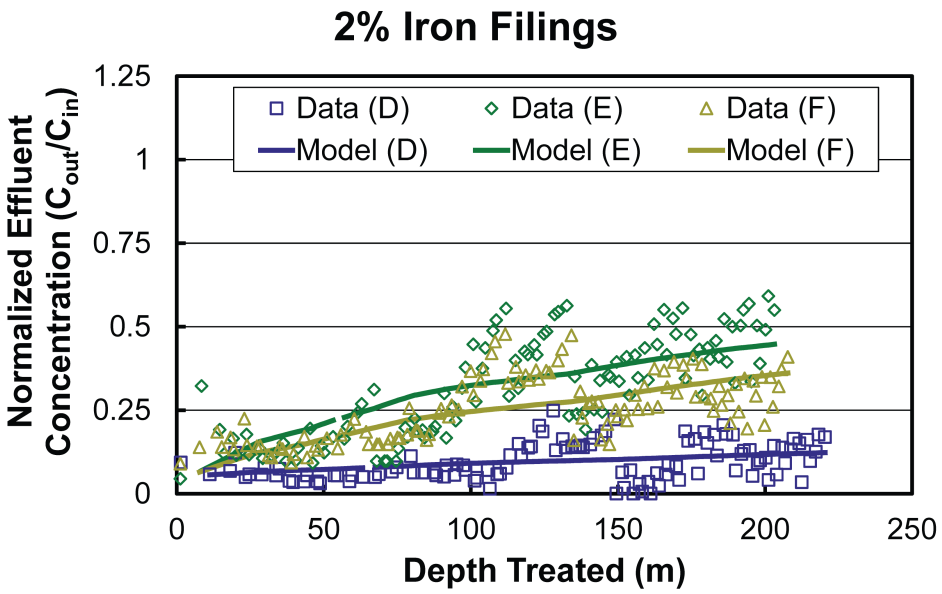

Figure 6. Effluent phosphate concentration normalized to the influent concentration (flow-weighted mean = 0.340 mg PO_4^{3-} -P/L, range = 0.233 to 0.531 mg PO_4^{3-} -P/L) and model prediction for 2% iron filings.

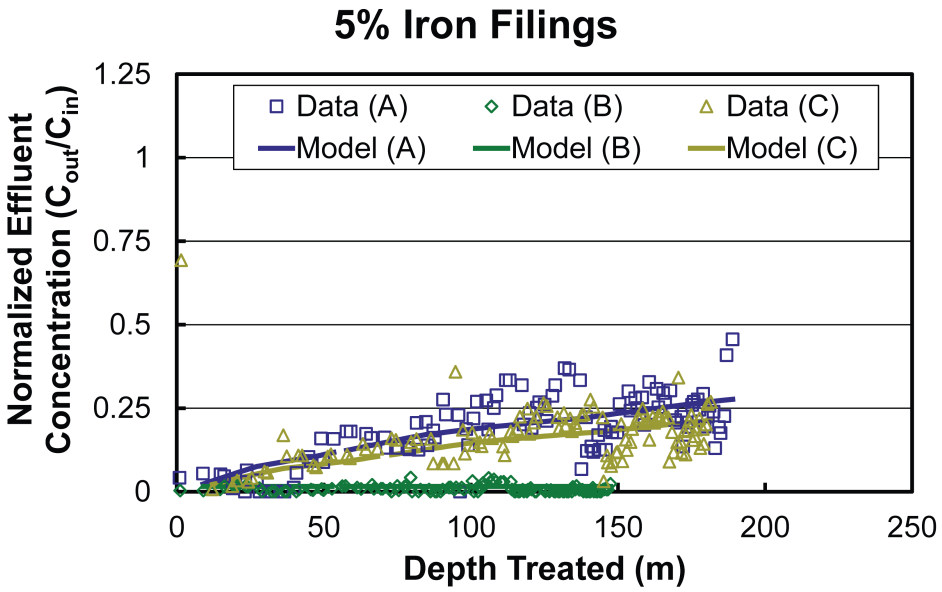

Figure 7. Effluent phosphate concentration normalized to the influent concentration (flow-weighted mean = 0.340 mg PO_4^{3-} -P/L, range = 0.233 to 0.531 mg PO_4^{3-} -P/L) and model prediction for 5% iron filings.

The model captures trends related to the capacity of the iron filings to retain phosphate despite the complexity of processes incorporated into the sum of mass retained term ($\sum M$). As discussed earlier, $\beta_0 = 1$ represents a retention capacity that equals or exceeds the initial phosphate concentration. As shown in Table 4, $\beta_0 \sim 1$ for the 5% and 2% iron-sand columns which means there is enough capacity at these mass fractions to capture phosphate from stormwater at the concentrations used in these experiments. For the 0.3% iron-sand columns, however, $\beta_0 \sim 0.6$ which means the capacity is not sufficient to capture all the phosphate in the synthetic stormwater; this is also evident from Figure 4.

The best-fit values for β_1 are best interpreted by considering the capacity term, ($e^{-\beta 1 \sum M}$), after the experiments were complete as listed in Table 4. Note that for most columns (excluding 2nd replicate of 5% and 1st replicate of 2%), the capacity term decreases with decreasing iron mass such that the final value of $e^{-\beta 1 \sum M}$ is close to zero for 0.3% iron-sand columns. This can be interpreted as $C^* \sim C_{in}$ for these columns and that $C_0 \sim C_{in}$ $(1 - \beta_0)$ for the 5% and 2% iron-sand columns. Note also from Table 4 that $\beta_0 \sim 1$ for 5% and 2% iron-sand columns and therefore $C^* \sim 0$ for these columns. The columns that do not follow this trend (2nd replicate of 5% and 1st replicate of 2%) both have small values for β_1 indicating that phosphorus removal is not affected by the sorption of previous phosphorus, or that the addition of new sorption sites through oxidation is much greater than the reduction of sorption sites by phosphate capture. While these experiments did not quantify oxidation or sorption independently, these columns likely had more contact time (e.g., 2nd replicate of 5%), better contact resulting in more sorption, or both. Another possible explanation is that the effective surface area varied in the columns due to stagnant areas or short-circuiting (not measured). It is also possible that these columns experienced better oxygenation resulting in development of more sorption sites than the other columns.

5 Field Application Results

Five tests were conducted for the stormwater pond fitted with two filtration trenches under various conditions as listed in Table 5. It is important to note that the limit of detection for the analytical method is 0.01 mg PO_4^{3-} -P/L and several effluent samples were

found to be below detection limits during this study (see Table 5). For calculation purposes, the concentration was assumed to be half of the detection limit (0.005 mg PO_4^{3-} -P/L) for all samples measured below detection limits (Kayhanian *et al.* 2002, Shumway *et al.* 2002).

Table 5. Testing results for an iron enhanced filtration trench mixed with 7.2% and 10.7% iron filings. Concentration assumed to be half of the detection limit (0.005 mg PO_4^{3-} -P/L) for all samples measured below detection limits Kayhanian et al. 2002, Shumway et al. 2002).

	Iron Content	**7/1/2010**	**7/13/2010**	**8/11/2010**	**8/12/2010**	**9/24/2010**
Average Filtration Rate ± 95% Confidence Interval (cm/hr)	7.2%	26.6 ± 4.30	14.0 ± 1.68	68.7 ± 1.67	45.9 ± 3.09	13.2 ± 0
	10.7%	10.3 ± 1.63	9.2 ± 1.57	16.4 ± 1.94	10.4 ± 0.61	10.1 ± 0.32
Influent Phosphate Flow-weighted Event Mean Concentration (mg PO_4^{3-} -P/L)	7.2%	0.032	0.027	0.101	0.077	0.140
	10.7%	0.033	0.025	0.101	0.077	0.140
Effluent Phosphate Flow-weighted Event Mean Concentration (mg PO_4^{3-} -P/L)	7.2%	0.023	0.012	0.016	0.021	0.020
	10.7%	0.013	< 0.01	0.015	0.017	0.013
Percent of effluent samples below detection (0.01 mg PO_4^{3-} -P/L)	7.2%	3.4%	25.0%	0%	18.2%	0%
	10.7%	33.3%	100%	15.8%	36.4%	22.2%
Flow-weighted Phosphate Event Mean Concentration Reduction Efficiency	7.2%	28.6%	57.1%	84.2%	72.8%	85.5%
	10.7%	61.7%	> 60.6%	85.2%	77.7%	90.9%
Prediction of Event Mean Concentration Reduction Efficiency	7.2%	93.3%	91.6%	90.5%	90.5%	86.9%
	10.7%	97.2%	96.7%	96.5%	96.5%	95.5%

The influent phosphate EMC for these tests varied from approximately 0.026 – 0.140 mg PO_4^{3-} -P/L and the effluent EMC was consistently between a non-detect level (< 0.01 mg PO_4^{3-} -P/L) and 0.023 mg PO_4^{3-} -P/L. The phosphate removal efficiency varied between approximately 29% and 91% but for most tests (only excluding July 1), phosphate capture is greater than 50%. From the data in Table 5, it is clear that as the influent phosphate EMC increased, the phosphate capture efficiency increased and the percentage of samples below detection limits decreased. The median phosphate concentration in

stormwater is 0.12 mg PO_4^{3-} -P/L (Pitt *et al.* 2005), which is greater than the influent concentration for the test on August 11 (84% phosphate retention) and less than the influent concentration for the test on September 24 (90% phosphate removal). Therefore, for most rainfall events the iron enhanced sand filtration trenches are expected to capture approximately 85 – 90% of the phosphate.

The model given in Equation (6) was used to predict the normalized effluent concentrations in the pond from the two trenches for the same conditions as the measured values reported in Table 5. The P8 Urban Catchment Model (Walker 1990) was used to estimate runoff and pollutant loading to the trenches prior to and between tests. The average filtration rate computed from all measured values from five tests (n = 100) was used to estimate the volume of stormwater treated by the trenches. Median values for the model coefficients fit to the 5% iron filings column data ($\beta_0 = 0.984$, $\beta_1 = 169.9$ g Fe per g P, $\beta_2 = 54.6$ per s) were used for this model prediction. The normalized effluent concentrations were converted to EMC phosphate reduction efficiency as reported in Table 5.

The model-predicted reduction efficiency is larger than measured efficiency for most tests but similar to the efficiency for the tests on August 11 and September 24. As mentioned previously, the influent concentration for these tests is most similar to median values for natural stormwater and therefore assumed to be representative of most natural rainfall events. Because the model-predicted efficiency is most similar to measured efficiency for these representative tests, the model adequately predicts field performance of iron enhanced sand filtration.

As mentioned above, the surface area of the filter trenches is approximately 0.24% of the impervious watershed, which is approximately an order of magnitude less than typical design values of 2 – 3% (Weiss *et al.* 2007). Therefore, the annual hydraulic loading rate for these experimental trenches will be considerably larger than typically designed trenches and will require more maintenance to remain effective. For this experimental facility, the iron-sand media may need to be replaced every 3 – 5 years based on the phosphate adsorption capacity (as estimated by the mathematical model) and corresponding useful life expectancy of the iron filings rather than approximately every 30 years when more typical filter/ impervious area ratios are utilized.

6 Potential Applications

The "Minnesota Filter," an iron enhanced sand filter for stormwater treatment, could be applied in several other applications. One such application is a horizontal-flow permeable weir in which stormwater runoff fills an upstream practice and begins to flow through a permeable weir wall constructed of vertical posts and horizontal composite planks. Permeable socks approximately 1.2 m long and 0.2 m in diameter could be filled with 5% or more by weight iron-sand media and installed between the horizontal planks to provide treatment of stormwater as it permeates through the weir. The permeable weir would treat all low-flow events and also treat stored stormwater after larger events. This type of permeable weir could be used at the downstream edge of wet detention basins.

A similar application would be a horizontal-flow iron-sand filter installed within ditch checks at frequent intervals in roadside swales (drainage ditches). Ditch checks are common erosion control structures composed of gravel or riprap designed to reduce the channelized flow velocity within roadside swales. When enhanced with iron-sand, particles will settle to the swale bottom and particulate and dissolved phosphorus will be captured within the ditch check as stormwater filters through the mix of gravel/riprap, sand, and iron filings.

Another application is an iron enhanced bioretention practice (i.e., rain garden). Bioretention practices have been shown to capture several stormwater pollutants (LeFevre *et al*. 2015). The use of compost in the soil of bioretention practices provides nutrients for the plants and has been found to capture dissolved metals (Davis *et al.* 2001, Morgan *et al.* 2010) and petroleum hydrocarbons (LeFevre *et al.* 2012) from stormwater. Others have shown the benefits of vegetation and soil amendments for pollutant uptake (Lucas and Greenway 2008, Lucas and Greenway 2011). Several studies have also shown that peat or compost can release nutrients due to the organic content of the material (U.S. EPA 1999, Koerselman *et al.* 1993, Stewart 1992, Morgan 2011). Thus, bioretention practices with compost can increase phosphate loads rather than decrease them. For sites where an under-drain is required, a bioretention practice designed with compost may not help to meet regulatory requirements because of the export of phosphate. To mitigate this, bioretention

facilities can be designed as a two-stage system where the top layer is constructed of compost-amended sand and the bottom layer is an iron enhanced sand filter. Stormwater runoff will flow through the compost-amended sand, where the suspended solids and dissolved metals will be removed. The stormwater will then flow through the iron enhanced sand filter where any phosphate in the stormwater runoff or exported from the compost will be captured before the stormwater reaches the under-drains. To ensure adequate oxygenation of the filter section, the bottom end of the under-drain should be open to the air.

7 Conclusions

Phosphate represents an average of approximately 45% of total phosphorus concentration in stormwater runoff and therefore, should be removed from stormwater in order to meet phosphorus load reduction requirements. The Minnesota Filter, composed of iron filings mixed with sand, is shown to capture significantly more phosphate than standard sand filtration for stormwater treatment. Sand filters mixed with 5% iron filings can capture, on average, 88% of the influent phosphate for at least 200 m of treated depth. Neither incorporation of iron filings into a sand filter nor capture of phosphate onto iron filings has a significant effect on the hydraulic conductivity of the filter at mixtures of 5% or less iron by weight. Field applications with up to 10.7% iron were operated over 1 year without detrimental effects upon hydraulic conductivity. A model is applied and fit to column study data to predict the field performance of iron-enhanced sand filters. The model predictions are verified through the measured performance of the filters in removing phosphate in field applications. Practical applications of the technology, both existing and proposed, are presented so stormwater managers can begin implementation. Iron enhanced sand filtration is suited for removing phosphate from stormwater because (1) it captures a significant portion of the phosphate without fouling, and (2) it has substantial capacity to capture phosphate for over 200 m of treated depth when mixed at 5% and sized appropriately.

Chapter 3: Monitoring and Maintenance of Phosphate Adsorbing Filters[2]

Abstract: Field installations of two iron enhanced sand filters (IESFs), designed to remove phosphate and particulates from stormwater runoff, were monitored and maintained for one to three years. One application, a traditional IESF in an agricultural watershed, retained over 64% of the influent phosphate load while the second, a pond perimeter IESF in a developing suburban watershed, retained 26%. The measured average effluent Event Mean Concentration (EMC) for the traditional IESF was 56.1 μg/L. All events exhibited positive removal of phosphate (i.e., effluent loads < influent loads). By contrast, the measured percent phosphate retained for the pond perimeter IESF in 2013, 2014, and 2015 was 18%, 25%, and 45%, respectively. In addition, the average effluent EMC for the three years was 64.1, 54.2 and 19.9 μg/L, respectively. Half of the events (14 out of 28) were found to have negative removal (i.e., effluent loads > influent loads). Events with negative removal tended to be smaller events with low influent phosphate concentrations (3.7 – 39.4 μg/L). Non-routine maintenance improved the hydraulic performance of the pond perimeter IESF and, after a rinsing event, also improved phosphate retention rates to an average of 45%. It is believed that there are at least two reasons for this difference in performance between the two IESFs: First, the traditional IESF was treating runoff from drain tiles with a low particulate phosphorus concentration, while the pond-perimeter IESF had a degrading mat of filamentous algae transported onto the surface, creating a source of phosphate that was not quantified. Second, the pond perimeter IESF had treated a relatively large volume of water for its size, resulting in substantial flow-through in the filter within 5 years of

[2] A version of this chapter has been accepted for publication in the Journal of Environmental Engineering as Erickson, A.J., Weiss, P.T., and Gulliver, J.S. (2017b, accepted). "Monitoring and Maintenance of Phosphate Adsorbing Filters." Journal of Environmental Engineering Special Issue: Environment and Sustainable Systems: A Global Overview. Permission was obtained from the American Society of Civil Engineers to reproduce the publication in this dissertation.

operations. This is greater than anticipated for an IESF, and may have partially caused the reduction in performance.

1 Introduction

Dissolved phosphorus, which in stormwater is usually in the form of phosphate (PO_4^{3-}) (Stumm and Morgan 1981), is typically the limiting nutrient for plant growth in temperate freshwater systems (Schindler 1997). In such systems, the addition of phosphate can lead to eutrophication, which is undesirable due to the corresponding negative environmental impacts such as low dissolved oxygen, fish kills and less biotic diversity, increased turbidity, etc. In fact, the United States Environmental Protection Agency (U.S. EPA) lists almost 3000 surface waters as impaired due to phosphate or phosphorus (U.S. EPA 2016). If a water body is designated as impaired, a corresponding total maximum daily load (TMDL) implementation plan must be developed. This plan specifies reduction goals for contaminant loads entering the water body such that, if implemented, the water body quality will improve and it will no longer be designated as impaired. For phosphorus impairments, one way to reduce phosphorus and/or phosphate loading to the water body is to reduce the phosphorus concentration in stormwater runoff.

Stormwater can be a major contributor of phosphorus load from sources such as fertilizer, vegetation, and detergents (U.S. EPA 1999, APHA 1998). Thus, removing phosphate from stormwater runoff can help improve water quality and achieve TMDL goals. In fact, in many situations, phosphate *must* be removed to meet TMDL goals. That is because, on average, the dissolved phosphorus fraction in stormwater is 48% (Maestre and Pitt 2005) and phosphate comprises 90% of dissolved phosphorus (Kayhanian *et al.* 2007). TMDL goals typically call for a reduction in phosphorus loads of 60% or more, so capturing the particulate fraction (on average 52% of the phosphorus load) is not enough. Some portion of the dissolved fraction must be removed to meet TMDL goals. Furthermore, Erickson *et al.* (2007) showed that dissolved phosphorus fractions over 90% are not uncommon in stormwater, which only increases the need to remove a portion of the dissolved fraction.

Typical stormwater control measures (SCMs, sometimes called best management practices or BMPs) such as detention basins, rain gardens, wet ponds, etc. do little to remove the dissolved phosphorus fraction. An iron-enhanced sand filter (IESF) has been documented to retain significant amounts of dissolved phosphorus (Erickson *et al.* 2007, 2012). The IESF uses iron shavings, typically at 5 – 7% by weight, mixed with typical concrete sand (e.g., American Standards for Testing and Materials type C33; ASTM 2002). When the iron is oxidized, it becomes positively charged. This positive charge binds with negatively charged phosphate ions through surface adsorption and complexation. In laboratory column studies, an IESF captured 80% or more of the influent dissolved phosphorus load (Erickson *et al.* 2007, 2012).

This chapter presents maintenance efforts and monitoring results of two field installations of the IESF technology, both of which are gravity flow IESFs. Performance of each installation in retaining soluble reactive phosphorus (SRP) will be shown. Because SRP is typically the phosphate ion in stormwater, this chapter will refer to phosphate as equivalent to SRP from this point forward. The first field installation of IESF is more of a traditional surface design, receiving runoff directly from farm land drain tiles (traditional IESF). The second is on the perimeter of a retention pond and treats suburban residential runoff that is temporarily retained in the pond. Therefore, it is referred to as a pond perimeter IESF. More details on the field installations and results follow.

2 Field Installations

2.1 Traditional Iron Enhanced Sand Filter

Martha Lake and Charlotte Lake, near the City of Buffalo in Wright County, Minnesota, United States of America (USA) have naturally low in-lake levels of phosphorus (~35 µg/L total P) but receive runoff from agricultural drain tiles through ditches and conveyances. Phosphate concentrations in nearby agricultural runoff, as determined by periodic grab samples, have ranged from 31 to 242 µg P/L. An IESF measuring 15.2 m by 7.6 m was installed with approximately 6% iron filings by weight,

near Martha Lake and Charlotte Lake. The sand filter receives runoff from drain tile associated with approximately 7.7 ha of farm land used for crops and livestock. The watershed to filter ratio of 660 to 1 is high because the watershed was fully permeable and the runoff peak was dampened due to filtration into the drain tile.

The cross-section of the IESF consists of, from top to bottom, 30 cm of ASTM C33 construction sand (ASTM 2002) with 6% iron shavings by weight, and 15-cm of 1-cm diameter pea gravel containing two 15-cm diameter perforated PVC underdrains (Figure 8). The filter was sealed from the surrounding soil with impermeable geotextile fabric. Flow monitoring equipment was installed on the downstream end of the filter to measure effluent flow rates. Automatic samplers (ISCO Brand, model 3700 and 6700) were installed to collect composite influent and effluent samples on a flow-weighted basis. Atmospheric data, including rainfall as measured by a tipping bucket rain gauge and air temperature, were also recorded.

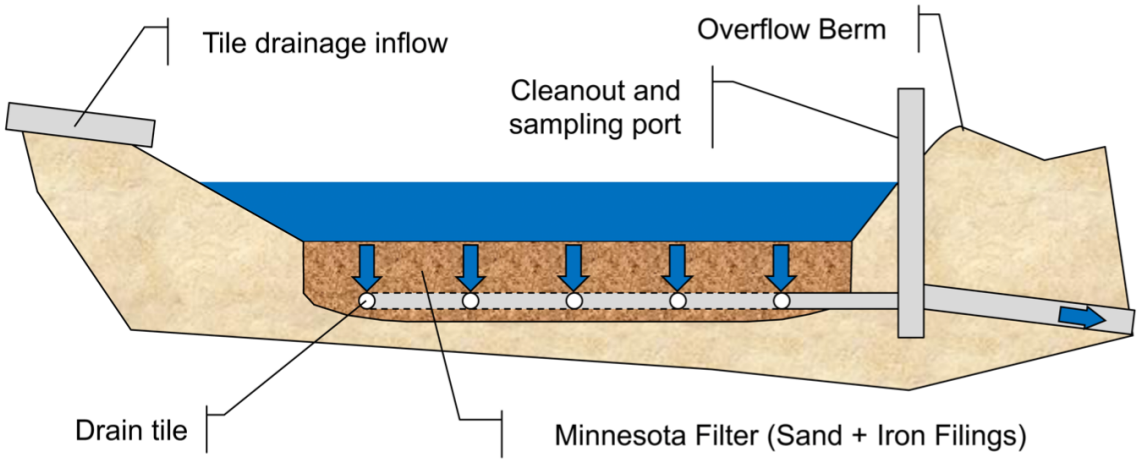

Figure 8. Cross-section of surface iron-enhanced surface sand filter.

2.2 Pond Perimeter Iron Enhanced Sand Filter

A pond perimeter IESF measuring 47 m by 3 m, with 5% iron shavings by weight, was installed along the perimeter of a wet pond in Prior Lake, MN in winter/spring of 2011 (Figure 9). Water draining from the wet pond discharges to a wetland that ultimately drains into Upper Prior Lake. Upper Prior Lake has a total watershed area of 6.5 ha, much of

which is being or will be developed. The pond perimeter IESF was designed with the filter surface at a new normal water level (NWL) that was below the water level control weir in the catch basin adjacent to the wet pond (Figure 10). When runoff flows into the wet pond, the design allows the water level in the pond to increase so that the surface of the IESF becomes temporarily submerged and water filtrates vertically downward through the sand-iron media. After flowing through the media, the filtered runoff enters a gravel reservoir where it is collected by a 10-cm diameter perforated PVC pipe drain tile and conveyed to the outlet structure (i.e., catch basin) of the wet pond. For rainfall events that do not increase the water level above the water level control weir crest, all water flows through the IESF until the water surface elevation returns to the NWL. In large runoff events, the IESF treats the first portion of the increase in wet basin storage volume while excess volume flows over the water level control weir and bypasses the IESF. Once the water level in the pond drops to the control weir crest elevation, the remaining excess water in the pond passes through the IESF. The filters are lined with an impermeable liner such that only stormwater that has been filtered by the IESF enters the drain tile and water enters the IESF only through the top surface. This will allow the filter to dry out between storms. Once stormwater enters the filter, the only way for it to leave the system is through the drain tile.

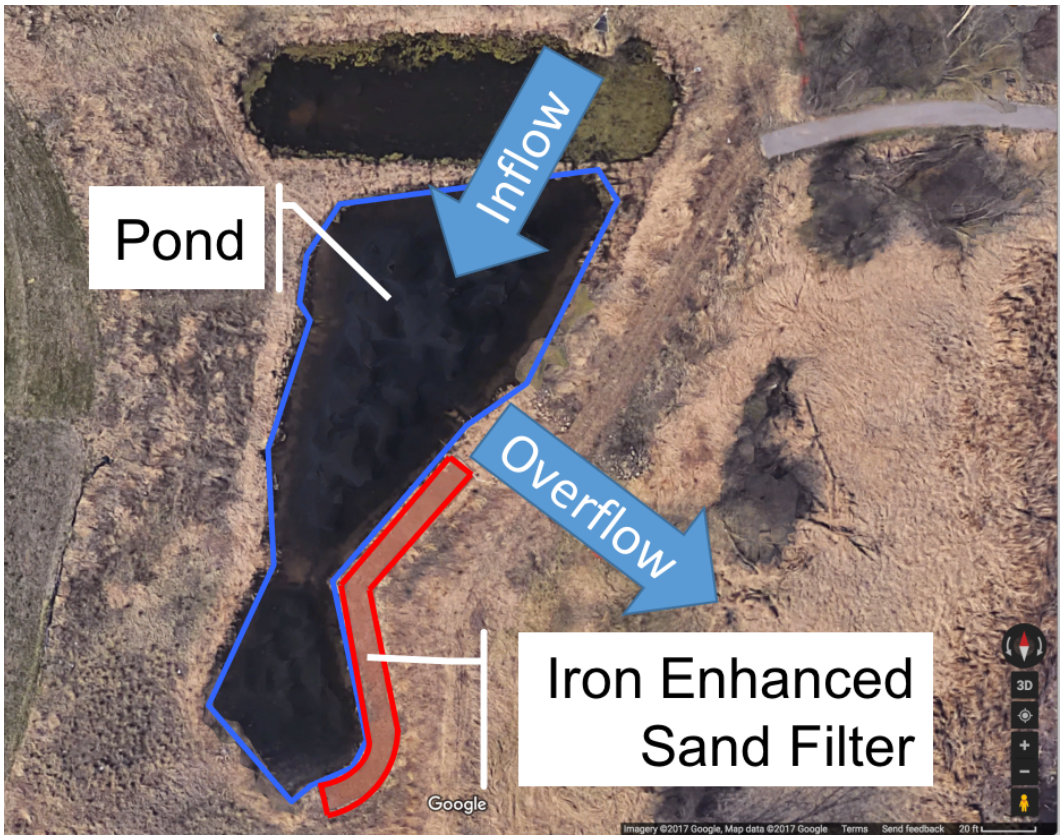

Figure 9. Pond perimeter iron-enhanced sand filter. (Photo Courtesy Google Maps)

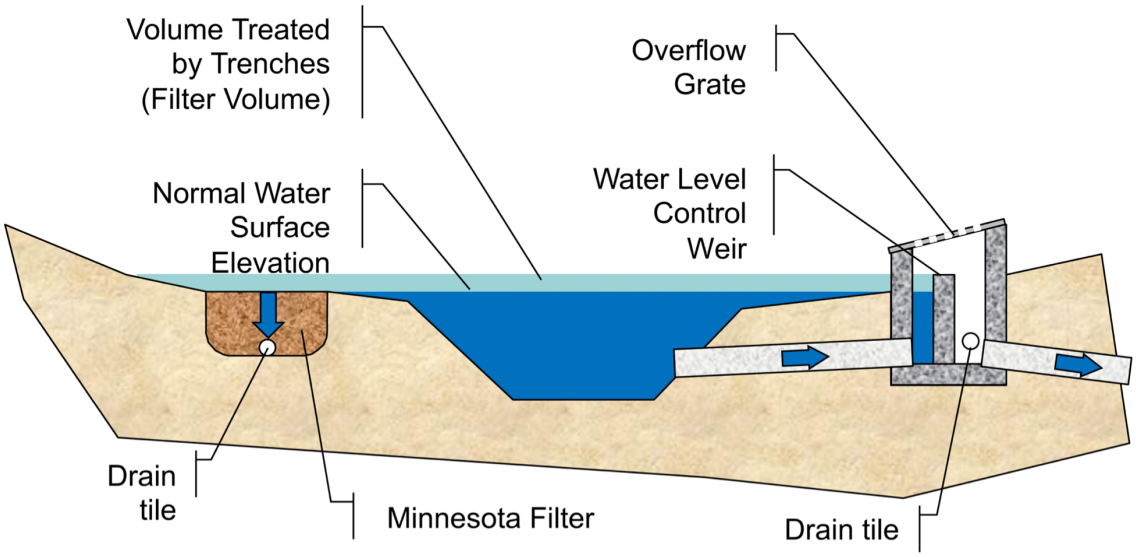

Figure 10. Pond perimeter iron-enhanced sand filter schematic.

3 Materials and Methods

3.1 Sample and Data Collection

To determine the performance of the IESF at each site with respect to phosphate retention, flow rates through the filters were measured and samples were collected. For the traditional IESF, composite, flow-weighted water samples were collected upstream of the filter and from the filter effluent (i.e., outflow from the drain tile). For the pond perimeter IESF, time-based individual samples were collected near the influent of the IESF and composite flow-weighted samples were collected at the effluent (i.e., outflow from the drain tile). For both sites, the phosphate concentrations of the influent and effluent samples were determined, and the percent phosphate retained (i.e., captured) in the filter was calculated. Rainfall was measured at both sites with a tipping bucket rain gage (ISCO Brand). All data was logged with Campbell Scientific CR1000 data loggers, and samples were collected by automatic samplers (ISCO Brand, model 3700 and 6700). The automatic samplers were programmed to begin sampling during a "rainfall event," which started when rainfall exceeded a minimum threshold of 0.05 cm and flow rate exceeded 0.28 L/s. The samplers continued sampling until the flow rate decreased to below the flow rate threshold (flow < 0.28 L/s) and when no rain was measured within the previous two hours (time of concentration << 2 hours). All equipment was powered by two, 12-volt deep cycle marine batteries located on site, except for the data logger, which had its own internal 12-volt battery. For the traditional IESF, two solar panels (43 W maximum power each) recharged the deep cycle marine batteries and the data logger internal battery between runoff events. For the pond perimeter IESF, an additional single solar panel (10 W maximum power) recharged the data logger internal battery.

3.2 Flow Rate Measurement

For the traditional IESF, the flow rate was calculated by measuring the depth of water flowing over a 39° V-notch weir, which was installed within an Agri Drain ™ inline water level control structure that was attached to the effluent drain tile from the IESF.

Because the weir would occasionally operate in submerged conditions, the water level on each side of the weir was measured by separate Campbell Scientific CS-450 pressure transducers located in the control structure (Villemonte 1947) and the weir was calibrated in a laboratory.

To measure flow rate passing through the pond-perimeter IESF, the 10-cm drain tile was extended by approximately 15 m through the outlet pipe (0.9 m diameter, reinforced concrete) of the catch basin to its discharge location near the receiving wetland. At the outlet of the drain tile extension, the pipe was expanded to a 1-m long, 15-cm diameter PVC pipe through an eccentric expansion fitting. A metal compound weir plate was attached to the end of the PVC pipe to allow for discharge measurement. The head on the weir was measured using a Campbell Scientific CS-450 pressure transducer located in an adjacent vertical, ~5-cm diameter cylinder that was connected to the bottom of the 15-cm PVC pipe by means of 0.5-cm diameter flexible tubing. This arrangement allowed the water elevation in the vertical cylinder to match the water elevation in the 15-cm diameter discharge pipe, with the dampening of rapid fluctuations due to surface waves and turbulence, and a minimum of 8 cm of water above the transducer's sensor (necessary for improved accuracy). The weir was calibrated in a laboratory so that the flow rate over the weir could be calculated from the known head on the weir. For more detailed information see Erickson *et al.* (2015).

3.3 Water Analysis

Phosphate concentrations of water samples were measured per Standard Methods section 4500-P, E - Ascorbic Acid (APHA 1998) and Lachat Instruments (a Hach Company brand) QuikChem® Method 10-115-01-1-M (Diamond 2002). The latter method has a statistically determined detection limit as determined in water of 5 µg P/L.

4 Results

4.1 Traditional Iron Enhanced Sand Filter

In 2015, a total of 13 rainfall-runoff events were monitored and total rainfall depth, total filtered volume, and the event mean concentration (EMC) of soluble reactive phosphorus (i.e., phosphate) of the influent and effluent for each event are given in Table 6. Also shown in Table 6 are the percent reduction in EMC, phosphate loads in and out, the percent load reductions for each event, and yearly and overall totals where relevant. The 13 rainfall events totaled 11.8 cm of rain and generated over 2.4 million liters of filtered volume. Influent EMC values ranged from 54 to 238 μg/L. Percent reductions in EMC ranged from 52% to 85% and, because there was no infiltration into the existing soil and inflow equaled outflow, the percent reductions in load for each event are equal to EMC percent reductions. Overall, the filter received 388 g of phosphate in the influent and discharged 138 g of phosphate in the effluent for an overall reduction in the phosphate load of 64.5%. The total load of phosphate entering the filter (388 g) divided by the total influent volume (2.45×10^6 L) gives an overall EMC of 158.2 μg/L for the influent. Similarly, the overall effluent EMC is 56.1 μg/L, which corresponds to an overall reduction in EMC of 64.5%.

Table 6. Traditional IESF Monitoring results from 2015. N/D = No Data; FW Average = Flow-weighted Average. "-" = Not applicable

Rainfall Start	Rainfall depth [cm]	Filtered Volume [10^6 L]	Percent Exceedance by Filtered Volume	EMC IN [µg/L]	EMC OUT [µg/L]	EMC Reduction [%]	Load IN [g]	Load OUT [g]	Load Removal [%]
07/06/15	3.91	0.136	42%	68	14	80%	9	2	80%
07/16/15	4.83	0.482	0%	238	42	82%	115	20	82%
07/24/15	1.98	0.079	83%	54	8	85%	4	1	85%
07/28/15	1.85	0.102	75%	56	12	79%	6	1	79%
10/08/15	1.78	0.028	100%	100	15	85%	3	0	85%
10/23/15	3.28	0.105	67%	68	17	76%	7	2	76%
10/27/15	3.71	0.323	17%	212	96	54%	68	31	54%
10/30/15	0.99	0.289	25%	202	89	56%	58	26	56%
11/02/15	N/D	0.159	33%	145	56	62%	23	9	62%
11/06/15	N/D	0.057	92%	102	53	48%	6	3	48%
11/11/15	2.06	0.108	50%	123	53	57%	13	6	57%
11/13/15	1.02	0.108	58%	112	65	42%	12	7	42%
11/16/15	4.55	0.476	8%	132	63	52%	63	30	52%
FW Average	3.09	-	-	158.2	56.1	64.5%	-	-	-
Totals	29.95	2.45	-	-	-	-	388	138	64.5%

To investigate if filter performance is a function of filtered volume, results were plotted as a function of percent exceedance by filtered volume in Figure 11. This plot shows filtered volume and phosphate loads in and out as a function of percent exceedance by filtered volume. All 13 monitored events are plotted in Figure 11; results corresponding to the largest filtered volume event (0.482×10^6 L) are plotted at zero percent exceedance because this event's filtered volume was not exceeded during the study period. Results corresponding to the second largest filtered volume event (0.476×10^6 L) are plotted at 8% exceedance because this filtered volume was only exceeded by one of the twelve other events, or 8% of the time. The results corresponding to the remaining eleven events are plotted in a similar manner.

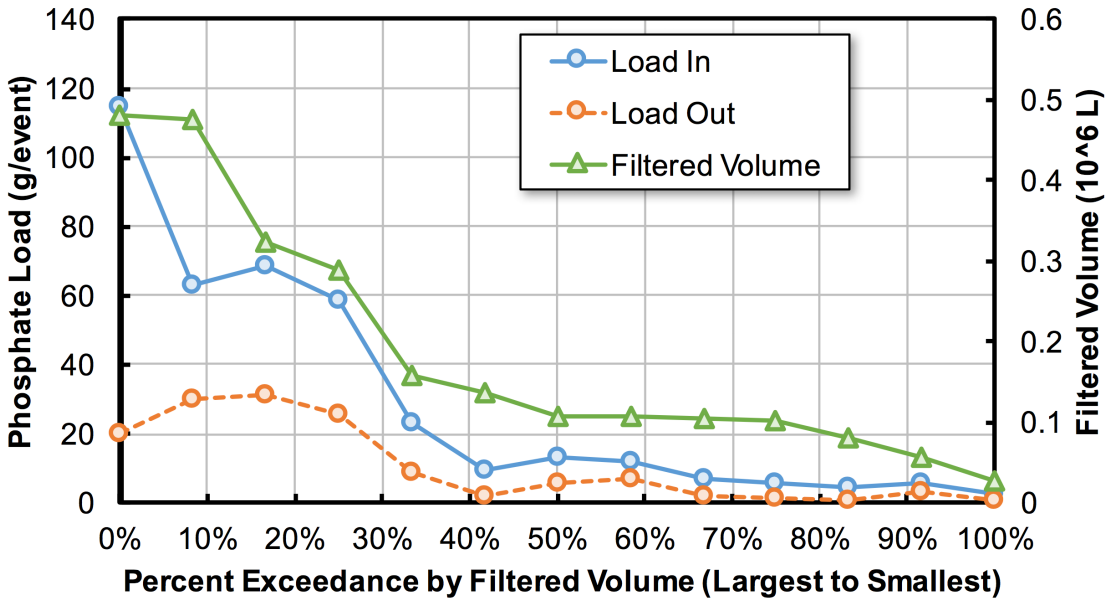

Figure 11. Event Phosphate Load In and Out by Percent Exceedance by Filtered Volume.

As shown in Figure 11, the filtered volume for the four largest events contributes most of the filtered volume, and the phosphate event load contributed by the four largest events (7/16/15, 11/16/15, 10/27/15, 10/30/15) is substantially more than the other nine events. This suggests that treatment of the largest events could have substantial impact on the overall average annual performance of the IESF. Figure 12 shows that the percent removal based on phosphate load is greater than 40% for all events. Four of the 13 events achieved 80% or more phosphate load removal. Figure 13 shows the influent and effluent phosphate load as well as the filtered volume for the traditional IESF as a function of event order (first to last). This also confirms that events with large filtered volumes (event 2, 7, 8, and 13) corresponded with events with a substantial difference between influent and effluent phosphate load (i.e., removal).

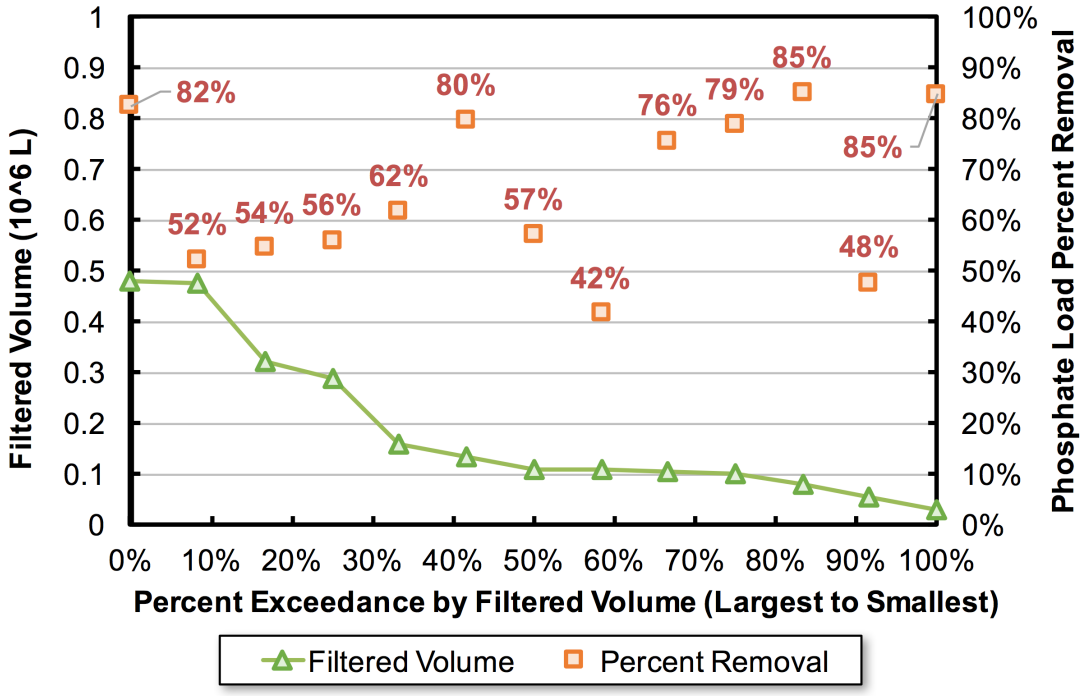

Figure 12. Filtered Volume and Phosphate Load Percent Removal by Percent Exceedance of Filtered Volume.

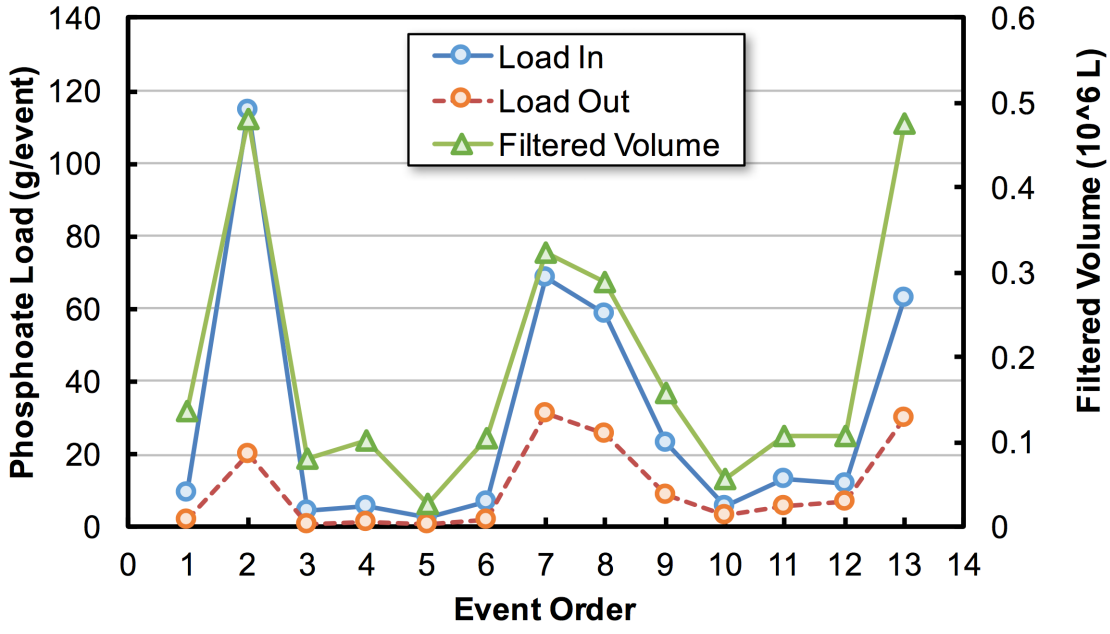

Figure 13. Traditional IESF Filtered Volume and Phosphate Load by Event Order.

Because the largest filtered volume events have higher loads than smaller filtered volume events, they have a greater impact on the overall phosphate load reduction. The largest event alone contributed nearly 30% of the total influent load (115 g of 388 g) and achieved 82% load reduction. Together, the four largest events produced over 78% of the total influent load (305 g of 388 g) and achieved a combined 64.9% load reduction. The overall phosphate load reduction was 64.5%, most of which can be attributed to the four largest events (out of 13 total).

4.2 Pond Perimeter Iron-Enhanced Sand Filter

The performance of the pond perimeter IESF was assessed by monitoring natural rainfall/runoff events for parts of each rainy season from 2013 through 2015. Data was compiled and separated (or grouped) into "events." The end of an event was indicated by the flow through the filter declining to zero or near zero. Altogether, the performance of the pond perimeter IESF was assessed for a total of 28 events (8 in 2013, 15 in 2014, and 5 in 2015).

Information regarding each of the monitored events is shown in Table 7. For events 3 through 6, valid rainfall data was not obtained due to rain gage errors. In these cases, rainfall daily amounts were obtained from other sources (e.g., Weather Underground; www.wunderground.com/) except for event 4 in which no data was available. Also, for event 25, more influent samples were collected by the sampler (24) than were recorded by the data logger (16). Because there was no method to determine which samples were the extra samples, the average phosphate concentration of all 24 bottles was used as the concentration of each of the 16 bottles recorded by the data logger and used in analysis. With an average influent concentration of the 24 bottles of 3.7 µg/L (range 2.0 to 6.2 µg/L) and a standard deviation of 0.7 µg/L, any error associated with this method was deemed acceptable.

Table 7. Pond Perimeter IESF Monitored events. Filtered volume is the measured flow that passed through the pond perimeter IESF. "-" = Not applicable

Rainfall Start	Rainfall depth [cm]	Filtered Volume [10^6 L]	Percent Exceedance by Filtered Volume	EMC IN [µg/L]	EMC OUT [µg/L]	EMC Reduction [%]	Load IN [g]	Load OUT [g]	Load Removal [%]
07/13/13	9.68	1.724	11%	125.2	57.2	54%	215.9	98.6	54%
Routine Maintenance: weeded & raked									
08/05/13	0.076	0.282	56%	11.7	147.5	-1163%	3.3	41.6	-1163%
08/06/13	0.71	0.155	74%	13.2	35.7	-170%	2.1	5.5	-170%
unknown	unknown	0.203	63%	11.5	108.3	-843%	2.3	22.0	-843%
09/19/13	0.61	0.144	78%	82.6	50.6	39%	11.9	7.3	39%
10/02/13	1.68	0.162	67%	11.5	24.7	-115%	1.9	4.0	-115%
10/14/13	2.59	0.546	44%	26.0	52.0	-100%	14.2	28.4	-100%
10/17/13	0.61	0.358	93%	32.3	26.4	18%	1.2	0.9	18%
2013 Totals	**16.0**	**3.252**	**-**	**77.7**	**64.1**	**18%**	**253**	**208**	**18%**
04/19/14	0.84	0.079	81%	8.1	46.2	-470%	0.6	3.7	-470%
04/23/14	11.4	4.241	4%	103.5	75.6	27%	438.8	320.6	27%
05/10/14	3.00	1.463	15%	58.5	38.8	34%	85.6	56.8	34%
05/19/14	1.93	0.635	41%	36.5	54.9	-50%	23.2	34.9	-50%
Routine Maintenance: weeded and raked									
05/27/14	0.28	0.075	85%	3.8	41.3	-981%	0.3	3.1	-981%
05/31/14	9.04	2.380	7%	110.7	63.2	43%	263.4	150.4	43%
06/07/14	1.85	0.543	48%	39.4	71.9	-83%	21.4	39.1	-83%
06/14/14	16.2	6.804	0%	79.2	54.0	32%	539.1	367.4	32%
06/28/14	3.73	0.856	30%	54.5	54.1	1%	46.7	46.3	1%
07/11/14	4.93	1.119	26%	15.8	28.7	-82%	17.7	32.1	-82%
Routine Maintenance: raked algae									
07/25/14	1.73	0.720	37%	10.0	29.2	-192%	7.2	21.0	-192%
Non-Routine Maintenance: raked, removed surface solids, broke up iron clumps									
08/17/14	3.53	0.835	33%	13.7	19.1	-39%	11.5	16.0	-39%
08/19/14	0.99	0.357	52%	16.4	13.1	20%	5.9	4.7	20%
09/10/14	0.25	0.040	89%	17.0	13.4	22%	0.7	0.5	22%
10/01/14	1.27	0.157	70%	42.8	29.7	31%	6.7	4.7	31%
2014 Totals	**61.0**	**20.306**	**-**	**72.3**	**54.2**	**25%**	**1469**	**1101**	**25%**
Routine Maintenance: weeded, broke up iron clumps									
06/17/15	0.15	0.005	100%	6.3	5.7	10%	0.034	0.031	10%
06/27/15	1.96	0.239	59%	3.7	20.0	-436%	0.9	4.8	-436%
06/29/15	0.43	0.027	96%	6.6	22.6	-243%	0.2	0.6	-243%
07/06/15	5.79	1.332	19%	35.6	22.0	38%	47.4	29.3	38%
07/12/15	4.19	1.195	22%	44.1	17.6	60%	52.7	21.1	60%
2015 Totals	**12.5**	**2.800**	**-**	**36.2**	**19.9**	**45%**	**101**	**56**	**45%**
Grand Totals	**89.48**	**26.358**	**-**	**69.1**	**51.2**	**26%**	**1823**	**1351**	**26%**

Table 7 lists the total load of phosphate in the influent and effluent for each event, for each year, and for the entire monitoring period along with the corresponding influent and effluent event mean concentration (EMC) and percentage of phosphate retained. Table 7 also shows, in time, when maintenance was performed on the filter and the kind of maintenance that was performed. Due to the assumption that the influent flow rate was

equal to the effluent flow rate (i.e., no infiltration), the percent phosphate retained as computed by EMC values and loads are identical (Erickson *et al.* 2013). Figure 14 shows the influent and effluent phosphate load as well as the filtered volume for the pond perimeter IESF as a function of event order (first to last), which corresponds to Table 7. As shown in Figure 14 and in Table 7, the four largest events (6/14/14, 4/23/14, 5/31/14, and 7/13/13) all achieved positive removal and contributed substantially to the overall performance of the pond perimeter filters.

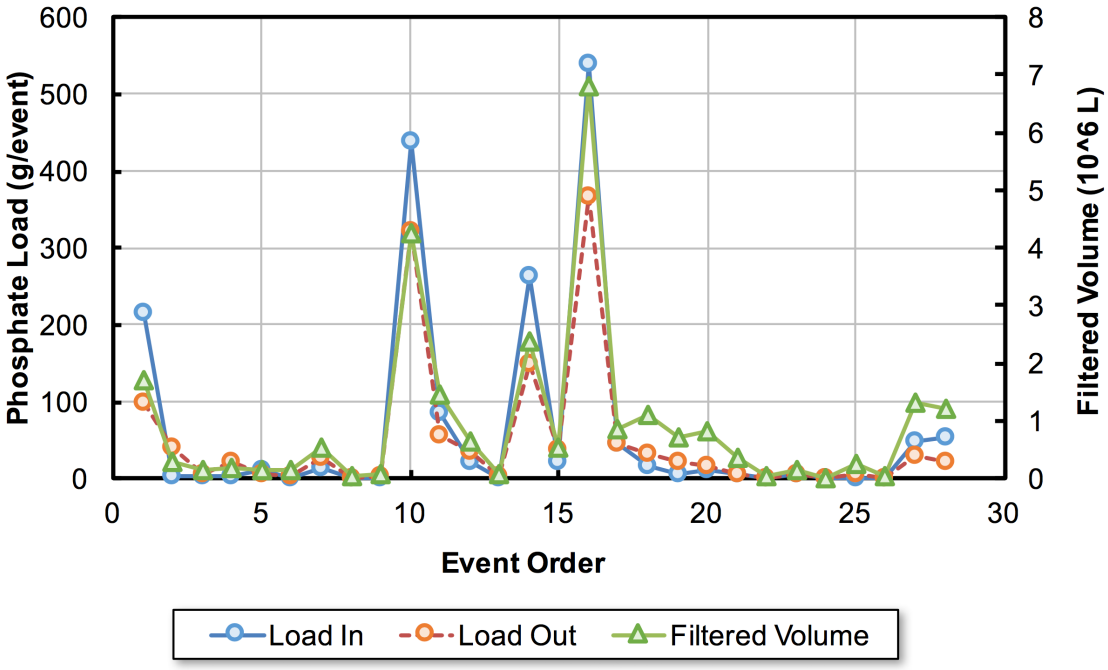

Figure 14. Pond Perimeter IESF Filtered Volume and Phosphate Load by Event Order.

As listed in Table 7, the percent phosphate retained in 2013, 2014, and 2015 was 18%, 25%, and 45%, respectively. It is also noteworthy that the average effluent EMC for the three years was 64.1, 54.2 and 19.9 µg/L, respectively. Half of the events (14 out of 28) were found to have negative removal (i.e., effluent loads > influent loads). Events with negative removal tended to be smaller events with low influent phosphate concentrations (3.7 – 39.4 µg/L). The negative removal is believed to be at least partially due to the accumulation of organic phosphorus in or on the filter media such that the degradation of this organic material (conversion of particulate phosphorus to soluble phosphate) caused

an unmeasured increase in the influent phosphate concentration. In other words, the influent samples did not accurately represent all sources of phosphate entering the IESF. Routine maintenance (Table 7) periodically removed this material, and this seems to have improved filter performance. More definite conclusions could not be made, however, because the relationship between maintenance and performance was not further investigated. Other than the accumulation of organic phosphorus, another possible explanation of negative removal is that equilibrium driving forces (i.e., concentration differences) caused phosphate to be released from the media at low concentrations and retained at high concentrations, but this effect has not been documented in any other IESF installation (Erickson *et al.* 2012) and is thus unlikely to have a significant impact on filter performance.

It should be noted that June 2014 was an unusually wet month that included frequent small storms with one large storm approximately equal to the 100-year return period (approximately 16.3-cm depth) on June 14, 2014. The frequent storms may have prevented the filter from drying and the large event could have led to atypical runoff characteristics. Beginning in July 2014 the filter began to infiltrate water at a much slower rate, presumably due to surface clogging.

5 Maintenance

As with any stormwater control measure, visual inspection and maintenance of IESFs is imperative if the practice is to remain functional and operate optimally for extended periods (Erickson *et al.* 2013). Routine maintenance occurs on a regular, relatively frequent schedule and non-routine maintenance occurs only as required by a change (often reduction) in performance, and thus occurs on an irregular, often infrequent schedule (Erickson *et al.* 2013).

5.1 Traditional Iron-Enhanced Sand Filter

The traditional IESF captures phosphate from agricultural drain tile, which has a low sediment concentration, so minimal sediment removal maintenance was required.

Vegetation and weeds, however, were removed 3 – 4 times per year. In addition, iron ochre developed on the surface of the traditional IESF, likely because the tile drainage had a measureable concentration of dissolved (ferrous) iron that was quickly oxidized by bacteria, which produce iron ochre as a waste product. Iron ochre was removed from the surface of the traditional IESF once per month or more. No other maintenance was necessary.

5.2 Pond Perimeter Iron-Enhanced Sand Filter

This study showed the necessity and impact of routine and non-routine maintenance on pond perimeter IESFs. Routine maintenance for this project included inspection, weeding, raking, and breaking up iron clumps. Non-routine maintenance was only performed once on this IESF trench between January 2011, when it was installed, and September 2015.

During runoff events, water carried duckweed, algae, and other vegetation from the pond to the filter. As water passed through the filter and water levels in the pond decreased, the vegetation was deposited on the filter surface. Routine maintenance was therefore undertaken to periodically remove the deposited vegetation from the filter surface. Routine maintenance activities also included removing vegetation (i.e., weeds) that were growing on the filter surface and raking the filter surface. Raking disturbed the surface of the filter to a depth of 2 – 7 cm with a metal rake. This broke through any minor "crust" of iron/sand, and allowed water to flow through the media. Raking, as opposed to removing by hand, was the most efficient means of removing smaller weeds from the filter surface. It is unclear from the data what effect routine maintenance had on the phosphate retention but field observations confirmed that routine maintenance preserved or restored adequate hydraulic (i.e., filtration rate) performance.

During the spring and early summer of 2014, the filter remained submerged for days following a rainfall/runoff event due to solids that had accumulated on or in the top portion of the filter media. These solids were in the form of duckweed and algae on the surface of the filter and a grey muck layer at or near the surface of the filter at some but not all locations. In some locations, the grey muck was observed up to 8 cm below the

surface. Thus, to improve flow through the filter, non-routine maintenance was performed in August 2014, which included scraping and removing algae from the filter surface, removing as much of the grey muck as possible, breaking up the sand media to a depth of 5 – 7 cm with metal rakes, and breaking up large clumps of iron shaving and sand conglomerates (some 30 cm or more in their longest dimension) with a sledgehammer. Iron clumps of this size tended to be isolated, relatively deep (10 – 20 cm below the surface), are less permeable, but scattered throughout the filter media and therefore likely had minimal impact on hydraulic performance. Iron clumps, however, may reduce iron-water contact because large particles have less contact area than smaller particles.

One of the primary purposes of this non-routine maintenance was to remove the grey muck that was observed near and just below the surface of the filter. It was hypothesized that the grey muck was gleyed sand, which is iron-rich sand that has been reduced to ferrous iron due to anaerobic conditions from prolonged water saturation. Gleyed soils exhibit a similar appearance and texture as the grey muck that was observed at (and removed from) the site. The grey muck may have also contained decomposing organic matter, which may have developed because of prolonged water saturation caused by the intense precipitation conditions observed in June 2014 (previously discussed). It is also possible that the grey muck was caused by the accumulation of fine organic material at or just under the surface of the filter from four previous rainy seasons. The grey muck has not been observed at any of the other 12 pond perimeter IESFs within the City of Prior Lake.

Permeable iron and sand clumping has been observed in this and other pond perimeter IESFs one or more years after construction. As occurred in this study, this tends to occur in IESFs that have been submerged for extended periods of time. The non-routine maintenance activities immediately improved hydraulic performance (i.e., increased filtration rates) and, after what appeared to be a rinse of the filter by the first runoff event after non-routine maintenance, improved phosphate retention.

6 Comparison of Practices

The traditional IESF retained significant amounts of phosphate for all events, including events with influent EMCs as low as 54 µg/L and 56 µg/L (85% and 79% retention, respectively). As described previously, plotting performance as a function of filtered volume percent exceedance (e.g., Figure 11) demonstrates the variation of performance for small storms compared to large storms. Large storms correspond to small values of percent exceedance because a small percentage of storm exceed the filtered volume of large events. Conversely, small storms correspond to large values of percent exceedance because a large percentage of storms exceed the filtered volume of small storms. When percent phosphate load removal is investigated as a function of the percent exceedance by filtered volume, the traditional IESF exhibited uniform phosphate retention rates from 50% to 80% for large events (small percent exceedance) and 40% to 85% for small events (large percent exceedance), as shown in Figure 12. The IESF was installed in October 2012, and it is estimated from nearby (8.7 km) airport data that approximately 250 cm of precipitation fell on the 7.7 ha watershed between construction and the end of the study period (December 2016). Assuming a runoff coefficient of 0.1 for the agricultural watershed, it can be assumed that approximately 19,250 m^3 of runoff flowed to the IESF. Dividing this volume by the surface area of the IESF (92.9 m^2) results in a depth treated of approximately 207 m. This is approaching the limits of known performance data (Erickson *et al.* 2007, 2012), where reduced performance may begin to become apparent.

The pond-perimeter IESF, however, exhibited a non-uniform performance trend. For large events with low percent exceedance values, retention rates are greater (i.e., 40 – 50%) than for small events with high percent exceedance values, for which retention rates are low and often negative (Table 7). The retention rates are substantially below the load-based average 71% removal of a pond-perimeter IESF that was monitored shortly after construction (Erickson and Gulliver 2010). The trend of the new pond-perimeter IESF reported by Erickson and Gulliver (2010) is similar to the traditional IESF in which low percent exceedance values had less percent retention than high percent exceedance values, but differs from the pond perimeter IESF investigated in this study. The volume of water

treated during this study on pond perimeter trenches divided by the IESF area results in 187 m of water measured and treated. The water treated in the two rainy seasons before the monitoring program started would increase this depth of water treated, resulting in the pond-perimeter being closer to the end of its useful life (Erickson *et al.* 2007) after four years.

The reason for these differences could be due to the differences in influent characteristics (i.e., high particulate phosphorus concentration), maintenance needs and actual maintenance frequency, load of phosphate already retained by the pond perimeter IESF, or release of phosphate from organic material on top of and in the filter. Low influent concentrations may result in water concentrations that are lower than that in equilibrium with the iron-bound or sediment-bound phosphate that has already been retained by the filter. This could cause a release of phosphate from the iron or sediment to the filtrating water. Thus, if the pond perimeter IESF had significantly higher amounts of phosphate retained (it has been in service for three years), there would be a greater possibility for phosphate release. Laboratory column studies with synthetic stormwater (Erickson *et al.* 2012) have indicated that an IESF with 5% iron filings by weight should retain greater than 70% of the phosphate after 180 m of treated water. However, when the five rainy seasons since construction of the pond-perimeter IESF are considered, it is apparent that much more than 180 m of water had been treated. The pond-perimeter IESF was thus undersized for the watershed. This could explain the relatively low performance of ~45% phosphate retention, even after non-routine maintenance. Another explanation for the reduced performance of the pond-perimeter filter before the non-routine maintenance is the filamentous algae that accumulated on the surface of the filter was degrading and releasing phosphate into the filter and effluent. The degradation could also have released small organic particles that moved through the filter and were further degraded in the filter. In this scenario, there would be an unmeasured source of phosphate on the surface and within the filter, which could distort the results. The authors believe that this latter explanation for the performance in 2013 and 2014 of the pond-perimeter IESF is the most likely.

Both the traditional IESF and the pond perimeter IESF captured phosphate, as illustrated by the cumulative phosphate load graphs shown in Figures 15 and 16. For both

IESFs, the cumulative load increases as percent exceedance increases, though the slope is larger for low percent exceedance values (large storms). For the traditional IESF, the four largest events (up to 25% exceedance) contributed most of the influent phosphate load (305 g out of 388 g total influent, 79%) and most of the phosphate removal (197 g out of 250 g total removed, 79%). The other nine events contributed 21% of the influent load (83 g) and 22% of the effluent load (30 g) and all event achieved positive removal (i.e., effluent loads < influent loads). Thus, the largest storms contributed most of influent load and contributed substantially to the overall performance. For the pond perimeter IESF, the four largest storms contributed most (1,457 g out of 1,823 g total influent, 80%) of the influent phosphate load, while the remaining 24 storms contributed approximately 20% of the influent phosphate load. The small storms, however, decreased the overall performance by contributing more effluent load (428 g out of 1365 g total effluent) than influent load (365 g out of 1,823 g total influent), which is attributed herein to an unmeasured source of phosphate on the surface of the IESF (degrading algae mat). Thus, for both IESFs the largest storms had the most load reduction in the overall performance.

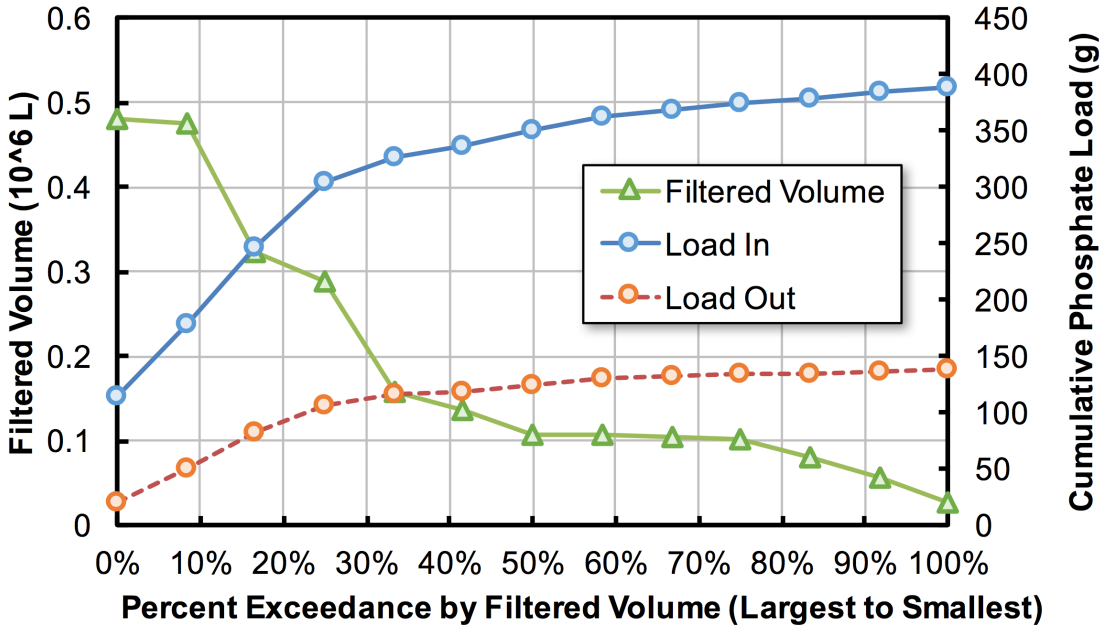

Figure 15. Traditional IESF Filtered Volume and Cumulative Phosphate Load by Percent Exceedance of Filtered Volume.

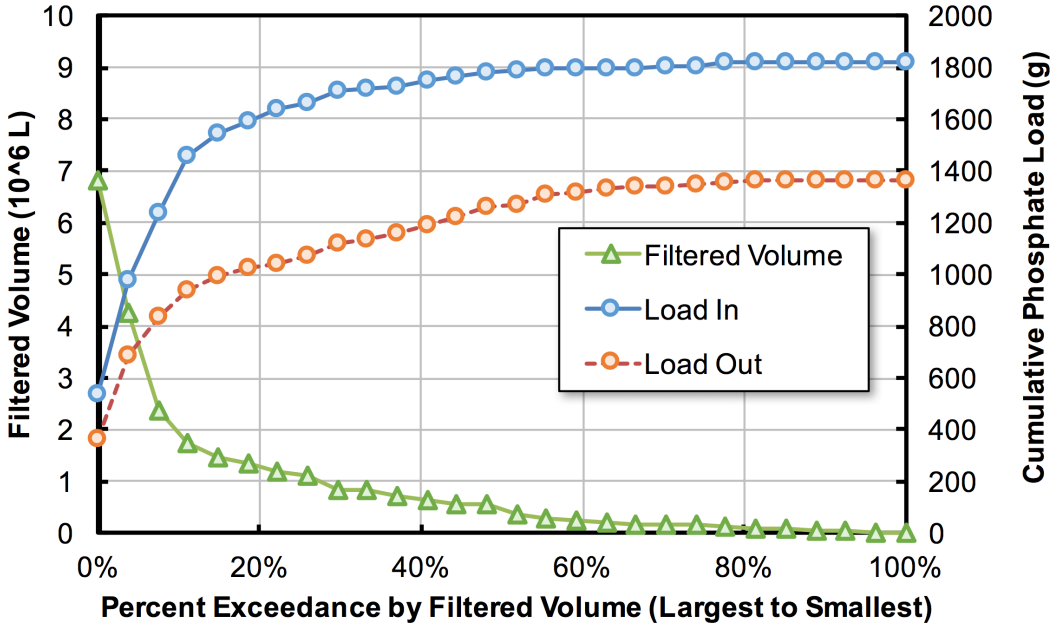

Figure 16.Pond Perimeter IESF Filtered Volume and Cumulative Phosphate Load by Percent Exceedance of Filtered Volume.

7 Lessons Learned

Two new field applications of iron enhanced sand filtration (IESF) were monitored over two or more rainy seasons to determine their performance with respect to phosphate retention. One application, a traditional IESF in an agricultural watershed, retained over 64% of the influent phosphate load while the second, a pond perimeter IESF in a developing suburban watershed, retained 26%. The retention rate of the traditional IESF was uniform as filtered volume increased whereas the pond perimeter IESF had higher retention rates for larger filtered volume events and negative removal for smaller filtered volume events. Non-routine maintenance improved the hydraulic performance of the pond perimeter IESF and, after a rinsing event, also improved phosphate retention rates to an average of 45%.

Overall, the traditional IESF seemed to perform better at removing phosphate from runoff. It is believed that there are two reasons for this difference in performance: First, the traditional IESF was treating runoff from drain tiles with a low particulate phosphorus

concentration (i.e., and large phosphate), while, the degrading mat of filamentous algae that was transported onto the surface of the pond-perimeter IESF created a source of phosphate that was not quantified. The design of pond-perimeter IESF should be altered so that filamentous algae do not accumulate on the filter surface, because it also created challenges in maintenance, in addition to performance degradation. Second, the pond perimeter IESF had treated a relatively large volume of water for its size, resulting in substantial flow-through in the filter within 5 years of operations. This is greater than anticipated for an IESF, and may have partially caused the reduction in performance.

Chapter 4: Phosphate Removal from Agricultural Tile Drainage with Iron Enhanced Sand[3]

Abstract: Can iron enhanced sand filtration capture total phosphorus and soluble phosphorus (phosphate) from agricultural tile drainage? A monitoring study measured the total phosphorus and phosphate capture performance of an iron enhanced sand filter (IESF) that was installed to treat agricultural tile drainage in Wright County, Minnesota, USA. Overall, for natural rainfall events that were monitored between June and November 2015 and again in 2016, the IESF captured 66% ± 7% (α = 0.05) of the influent total phosphorus mass (n = 21) and 64% ± 8% (α = 0.05) of the influent phosphate mass (n = 33). Removal of total phosphorus and phosphate was approximately uniform for large and small rainfall events and varied from 42% to 95% for total phosphorus and 9% to 87% for phosphate. The IESF treated 290 m of treated depth since installation, and results indicate that performance may be decreasing due to exhaustion of sorption media. Routine and non-routine maintenance was performed throughout the project to ensure adequate flow through the IESF and adequate performance. Detailed results, maintenance activities, design and operating & maintenance recommendations, and lessons learned are given within this chapter.

1 Introduction

Rainfall and snowmelt on urban or agricultural landscapes typically produces enough water to generate flow over the surface of the landscape, which is called stormwater runoff. In agricultural watersheds, there are often buried perforated pipes called drain tiles that collect soil moisture and discharge it downstream, which allows the soils to be farmed. This drain tile flow has quantitative characteristics such as volume and flow rate as well as

[3] A version of this chapter has been submitted for publication in Water, as Erickson, A.J., Gulliver, J.S., and Weiss, P.T. (2017a, submitted). "Phosphate Removal from Agricultural Tile Drainage with Iron Enhanced Sand." Water: Special Issue: Additives in Stormwater Filters for Enhanced Pollutant Removal. Water is an open-access journal, so permission is not required to reproduce the publication in this dissertation.

qualitative characteristics such as temperature, pH, and pollutant concentrations. One such pollutant of concern is phosphorus, which can be either particulate (> 0.45 μm in size) or soluble (< 0.45 μm). In stormwater runoff, drain tile flow, and surface water bodies, soluble phosphorus is most often in the form of phosphate (PO_4^{3-}) (Stumm and Morgan 1981). Though phosphate is often also known as dissolved phosphorus, soluble reactive phosphorus, and ortho-phosphorus, this chapter will use the term "phosphate" to describe the soluble reactive phase of phosphorus.

In agricultural watersheds, phosphate sources include natural organic matter, crop biodegradation, natural and synthetic fertilizers, livestock waste, among others. Phosphate is more bioavailable than particulate phosphorus (Sharpley *et al.* 1992), and thus typically limits biological growth in temperate non-marine surface water ecosystems (Aldridge and Ganf 2003, U.S. EPA 1999, Schindler 1977). When in excess, however, phosphate often generates nuisance algae blooms and eutrophic conditions in these ecosystems.

Sedimentation (i.e., particle settling) and filtration (i.e., sieving) are two mechanisms used by typical stormwater control measures (SCMs) such as wet ponds, dry ponds, and sand filters to capture particulate forms of phosphorus. Phosphate, however, is often not captured by most SCMs because a chemical or biological process is necessary to do so. For example, sand filters can capture approximately 80% of total suspended solids (Weiss *et al.* 2007), which primarily consists of particulates that can be captured by filtration. Particulate phosphorus will also be captured by sand filters, but only about 45% of the total phosphorus is captured (Weiss *et al.* 2007) because phosphate is allowed to pass through the sand filter with the water.

SCMs can be improved to capture soluble pollutants such as phosphate. Previous studies have found that adding metals such as steel wool or elemental iron to sand filter media resulted in the capture of a significant amount of phosphate (Erickson *et al.* 2007, 2012, 2015). As stormwater passes through the sand mixed with iron filter media, the elemental iron rusts to form iron oxides, which bind with phosphate via surface adsorption to remove phosphate from the stormwater. With this knowledge, Wright Soil and Water Conservation District (SWCD) of Minnesota installed an iron-enhanced sand filter (IESF) in 2012 to limit the phosphate load moving from the landscape into surface water bodies

within their jurisdiction. A drain tile from an agricultural field was intercepted and re-routed away from an existing ditch system and into the IESF. The performance of this IESF was then assessed by monitoring natural rainfall/discharge events for two rainy seasons. The main objectives of the study described in this chapter were to 1) assess the performance of a three- to four-year-old IESF with regards to the capture of total phosphorus and phosphate from agricultural drain tile flow, 2) investigate maintenance requirements, and 3) compare measured data to previously published performance of IESFs.

2 Materials and Methods

2.1 Site Location

This monitoring project was performed in Wright County, near the cities of Buffalo and Rockford, MN, USA. To protect the water quality of nearby lakes, Wright SWCD installed an IESF in 2012 to treat water from approximately 7.45 ha of farmland (90% corn and soybean crops and 10% pasture) that drains towards a shallow wetland and into a tile drainage system. Before 2012, the tile drain discharged into a ditch that carried the water a few hundred yards to a nearby lake.

An unknown portion of the watershed has random (not patterned) 20-cm diameter clay tile drainage with no surface inlets. The extent and quality of the clay tile is unknown. The extent to which the shallow wetland interacts with the tile drainage system is also unknown, and thus it is not known how the wetland hydrology and water quality may have affected the results of this study. The wetland is identified as a Palustrine, Emergent, Persistent, Temporary Flooded, and Farmed (PEM1Af) according to the Minnesota Department of Natural Resources National Wetland Inventory (MDNR 2017).

2.2 Iron-Enhanced Sand Filter Design

The iron enhanced sand filter (IESF) was designed with the filter media surface just below the natural topography. The intercepted drain tile discharges onto the surface of the IESF, and berms were installed around the IESF to provide storage volume up to

approximately 30 cm above the IESF surface. The berms also prevent overland flow from entering the IESF from the surrounding areas and the nearby ditch. A photo of the IESF shortly after construction is provided in Figure 17.

Figure 17. Site photo of Iron Enhanced Sand Filter (IESF) shortly after construction.

The IESF is approximately 6.1 m wide, 15.2 m long, 30 cm thick and contains 95% ASTM C-33 concrete sand (ASTM 2002) and 6% iron filings by weight. Below the IESF media is a layer of approximately 15 cm of pea gravel encompassing a 15-cm diameter PVC perforated pipe underdrain system designed to collect water after it filters through the media. This underdrain system consists of two longitudinally-oriented pipes along the length of the IESF (from inflow to outflow). This system connects to a single 20-cm diameter outlet pipe and to a vertical pipe extending above the IESF surface to allow for cleanout access and sample collection (white vertical pipe visible in Figure 17 and illustrated in Figure 18). The IESF is lined with an impermeable liner such that only water

that has been filtered by the IESF enters the underdrain system and water only enters the IESF through the top surface. After water is filtered by the media and collected by the underdrain system, it is routed through a 20-cm diameter solid pipe for roughly 61 m where it is discharged into the nearby ditch.

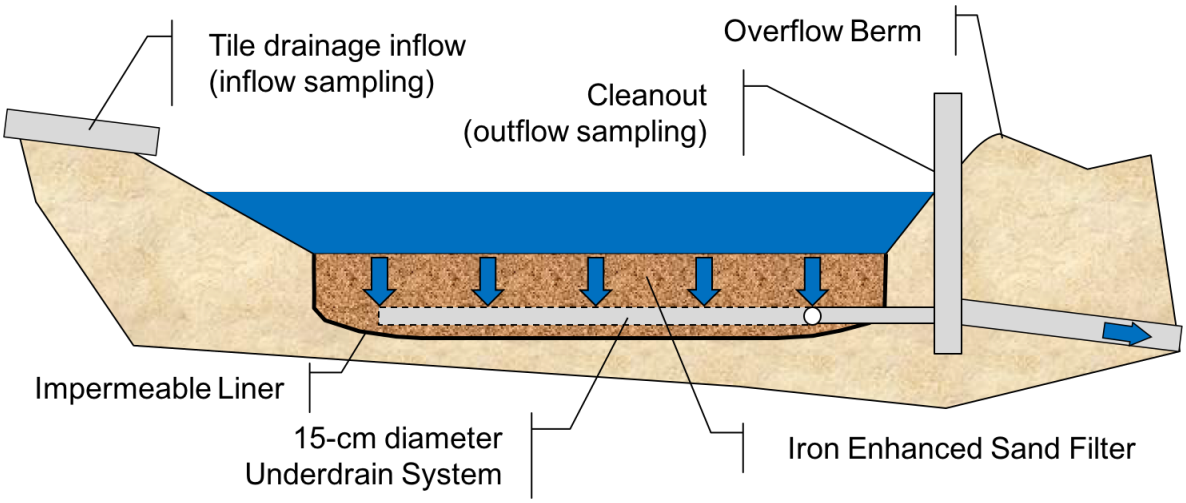

Figure 18. Iron enhanced sand filter (IESF) schematic.

Previous studies have recommended that IESF media must dry out between flow events to allow for continuous oxidation (i.e., rusting) of the iron particles, which creates more sorption sites (Erickson *et al.* 2007, 2012). For this site, this is achieved because the underdrain outlet is rarely submerged from downstream; allowing water to freely drain out by gravity and oxygen in the air to reach the bottom of the IESF media through the underdrains. When water is not standing on top of the IESF during or shortly after a rainfall event, air can also reach the surface of the IESF. In addition, the impermeable liner prevents adjacent groundwater from saturating the media between flow events.

2.3 Measurements

The total phosphorus and phosphate capture performance of the IESF was determined by monitoring natural rainfall events in 2015 and 2016. The parameters measured during the study included rainfall at the site, total flow volume, flow rate through the IESF, and total phosphorus and phosphate concentration in water samples collected

from the influent and effluent. For each monitored event, water samples were collected where the agricultural drain tile flow entered and exited the IESF. Rainfall and flow data were stored on a Campbell Scientific CR1000 data logger and were either downloaded directly from the data logger or transmitted by cellular modem (Sierra Wireless Raven XT model V2227-VD). Samples were collected by ISCO automatic samplers (described below) or manually as grab samples. All equipment was powered by two, 12-Volt deep cycle marine batteries located on site. Two Renogy 50-Watt, 12-Volt Polycrystalline Solar Panels and two Renogy Wanderer 30-Amp PWM Charge Controllers sufficiently recharged the deep cycle marine batteries between flow events. Rainfall was measured by a Texas Electronics model TR-525I tipping bucket rain gauge and air temperature was measure by an RM Young shielded air temperature sensor, both located at the site.

2.3.1 Flow Rate Measurement

Influent flow rate was not measured due to minimal elevation change, (i.e. low available head) that prevented the use of a weir or flume, and low velocity and flow rate values that prevented the use of a flow meter. Because the IESF has an impermeable liner, however, it was assumed that all water that entered the IESF from the surface would also exit through the underdrain collection system. Thus, outflow of the IESF was measured and assumed to be similar to the inflow.

The effluent flow rate was measured with a V-notch weir that was fabricated, calibrated, and installed within an Agri Drain flow control structure (20 cm pipe connection, 60 cm tall, 29.5 cm wide, 30 cm long; https://www.agridrain.com/). The Agri Drain structure was installed at the end of the 20-cm diameter discharge pipe that conveyed water downstream from the IESF's underdrain system. Measuring the flow rate near the discharge location allowed the maximum possible drop in elevation between the underdrains within the IESF and the weir crest within the Agri Drain. This minimized the potential for water backup into the underdrains and maximized the allowable water depth over the weir. Because backwater from the downstream culvert could affect flow over the weir, the water level upstream and downstream of the weir was measured using two separate Campbell Scientific CS450 pressure sensors. These sensors were fixed in

elevation and protected from debris by placing them within 2.5-cm PVC pipes. With the upstream and downstream water levels measured, the flow rate was calculated using Equation (7) (Franzini and Finnemore 1997, Villemonte 1947),

$$Q = \left(\frac{8}{15} C_{dv} \left[\tan\left(\frac{\theta}{2} \right) \right] \left(\sqrt{2g} \right) \left(H_1^{2.5} \right) \right) \left(1 - \left(\frac{H_2}{H_1} \right)^{1.5} \right)^{0.385} \quad (7)$$

where:

Q = discharge (m^3/s),

C_{dv} = weir discharge coefficient (C_{dv} = 0.601),

θ = angle of V-notch (38.9° = 0.680 rads),

g = acceleration of gravity (9.81 m/s^2),

H_1 = total upstream head (i.e., water depth) above the vertex of the V-notch (m)

H_2 = total downstream head (i.e., water depth) above the vertex of the V-notch (m).

The accuracy of Equation (7) was tested in the laboratory by measuring flow rate and comparing the measured value to the predicted flow rate based on Equation (7). The Root Mean Square Error for the use of Equation (7) to predict the measured flow data was found to be 0.22 L/s for 634 flow calibration measurements, up to a maximum of ~6 L/s. It can be noted that Equation (7) collapses to the V-notch equation (Franzini and Finnemore 1997) when the downstream head (H_2) becomes zero.

2.3.2 Water Sample Collection and Storage

Water samples were collected from within the pipe that discharged tile drainage water from the agricultural watershed onto the surface of the IESF, and were called influent samples. Water samples were also collected from a cleanout on the downstream end of the IESF where the underdrain system below the IESF connected to the outflow pipe, and were called effluent samples.

Two ISCO 6712 automatic water samplers were used to collect two individual flow-weighted composite samples, one from the influent and one from the effluent, for each monitored rainfall event. Sample collection began when rainfall exceeded a minimum

threshold of 0.05 cm and flow rate exceeded 0.28 L/s. For the calibrated weir equation provided in Equation (7), a flow rate of 0.28 L/s over the V-notch weir corresponds to a water depth of approximately 5 cm. Sampling continued until the flow rate decreased to below 0.28 L/s. During sampling, the automatic water samplers collected a subsample of 90 mL for every 5.66 m^3 of flow over the weir, and added the 90-mL subsample to the composite sample bottle stored within the sampler.

In most cases, automatically-collected water samples were retrieved from the site within 24-48 hours of the end of the sampling event and returned to the laboratory where a portion of each sample (typically three separate ~45 mL sub-samples) was immediately separated and labeled for total phosphorus analysis. Another portion (typically one ~45 mL sub-sample) was immediately filtered through a 0.45-micron filter in preparation for analysis of phosphate. Samples were frozen immediately after subsampling and 0.45-micron filtering if they could not be analyzed immediately.

Grab samples were also collected irregularly from the influent and effluent sampling locations by Wright SWCD staff, starting shortly after construction of the IESF in 2012 and continuing through 2017. These samples were collected and stored in 500 mL plastic bottles supplied by the analytical laboratory (RMB Laboratories, Inc.).

2.3.3 Water Sample Analysis

Grab samples were analyzed by RMB Laboratories, Inc. in Detroit Lakes, MN, USA. The analytes and associated analysis methods were as follows:

- Orthophosphate, as P (dissolved) (EPA 365.3)
- Phosphorus, Total as P (EPA 365.3)
- Iron (EPA 200.7)

Flow-weighted composite samples were analyzed at St. Anthony Falls Laboratory, Minneapolis, MN, USA. Total phosphorus analysis of water samples followed standard methods section 4500-P B5 - Persulfate Digestion method (APHA 1998) and phosphate concentrations of water samples were measured according to standard methods section 4500-P E - Ascorbic Acid (APHA 1998) with a minimum detection level of 10 μg P/L.

3 Results & Discussion

The performance of the IESF for capturing total phosphorus and phosphate from agricultural drain tile flow was assessed by monitoring natural rainfall/discharge events during 2015 and 2016. In addition, grab samples were collected from 2012 through 2017 to record the influent and effluent pollutant concentrations, though grab samples were not used to calculate performance. The results of grab sample collection and performance of the IESF based on monitoring is discussed in the following sections.

3.1 Grab Samples

Grab samples were collected by Wright SWCD beginning when the IESF was installed through the duration of the project. Several parameters were analyzed in the grab samples, though only iron, total phosphorus, and phosphate will be discussed here. Influent iron concentration varied from 120 µg/L to approximately 1,500 µg/L, and the iron concentration decreased when moving through the IESF (i.e., iron captured by the IESF), with effluent concentrations varying from below detection (50 µg/L) to approximately 410 µg/L. It is possible that iron is captured by the IESF because an ionic double layer develops. In this process, iron particles within the IESF would attract ions of opposing charge (negative charge, including phosphate), which would alter the surface charge of the iron particles. Iron ions in the influent water would then be attracted to these negatively charged ions, forming a double layer. Another possible explanation is the conversion of Ferrous (Fe^{2+}) dissolved iron to ferric (Fe^{3+}) particulate iron, which could be captured on the surface or within the iron media. This explanation is supported by the development of iron ochre on the surface of the IESF, which is a waste product from bacteria that oxidize dissolved minerals such as iron. Iron ochre was visible on the IESF as a rust colored sludge when wet and as a rust colored thin crust/cake when dry.

The concentration of total phosphorus in grab samples (Figure 19) decreased from influent to effluent through the IESF (i.e., total phosphorus capture) for nearly all samples collected. Total phosphorus decreased from an influent range of 73 to 577 µg/L (average = 227 ± 44 µg/L, $\alpha = 0.05$) down to an effluent range of 6 to 293 µg/L (average = 74 ± 22

µg/L, α = 0.05). One total phosphorus sample had an effluent concentration substantially larger than the other samples (3,120 µg/L on 15 Sep 2016), though it is unclear why this sample had a concentration of this magnitude, and the concentration was considered an outlier and removed from further analysis of the data set.

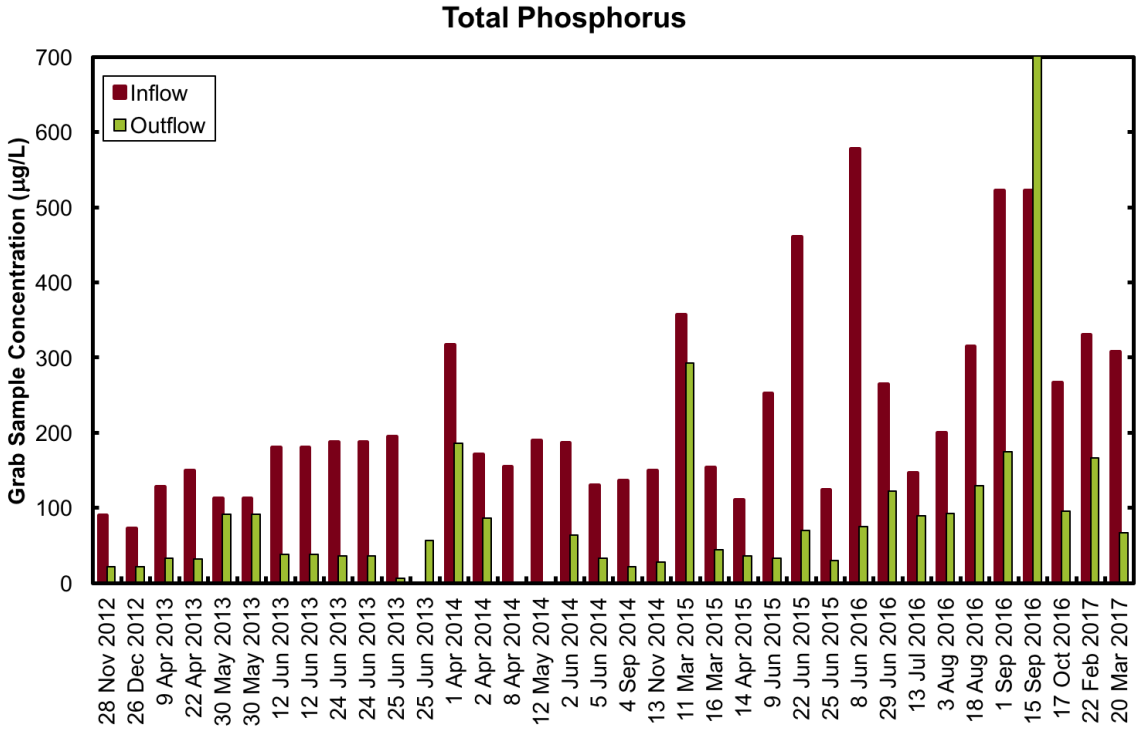

Figure 19. Grab sample data for total phosphorus.

From Figure 19 it appears that the influent and effluent total phosphorus concentration increased beginning with samples in 2014. As reported in Table 8, the average influent total phosphorus (TP) concentration increased from 145 ± 29 (α = 0.05) µg/L in 2012 – 2013 to 264 ± 59 (α = 0.05) µg/L in 2014 – 2017, which is approximately an 82% increase. The average effluent concentration increased by approximately 119% from 42 ± 16 (α = 0.05) µg/L in 2012 – 2013 to 92 ± 31 (α = 0.05) µg/L in 2014 – 2017. Influent phosphate samples varied in concentration from 30 to 329 µg/L and were reduced by the IESF to between 4 and 214 µg/L from 2012 to early 2017 (Figure 20). From Figure 20 it is apparent that the effluent phosphate concentration also increased beginning with

samples in 2014. As shown in Table 8, the average effluent concentration increased from 11 ± 3 (α = 0.05) µg/L in 2012 – 2013 to 67 ± 21 (α = 0.05) µg/L in 2014 – 2017. The influent concentrations were similar in each period with an average of 103 ± 15 (α = 0.05) µg/L in 2012 – 2013 compared to an average of 119 ± 30 (α = 0.05) µg/L for 2014 – 2017. It is possible that the increase in effluent concentration of both total phosphorus and phosphate is due to one or more of the following possible explanations, though none have been confirmed:

1) short-circuiting because of vegetation (harvested periodically) that create macropores from the surface to the underdrains,
2) the capacity of the IESF to capture phosphate had decreased.

Table 8. Influent and effluent total phosphorus (TP) and phosphate (PO_4) grab sample minimum, average ± 95% confidence interval, and maximum for 2012-2017.

	Influent (µg/L)		**Effluent (µg /L)**	
	2012-2013	**2014-2017**	**2012-2013**	**2014-2017**
TP Minimum	73	111	6	22
TP Average	145 ± 29	264 ± 59	42 ± 16	92 ± 31
TP Maximum	195	577	91	293
PO_4 Minimum	78	31	4	19
PO_4 Average	103 ± 15	119 ± 30	11 ± 3	67 ± 21
PO_4 Maximum	136	329	20	214

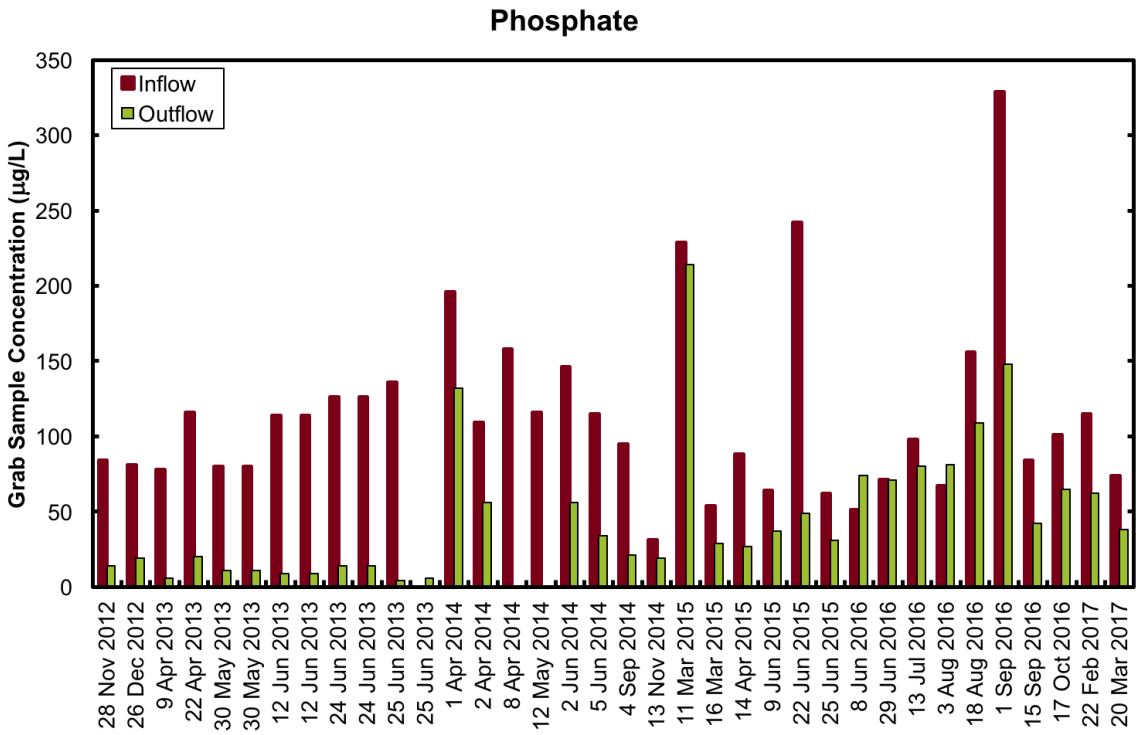

Figure 20. Grab sample data for phosphate.

3.2 Rainfall Event Performance and Continuous Monitoring

One goal of this section is to determine if this agricultural watershed is representative of the region. Monitoring natural rainfall events began on 26 June 2015 and continued until 20 November 2015. Monitoring equipment was removed for the winter and reinstalled on 14 May 2016 where it remained until 7 November 2016. It is important to note that several precipitation events occurred during December through May, outside the periods when monitoring equipment was installed, and are not discussed in this report.

For the periods in which monitoring equipment was installed, flow data were compiled and separated into "events" and "baseflow." As previously described in section 2.3.2 above, rainfall-induced events occurred when rainfall and flow rate exceeded preset thresholds. Any flow that occurred between events was considered baseflow. In addition, equipment failure occurred during some events and thus samples were not collected properly. For these events, the flow rate was considered "non-sampled rainfall event flow." For other events, equipment malfunction or extreme flow conditions resulted in flow rate

data that was unreliable. These events are not reported and considered "missed." Finally, total phosphorus was not measured in samples collected in 2015. With this grouping of events, the performance of the IESF was assessed for a total of 33 flow events (13 in 2015 and 20 in 2016). Of these events, rainfall was measured for 30 events (11 in 2015 and 19 in 2016), total phosphorus performance for 20 events (all in 2016), and phosphate performance for 31 events (13 in 2015 and 18 in 2016).

3.2.1 Rainfall and Flow Volume

Rainfall depth varied from 0.05 to 7.32 cm per event with an average of 2.23 ± 0.70 (α = 0.05) cm for 30 events. The average (2.23 cm) is greater than the median (1.82 cm) for the rainfall depth, which is also true for the rainfall duration, average rainfall intensity and flow volume because several large rainfall events skew the average towards larger values and many small events skew the median towards smaller values. Annual precipitation measured at a municipal airport (Buffalo, MN; KCFE) approximately 8.7 km northwest of the IESF was 53.7 cm for the 2015 water year (1 October 2014 – 30 September 2015) and was 82.4 cm for the 2016 water year (1 Oct 2015 – 30 Sept 2016). The total measured rainfall depth at the IESF site in 2015 was 29.97 cm and was 37.1 cm in 2016. These values are approximately 50% less than the average annual precipitation for south central Minnesota, USA because it excludes precipitation that occurred during non-sampled rainfall events and several snowmelt and rainfall events that occurred during December through May but were not measured as part of this project.

Flow volume varied from 28.2 to 487 m^3 with an average of 178.5 ± 48.4 (α = 0.05) m^3 per event. The total rainfall for 2015 and 2016 was 66.95 cm which produced a total drain tile flow volume of 5,891 m^3. Distributing this flow volume over the contributing watershed (~7.45 ha of crop and pasture) results in a drain tile flow depth of approximately 7.91 cm, which corresponds to a drain tile flow "runoff coefficient" of approximately 0.12. This drain tile flow "runoff coefficient" simply represents the approximate ratio of drain file flow volume to rainfall volume.

The total flow volume for 2015 was 2,451 m^3, which corresponds to approximately 3.29 cm of drain tile flow and a "runoff coefficient" of 0.11. As reported in Table 9, these values can be compared to values from the IESF in 2016 and several sites that are part of the Discovery Farms Minnesota program (https://discoveryfarmsmn.org/). For this comparison, monthly data from the Discovery Farms sites were summed to estimate total rainfall depth, drain tile flow depth, and "runoff coefficient" for June through November in each year reported by Discovery Farms Minnesota (DFM). One DFM site is located in Wright County and is approximately 35.4 km southwest of the IESF studied in this project. DFM data reported in Table 9 are average values from six years of measurements at nine different sites, including the site in Wright County.

Table 9. Rainfall Depth, Drain Tile Flow, and "Runoff Coefficient" for June through November. IESF is the iron enhanced sand filter studied in this report. Measurements at IESF in 2015 and 2016. Measurements at Discovery Farms Minnesota (DFM) sites averaged over six years (2011 - 2016).

	Rainfall Depth [cm]	**Drain Tile Flow [cm]**	**"Runoff Coefficient"**
IESF (2015)	29.97	3.30	0.11
IESF (2016)	37.08	4.62	0.125
DFM: 9 Sites (2011 – 2016)	40.92	5.11	0.125
DFM: Wright County Site (2011 – 2016)	46.84	3.05	0.065

As shown in Table 9, the rainfall depth at the IESF site was less than the average rainfall measured at the DFM sites because equipment failure at the IESF site prevented measurement of some rainfall events during the monitoring period of June through November in both 2015 and 2016. The drain tile flow depth measured at the IESF was also less than the nine DFM sites, but approximately the same as the average drain tile flow depth reported by the Wright County DFM site. The drain tile flow "runoff coefficient" for the IESF was similar to the average "runoff coefficient" measured at the nine DFM sites, suggesting that even though some rainfall events were unmeasured at the IESF site, the drain tile flow characteristics for the events that were measured are similar to other

agricultural sites in a similar climate that are measured year-round and over several continuous years (2011 – 2016).

The rainfall depth and drain tile flow depth for the IESF site, nine DFM sites, and the Wright County DFM site for June through November are also shown in Figure 21. The IESF data are consistent with the best-fit linear regression of the DFM data, further suggesting that drain tile flow characteristics of the IESF site are consistent with other agricultural sites in a similar climate for the time period between 2011 and 2016. When compared directly to the Wright County DFM site, the IESF site exhibited similar drain tile flow depth but less rainfall depth and thus a larger drain tile flow "runoff coefficient."

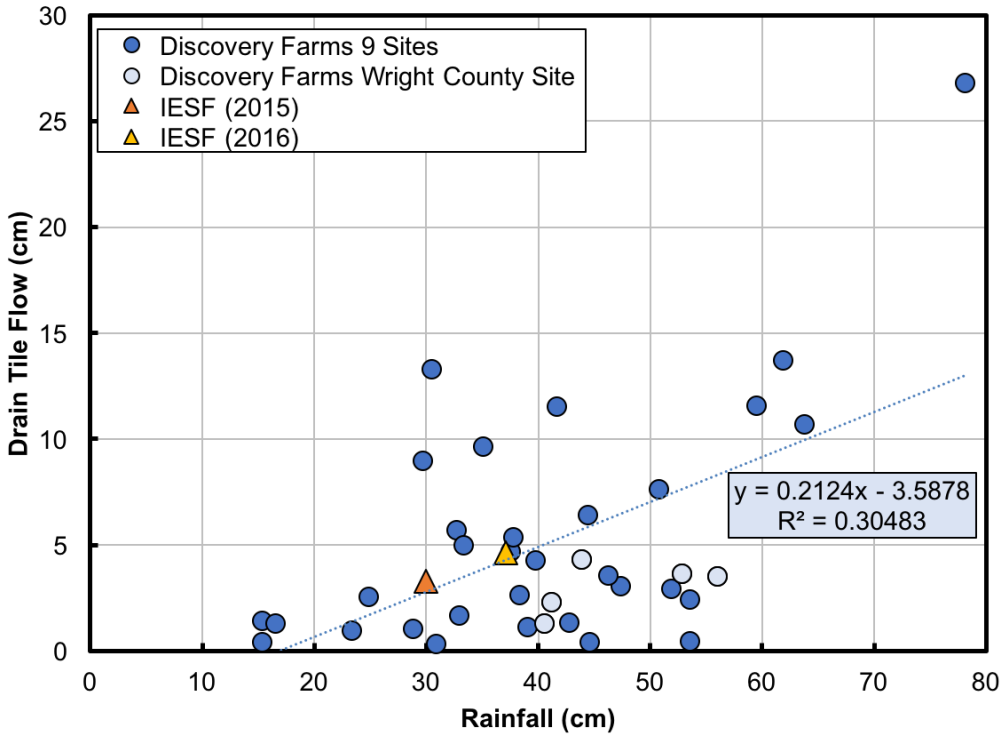

Figure 21. Total drain tile flow depth vs. total rainfall depth for June through November. IESF is the iron enhanced sand filter studied in this report. Measurements at IESF in 2015 and 2016. Measurements at Discovery Farms Sites averaged over six years (2011 - 2016).

3.2.2 Rainfall-induced flow vs. Baseflow

Urban watersheds typically produce runoff in response to rainfall events within a few minutes to a few hours, and runoff typically persists for a few hours to a few days. By contrast, agricultural watersheds can produce drain tile flow whenever there is excess soil moisture. As a result, this project measured drain tile flow near-continuously when monitoring equipment was operational at the site. It is unclear whether this is typical at this site, or if rainfall and runoff characteristics for 2015 and 2016 were unusual. It is also unclear if or to what extent the upstream wetland affected the flow conditions during the monitoring study.

Flow data were separated into rainfall event flow and baseflow, as described in section 3.2 above. In 2015, several rainfall events were not captured by the monitoring equipment due to equipment failure, excessive downstream flooding, interference from frogs and/or other animals, among others. Despite this loss of data, approximately 3,167 m^3 of flow was measured through the IESF from 26 June to 20 November 2015. Of this flow, approximately 2,489 m^3 was rainfall event flow in which samples were collected, approximately 221 m^3 was non-sampled rainfall event flow, and approximately 457 m^3 was baseflow. This corresponds to approximately 86% rainfall event flow (7% non-sampled) and 14% baseflow.

Equipment failure, flow exceeding the calibration range, and a vehicular collision with the Agri Drain unit contributed to loss of data during the 2016 monitoring season. However, approximately 6,388 m^3 of flow was measured through the IESF from 14 May to 7 November 2016. Of this flow, approximately 3,653 m^3 was sampled rainfall event flow, 2,282 m^3 was non-sampled rainfall event flow, and approximately 454 m^3 was baseflow. This corresponds to approximately 93% rainfall event flow (36% non-sampled) and 7% baseflow.

Overall, approximately 9,555 m^3 of flow was measured through the IESF in 2015 and 2016. Of this, approximately 6,142 m^3 was sampled rainfall event flow, 2,503 m^3 was non-sampled rainfall event flow, and approximately 910 m^3 was baseflow, which corresponds to 90% rainfall event flow (26% non-sampled) and 10% baseflow.

Approximately twice as much flow was measured in 2016 compared to 2015, though the baseflow amount was nearly identical (457 m^3 in 2015 vs. 454 m^3 in 2016). This is expected because the increase in total flow is in response to more rainfall event flow.

3.2.3 Total Phosphorus

Summary statistics for total phosphorus are shown in Table 10 and Figure 22. The concentration of flow-weighted composite samples is equivalent to the event mean concentration (EMC) (Erickson *et al.* 2013). Analysis of flow-weighted composite samples collected as part of this project revealed that the influent total phosphorus EMC varied from 138 to 1,516 µg/L with a flow-weighted average EMC of 370 ± 168 (α = 0.05) µg/L. The flow-weighted average EMC is equivalent to the total influent load (e.g., 1,273 g) divided by the total flow volume (5,891 m^3) for all the rainfall events. Capture of total phosphorus within the IESF is the combination of particulate phosphorus captured on the surface of the IESF and capture of phosphate within the IESF media through a sorption reaction with iron. As a result, the effluent EMC varied from 56 to 343 µg/L with a flow-weighted average EMC of 125 ± 30 (α = 0.05) µg/L. The total phosphorus capture performance can be expressed as the percent reduction in load between the influent and effluent (Erickson *et al.* 2013). Thus, the total phosphorus load decreased by 66.3% ± 6.7% (α = 0.05) from an average of 63.7 ± 22.1 g in the influent to 21.5 ± 9.6 g in the effluent.

Table 10. Total phosphorus summary statistics. NOTE: ± 95% confidence interval; "-" = Not applicable

	EMC IN [µg/L]	EMC OUT [µg/L]	Load IN [g]	Load OUT [g]	Load Capture [%]
Minimum[1]	138.4	56.4	6.3	2.6	42%
Average	-	-	63.7 ± 22.1	21.5 ± 9.6	-
Flow-Weighted Average	370.3 ± 167.8	124.7 ± 30.5	-	-	-
Maximum[1]	1,516	342.5	178.3	86.0	95%
Count	20	20	20	20	20
Total	-	-	1,274	429	-
Load Capture Efficiency	-	-	-	-	66.3% ± 6.7%

[1] *NOTE: Minimum and maximum values were calculated for all rainfall events, and are independent of min and max values for other parameters. For example, the minimum Load IN for all events was 6.3 g (occurred on 10 July 2016); the minimum Load OUT was 2.6 g (also occurred on 10 July 2016), and the minimum Load Capture for all events was 42% (occurred on 16 October 2016).*

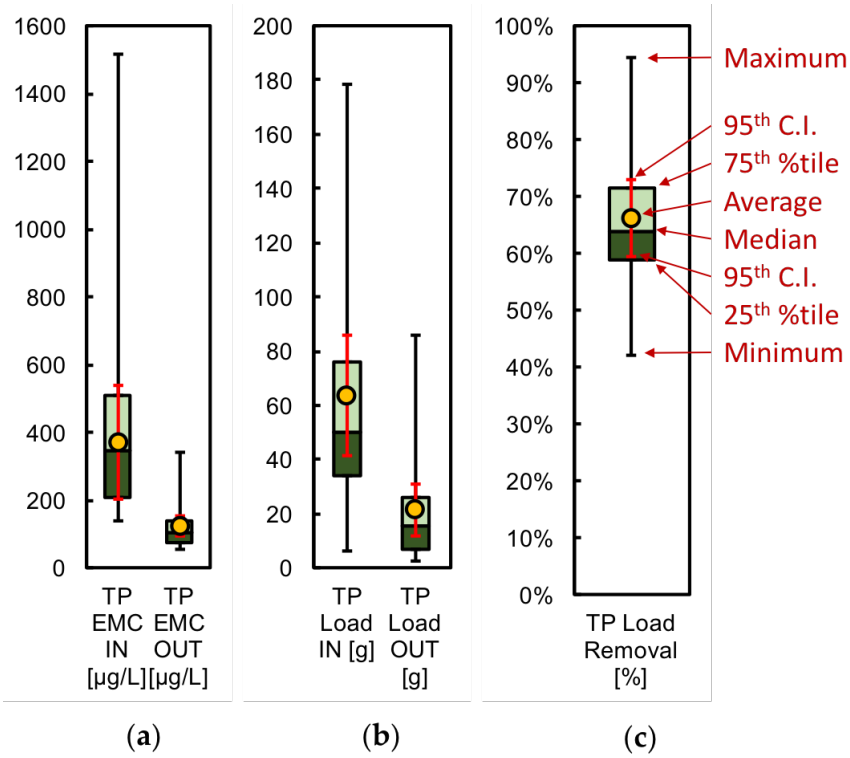

Figure 22. Total phosphorus (TP) statistics for n = 20 events in 2016 for (a) influent (IN) and effluent (OUT) EMC, (b) influent (IN) and effluent (OUT) load, and (c) load capture (%). Note: %tile = Percentile and C.I. = Confidence Interval

Flow volume, total phosphorus EMC and load for each event in 2016 are shown in Figure 23 and Figure 24. All events exhibited positive total phosphorus capture (i.e., effluent EMC < influent EMC). Two events had influent EMCs greater than 1000 µg/L, but most events had influent EMCs between 200 and 800 µg/L. By contrast, only one event had an effluent EMC greater than 200 µg/L and approximately half of the events (9 out of 20) had effluent EMCs less than 100 µg/L for total phosphorus.

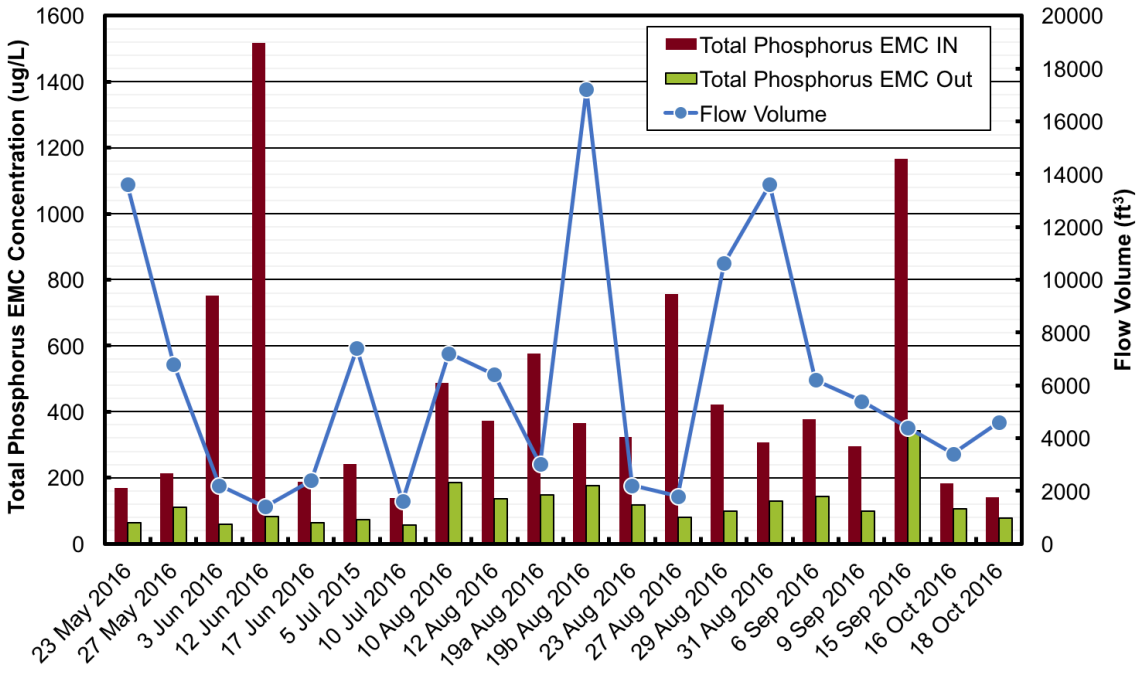

Figure 23. Flow volume, total phosphorus EMC influent and effluent for 2016.

The total phosphorus load reduction for each event varied from 42% to 95% for 20 events with an overall total phosphorus load reduction of 66.3% ± 6.7% (α = 0.05). A substantial portion of the influent total phosphorus load (323.6 grams, 25%) was contributed by two events: 19b Aug 2016 (178.3 grams) and 15 Sep 2016 (145.3 grams), as shown in Figure 24. These two events contributed approximately 17.8% of the flow in 2016. Three other events each contributed between 100 and 130 grams of total phosphorus load, which accounts for approximately 344.6 grams (27%) of the overall influent total phosphorus load and 26% of the flow volume (31,430 ft^3). Thus, five of the 20 events

(25%) contributed approximately 52.5% of the influent total phosphorus load and 43.7% of the flow volume. This shows that a relatively small number of large events contributed most of the total phosphorus load and flow volume.

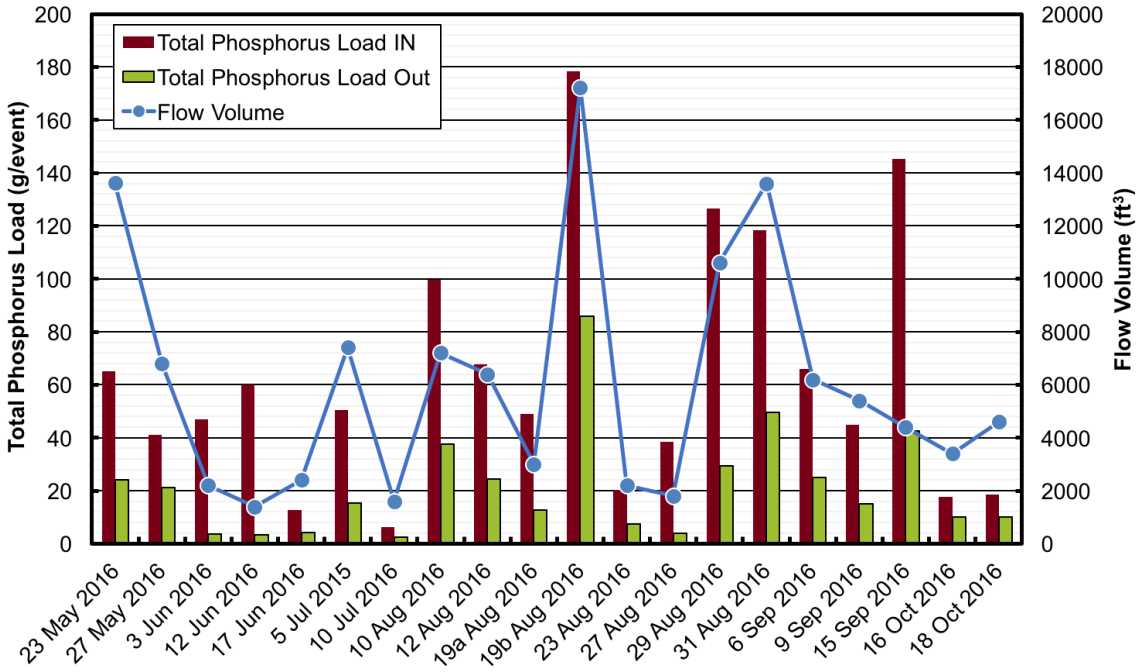

Figure 24. Flow volume, total phosphorus influent and effluent load for 2016.

Total phosphorus was not measured in samples from 2015, but the total phosphorus influent load for all 2016 events was 1,273.6 grams (Table 10). If this load is attributed to the entire 7.45-ha contributing watershed, the total phosphorus load per land area is approximately 171 grams per ha (g/ha). This load only represents load from flows between June and November 2016, and excludes any load that may have been contributed by non-sampled events and events prior to June 2016 and after November 2016. Thus, the 2016 water year (October 2015 - September 2016) total phosphorus load for the IESF site is expected to be greater than 171 g/ha. By comparison, ten Discovery Farms Minnesota (DFM) sites reported total phosphorus loads for the entire 2016 water year ranging from 11.2 to 157 g/ha for tile drainage flow (DFM 2016). The IESF site appears to be contributing more total phosphorus load per area in tile drain flow than the DFM sites.

3.2.4 Phosphate

Summary statistics for phosphate are shown in Table 11 and Figure 25. The influent total phosphorus EMC varied from 18 to 358 µg/L with a flow-weighted average EMC of 162 ± 33 (α = 0.05) µg/L. All events exhibited positive capture (i.e., effluent EMC < influent EMC) of phosphate, likely due to chemical reactions between the iron oxide surfaces in the IESF and phosphate in the water. As the iron rusts and becomes iron oxide, phosphate can sorb to the surface of the iron oxide and become captured within the IESF. As a result, the effluent EMC varied from 8 to 127 µg/L with a flow-weighted average EMC of 57 ± 13 (α = 0.05) µg/L, and the phosphate load decreased by 63.9% ± 7.7% (α = 0.05) from an average of 30.8 ± 13.9 g in the influent to 11.1 ± 5.1 g in the effluent.

Table 11. Phosphate summary statistics. NOTE: ± 95% confidence interval; "-" = Not applicable

	EMC IN [µg/L]	**EMC OUT [µg/L]**	**Load IN [g]**	**Load OUT [g]**	**Load Capture [%]**
Minimum[1]	18.3	8.1	2.8	0.4	9%
Average	-	-	30.8 ± 13.9	11.1 ± 5.1	-
Flow-Weighted Average	162.3 ± 33.4	58.6 ± 12.7	-	-	-
Maximum[1]	358.3	126.6	157.0	61.7	87%
Count	31	31	31	31	31
Totals	-	-	956.1	345.1	-
Load Capture Efficiency	-	-	-	-	63.9% ± 7.7%

[1] *NOTE: Minimum and maximum values were calculated for all rainfall events, and are independent of min and max values for other parameters. For example, the minimum Load IN for all events was 6.3 g (occurred on 10 July 2016); the minimum Load OUT was 2.6 g (also occurred on 10 July 2016), and the minimum Load Capture for all events was 42% (occurred on 16 October 2016).*

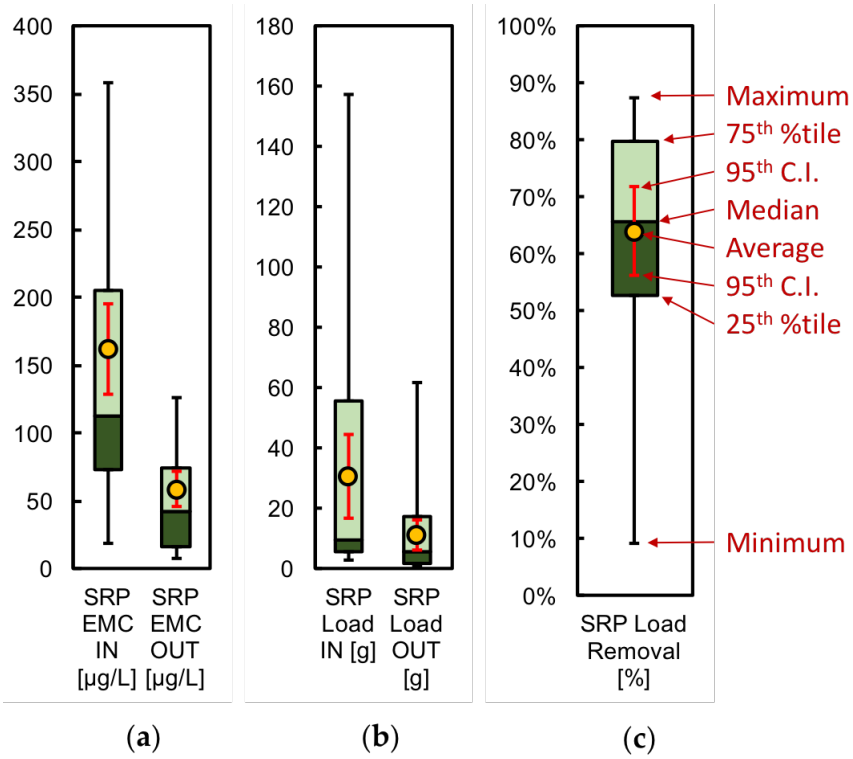

Figure 25. Phosphate (SRP) statistics for n = 31 events in 2015 and 2016 for (a) influent (IN) and effluent (OUT) EMC, (b) influent (IN) and effluent (OUT) load, and (c) load capture (%). Note: %tile = Percentile and C.I. = Confidence Interval

Flow volume, phosphate EMC and load for each event in 2015 and 2016 are shown in Figure 26 and Figure 27. While the influent phosphate EMC for most events in 2015 were less than 150 µg/L (Figure 26), the influent EMC for several events in 2016 were 200 – 350 µg/L. Thus, the influent EMCs appear to increase from 2015 to 2016. The effluent EMCs, however, were less than 70 µg/L for most events in 2015 and less than 50 µg/L for more than half of the events (10 out of 18) in. This reveals that the influent phosphate EMCs increased from 2015 to 2016, but the effluent EMCs were nearly the same.

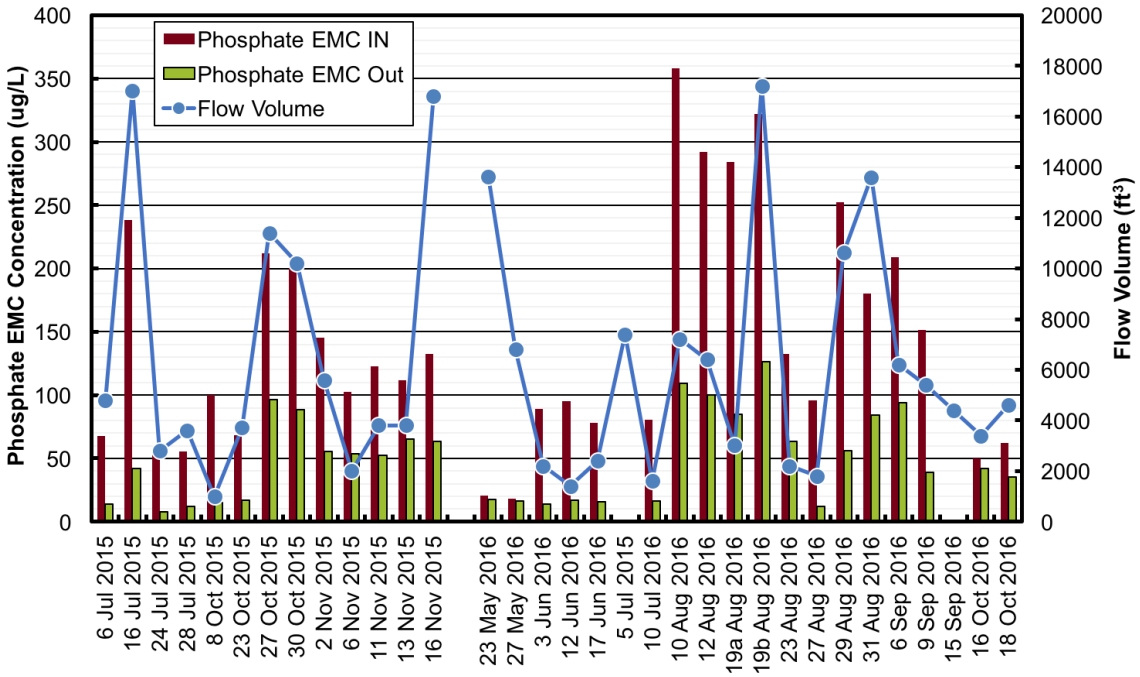

Figure 26. Flow volume, phosphate EMC influent and effluent for 2015 and 2016.

The IESF captured a fraction of the phosphate load for all events during the 2015 and 2016 monitoring seasons. The influent phosphate load varied from 2.8 to 157 grams per event with an average load of 31 ± 14 (α = 0.05) grams per event and a total influent load of 956.1 grams. The effluent load varied from 0.4 to 61.7 grams per event with a flow-weighted average of 15.6 (α = 0.05) grams per event and a total effluent load of 345.1 grams. The load reduction for each event varied from 9% to 87% for 31 events with an overall phosphate load reduction of 63.9% ± 7.7% (α = 0.05).

The influent phosphate load for all events in 2015 and 2016 was 956.1 grams (Table 11). A substantial portion of that load (271.9 grams, 28%) was contributed by two events: 19b Aug 2016 (157 grams) and 16 Jul 2015 (114.8 g), as shown in Figure 27. These two events only contributed 16.5% of the flow volume (34,230 ft^3). Seven other events each contributed between 50 and 80 grams of phosphate load in 2015 and 2016, which accounts for approximately 461 grams (48%) of the overall influent phosphate load and 36.7% of the flow volume (76,257 ft^3). Thus, nine of the 31 events (29%) contributed approximately 76.7% of the influent phosphate load and 53.1% of the flow volume. This shows that a

relatively small number of large events contributed most the phosphate load and flow volume.

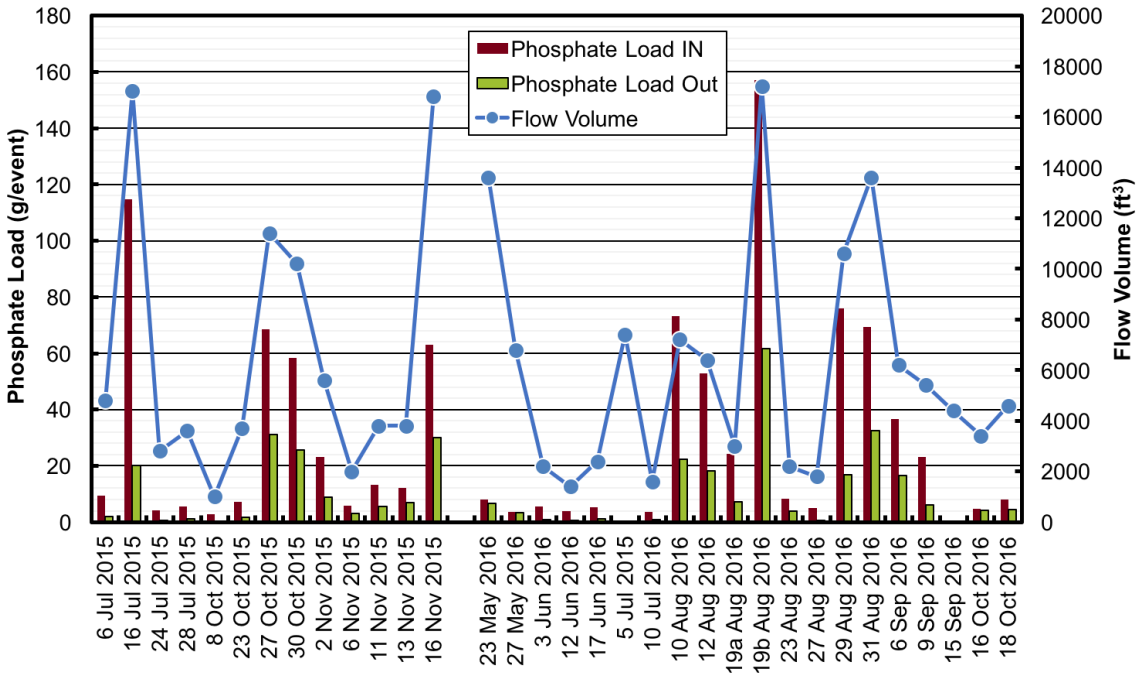

Figure 27. Flow volume, phosphate influent and effluent load for 2015 and 2016.

3.3 Soluble Fraction

A pollutant can either exist in soluble phase (e.g., molecule) or in particulate phase (e.g., sand grain). The total concentration is the sum of the soluble concentration and particulate concentration, where the soluble portion is defined as smaller than 0.45 µm (APHA 1998). From this, the soluble fraction can be calculated by dividing the soluble concentration by the total concentration. Stormwater runoff from nationwide highways and urban areas, on average, has 30 – 45% soluble and 55 – 75% particulate phosphorus (Kayhanian *et al.* 2007, Pitt *et al.* 2005), but the soluble fraction ranges from 3 – 100% (Erickson *et al.* 2007).

When evaluating performance of a stormwater control measure such as the IESF studied in this project, calculating the soluble fraction can provide insight into the relative performance of the different treatment mechanisms. For sand filters, a portion of the

particulates are captured by physical sieving on the surface and within the media of the filter. The IESF will also capture a portion of the soluble phase of phosphorus (phosphate) through reaction with the iron.

Figure 28 shows summary statistics of the soluble fraction in percent for both the rainfall event samples and grab samples collected throughout this project. For the rainfall event samples (Figure 28a), the influent soluble fraction varied from approximately 5% to 90%, with an average of 43.2% ± 12.6% ($\alpha = 0.05$), which is similar to values measured in urban stormwater (Erickson *et al.* 2007, 2012). The effluent varied from approximately 15% to 75% with an average of 43.5% ± 10.0% ($\alpha = 0.05$). For comparison, nine Discovery Farms Minnesota (DFM) sites reported an average of 60% soluble fraction for tile drainage flow samples collected between 2011 and 2016. This higher soluble fraction is expected because drain tile flow has already been filtered by the soil. For unknown reasons, the 2015 – 2016 influent to the IESF had an unusually high percentage of particulate phosphorus.

Performance data previously discussed in section 3.2 show that phosphate and total phosphorus were captured by the IESF. It is likely that both particulate and soluble phosphorus (phosphate) were captured by the IESF and it is also likely that this occurred at approximately the same rate because 1) the IESF showed positive capture of soluble and total phosphorus, 2) the average soluble fraction of influent and effluent were similar (i.e., 43 and 44%, respectively), and 3) the variability in soluble fraction decreased from the influent to the effluent. Relative to sand filters in urban settings, the particulate phosphorus capture performance is low, likely due to the smaller size of particulates in the agricultural drain tile flow.

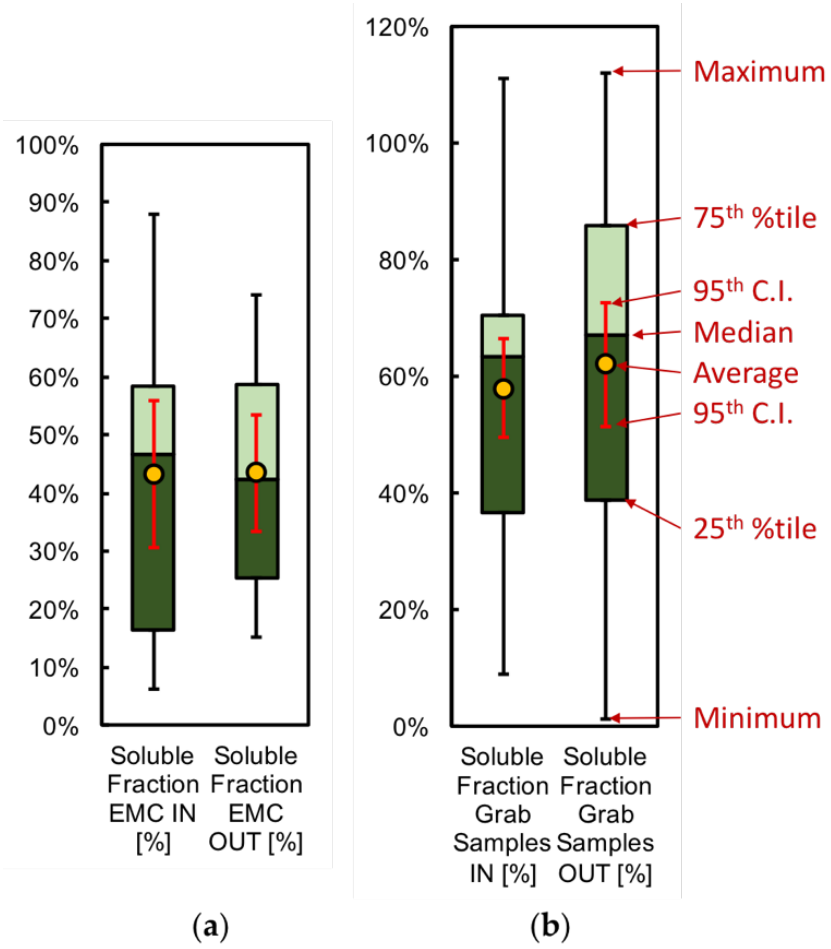

Figure 28. Soluble phosphorus fraction = phosphate / total concentration of (a) rainfall event sample data for n = 18 influent (IN) and effluent (OUT) events in 2016 and (b) grab sample data for n = 35 influent (IN) events and n = 33 effluent (OUT) events from 28 Nov 2012 – 20 Mar 2017. Note: %tile = Percentile and C.I. = Confidence Interval

When considering the grab sample data (Figure 28b), the soluble fraction varied from approximately 10% to 110% in the influent with an average of 58% ± 8% ($\alpha = 0.05$). The effluent grab sample soluble fraction varied from approximately 1% to 110% with an average of 62% ± 10% ($\alpha = 0.05$). The reason the soluble fraction in some grab samples was greater than 100% was because the measured soluble (phosphate) concentration was greater than the measured total concentration. There is no physical explanation for this condition, and it is attributed to the time lag that exists between similar inflow and outflow volumes, which is not accurately sampled in instantaneous grab samples, or measurement

error as reported from the laboratory. The soluble fraction of the grab samples is higher than the monitored data, which could be due to the fact that grab samples ignore the high peaks in the runoff, when a greater particle concentration may be present in the drain tile flow. Despite the possible uncertainty in these measurements, the soluble fraction of the grab samples collected through this project (58% influent, 62% effluent) is similar to the average of 60% soluble fraction for tile drainage flow samples from nine DFM sites collected between 2011 and 2016.

3.4 Hydraulic and Phosphate Loading Rate

A common metric for understanding the longevity of IESFs is the depth of water treated (Erickson *et al.* 2007, 2012). This depth represents the amount of water that has passed through the IESF since its construction, and indirectly represents the amount of phosphate that has been captured by the IESF. To calculate the treated depth, the total volume of water treated by the IESF from the time it was constructed is divided by its surface area. The total volume of water treated can be estimated from the hydraulic loading rate, historical rainfall and flow data, computer modeling of hydrologic processes, or some combination thereof.

The IESF in this study was constructed around October 30, 2012. Rainfall and flow data were not collected at the IESF until June 2015 and is thus unknown. Rainfall, however, is measured at a municipal airport (Buffalo, Minnesota, USA; KCFE) approximately 8.7 km northwest of the IESF. The rainfall data measured at KCFE was correlated ($R^2 = 0.869$) to the rainfall data measured at the IESF during this project, as shown in Figure 29 and given by Equation (8),

$$Rain_{IESF} = 1.1875\left[Rain_{KCFE} \right] \tag{8}$$

where:

$Rain_{IESF}$ = precipitation measured at the IESF site,

$Rain_{KCFE}$ = precipitation measured at the Buffalo Municipal Airport (KCFE)

Using Equation (8), the precipitation at the IESF can be predicted from historical rainfall data at KCFE for the periods when precipitation was not measured at the IESF. Approximately 253.6 cm of precipitation fell at KCFE between 30 October 2012 and 18 October 2016, which can be extrapolated to total precipitation depth of approximately 301.2 cm at the IESF using Equation (8).

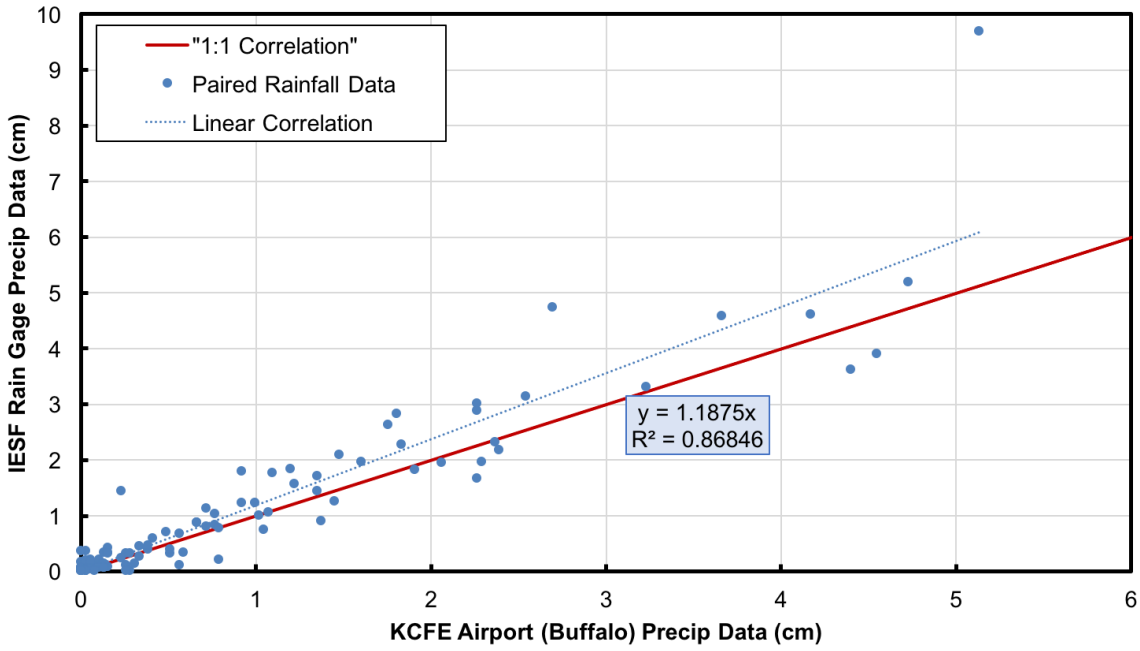

Figure 29. Relationship between rainfall data measured at IESF and rainfall data measured at Buffalo, Minnesota, USA Municipal airport (KCFE) for events between 26 June 2015 and 29 October 2016.

The watershed contributing to the IESF studied in this project is approximately 7.45 ha. Multiplying this area by the rainfall depth (301 cm) yields a predicted rainfall volume of approximately 224,500 m^3. As previously discussed in section 3.2, an estimated drain tile flow "runoff coefficient" for this watershed is approximately 0.12. Applying this to the predicted rainfall volume yields an estimated drain tile flow volume of approximately 27,000 m^3, which corresponds to the total volume of water treated by the IESF since it was constructed. The total volume of water treated by the IESF can be converted to a depth treated, which adjusts the volume for the size of the IESF and accounts for over- or under-

sizing. Dividing the volume treated (27,000 m^3) by the surface area of the IESF (92.9 m^2) yields a depth treated of approximately 290 m.

Overall, the performance of the IESF in this study (63.9% ± 7.7% (α = 0.05) phosphate load reduction, 66.3% ± 6.7% (α = 0.05) total phosphorus load reduction) is comparable to other studies of IESFs. Laboratory experiments of IESFs in previous studies found an average of 88% phosphate capture with a total treated depth of 200 m (Erickson *et al.* 2012). Field applications of an IESF trench after less than one year of operation exhibited an average of 60% phosphate load reduction for 7.2% iron by weight, and 78.8% phosphate load reduction for 10.7% iron by weight (Erickson *et al.* 2010). The amount of water treated by the IESF in this study from the time it was constructed until the end of the study (October 2012 - October 2016) was approximately 290 m of treated depth, which exceeds previously investigated treated depths (200 m) (Erickson *et al.* 2007, 2012). As shown in Figure 20 and discussed previously, the effluent concentration of phosphate increased from 2012 – 2013 to 2014 – 2017, which may be an indication that the IESF capacity for phosphate capture has decreased over time.

3.5 Maintenance

Regular, routine maintenance began within one or two years of construction and consisted of Wright SWCD staff visiting the site once or twice per month to 1) remove vegetation, iron ochre, and algae from the IESF, and 2) scrape and level the surface as needed. These activities occurred during the months of May through September of each year and required one or two individuals less than approximately one hour each to complete per site visit. In addition, non-routine maintenance was needed in May 2016 to remove a substantial accumulation of vegetation, iron ochre, and algae from the surface and required two individuals for approximately 2 hours each.

Iron ochre is a waste product from bacteria that oxidize dissolved minerals such as iron. Iron ochre is visible on the IESF as a rust colored sludge when wet and as a rust colored thin crust/cake when dry. It is likely that the dissolved iron in the water from the tile drainage was sufficient to support bacteria that produce iron ochre.

The accumulation of iron ochre and subsequent biofouling reduced the hydraulic capacity of the IESF in locations near the inlet, resulting in small pools of water between rainfall events. Algae sometimes grew within standing water on the IESF surface, and was also removed during routine maintenance. The combination of iron ochre, algae, and biofouling caused "creeping failure" on the surface of the IESF, moving slowly from the inlet towards the outlet. If vegetation, iron ochre, and algae were not removed during routine maintenance, accumulation would begin to clog the entire IESF surface and prevent treatment of influent water.

4 Application to Other Locations

The intention of this project was to measure the performance of an IESF with regards to the capture of total phosphorus and phosphate from agricultural tile drainage. The performance of this IESF is specific to this design, this location, and the period of time over which it was monitored. It is feasible, however, that an IESF could be installed in other locations to capture total phosphorus and phosphate from agricultural runoff. To aid designers, several important design considerations are listed below and a design example is provided.

4.1 IESF Design Considerations:

- The IESF must be allowed to drain, and therefore the outlet of the underdrain system below the IESF must be placed above the high-water elevation of the downstream conveyance system and/or waterbody. This will prevent inundation of the IESF.
- Intermittent flow onto the IESF is recommended. As the current study has shown, however, near-continuous flow may be feasible if the underdrain system of the IESF allows air flow to reach the IESF media and the surface is not continuously inundated.
- The IESF should be designed with 8% or less of iron by weight. Iron content greater than 8% may become clogged and not allow flow through the system (Erickson *et*

al. 2010, 2012). Many IESF systems, including the one studied in this project, have used ~5% iron by weight. In addition, it is recommended that the iron be mixed thoroughly with clean washed sand such as ASTM C33 (ASTM 2002). Too much mixing may cause stratification of iron within the sand, due to density and size differences. Previous projects have found that roto-tilling the iron into the sand in layers of approximately 5 – 10 cm deep adequately mixes the iron into the sand.

- The iron used in the IESF should be high purity (≥ 90% elemental iron) with little or no toxic impurities (e.g., copper, cadmium, lead, etc.). In addition, the iron should be reactive with phosphate. Iron and impurity content should be verified independently of the supplier to ensure purity and prevent the leaching of contaminants into the filtered runoff.
- For maintenance considerations, a filtration rate of 10 cm/hr vertically down and through the IESF media can be used to estimate the IESF surface area needed to treat a known or estimated (peak) flow rate. The smaller the IESF surface area, the greater the frequency of required maintenance.
- For lifetime capacity considerations, a sorption capacity of 5 mg P per gram Fe (Erickson *et al.* 2012) can be used to estimate the amount of iron needed to treat a known or estimated phosphate load.

4.2 Example Design Calculation:

An agricultural watershed may produce approximately 10 – 15% tile drainage flow. Assuming an annual precipitation of 76 cm and 15% tile drainage runoff, an 8-ha agricultural watershed may produce approximately 9,120 m^3 of tile drainage flow per year. Assuming an influent phosphate concentration of 0.1 mg/L, approximately 912 grams of phosphate will be contributed per year from the watershed. Assuming a sorption capacity of 5 mg P per gram of Fe (Erickson *et al.* 2012), a 20-year lifetime would require approximately 3,648 kg of Fe to be installed in the IESF. Assuming 5% iron by weight, the total IESF media weight would be 72,960 kg (69,312 kg sand + 3,648 kg Fe). With a bulk

density for iron-sand media of 1,760 kg/m^3, the total IESF media volume is approximately 41.4 m^3.

The peak flow rate could be measured for a specific site, or estimated using a Rationale method or other peak flow estimation technique. Assuming a peak flow rate of 20 m^3/hr = 5.5 L/s (typical peak flow measured in this study for a 7.45-ha agricultural watershed and "runoff coefficient of 0.12) and a design hydraulic loading rate of 10 cm/hr as recommended in section 4.1 above, approximately 200 m^2 will be needed for the surface area of the IESF. With a total IESF media volume of 41.4 m^3 and a surface area of 200 m^2, the media depth is approximately 20.7 cm. It is often best to include extra IESF media to allow for years with higher phosphate concentrations, which will deplete the iron capacity more quickly. For this example, the media depth (20.7 cm) could be increased by 20% to 25 cm or by 45% to 30 cm. The amount of iron and sand should also be increased accordingly.

5 Conclusions

An iron enhanced sand filter (IESF) was installed in Wright County, Minnesota, USA in order to treat agricultural tile drainage to reduce soluble (phosphate) and total phosphorus loads received by nearby lakes. For this study, grab samples were collected from 2012 through 2017 and monitoring equipment was installed to collect flow-weighted composite samples for analysis of total phosphorus and phosphate capture performance during rainfall-induced tile drainage flow events of 2015 and 2016. Approximately 90% of the measured total flow volume corresponded to rainfall event flow and approximately 10% corresponded to baseflow. Samples were not collected from several events throughout the two-year period due to equipment errors, resulting in several non-sampled rainfall events corresponding to approximately 26% of total flow. During the study period, 33 rainfall events were monitored and IESF capture performance was determined for phosphate and total phosphorus.

The rainfall depth of events measured from approximately June through November in 2015 and again in 2016 varied from 0.05 to 7.32 cm per event with an average of 2.23 ± 0.70 (α = 0.05) cm for 30 events and totaled 66.95 cm. These events produced an

agricultural tile drainage flow depth of 7.91 cm, corresponding to an effective "runoff coefficient" of 0.12. The total phosphorus load reduction varied from 42% to 95% with a flow-weighted mean reduction of 66.3% ± 6.7% (α = 0.05) for 20 events in 2016. The phosphate load reduction varied from 9% to 87% with a flow-weighted mean reduction of 63.9% ± 7.7% (α = 0.05) for 31 events in 2015 and 2016. In addition, the influent soluble fraction for monitored rainfall events varied from approximately 5% to 90% with an average of 43.2% ± 12.6% (α = 0.05) and effluent soluble fraction varied from approximately 15% to 75% with an average of 43.5% ± 10.0% (α = 0.05).

Maintenance of the IESF consisted of 1) removal of vegetation, iron ochre, and algae and 2) leveling and scraping of the IESF surface. This occurred approximately once or twice per month during the growing season (May - September) of each year and each occurrence required typically less than one hour per person for one or two people. This level of maintenance was satisfactory to ensure proper flow and contact between the water and the IESF media and is expected to continue throughout the life of the IESF.

Chapter 5: Abiotic Capture of Stormwater Nitrate with Granular Activated Carbon[4]

Abstract: Stormwater runoff from urban and agricultural watersheds carries nitrate, which is difficult to remove because it is highly soluble and thought to be relatively inert in abiotic processes such as ion exchange and sorption. Thus, current practice relies on denitrification to capture nitrate in stormwater treatment practices, requiring storage of captured stormwater, anaerobic conditions, and enough residence time for the bacteria to convert nitrate to nitrogen gas. The purpose of this research was to (1) quantify abiotic nitrate removal and removal capacity of two granular activated carbons (GACs), and (2) illustrate use of GACs in stormwater treatment practices. Batch and upflow column experiments found that two commercially available GACs captured nitrate abiotically, although competition between (bi)carbonate and nitrate limited removal of nitrate. Compared with removal of nitrate by denitrification, abiotic capture of nitrate during rainfall events requires less stormwater storage volume and less residence time to remove nitrate because it accumulates on the media as stormwater passes through the filter. This suggests that nitrate can be removed from stormwater with less storage and smaller treatment practices.

1 Introduction

Urbanization increases the amount of impervious land surfaces such as roads, parking lots, and rooftops, which results in less infiltration of rainfall and more surface runoff. This nonpoint source stormwater runoff is typically conveyed to and through storm sewers, often carrying pollutants (e.g., sediments, nutrients, and metals) to receiving water bodies, resulting in water quality impairments (U.S. EPA 2000). One such pollutant, nitrate (NO_3^-), has water quality limits to reduce biological overproduction (eutrophication) in

[4] A version of this chapter was published in Journal of Environmental Engineering Science in 2016, as Erickson, A.J., Gulliver J.S., Arnold W.A., Brekke C., and Bredal M. (2016). "Abiotic Capture of Stormwater Nitrates with Granular Activated Carbon." Environmental Engineering Science. May 2016, 33(5): 354-363. Permission was obtained from Mary Ann Liebert to reproduce the publication in this dissertation.

marine environments, such as the hypoxic zone in the Gulf of Mexico near the mouth of the Mississippi River in the United States (U.S. EPA 2007a). In addition, nitrate causes methemoglobinemia (U.S. EPA 2012) in human infants when drinking water with a concentration > 10 mg NO_3^--N/L is consumed by the mother (breast milk) or baby. Sources of nitrate in urban runoff include fertilizers, plant debris, and animal waste (U.S. EPA 1999). Kayhanian *et al.* (2007) analyzed the results from 34 highway water quality stations and a total of 634 storms to determine that nitrate and total Kjeldahl nitrogen (TKN) concentrations increased with increasing antecedent dry period and traffic counts and decreased with an increase in storm rainfall and seasonal cumulative rainfall. The mean, median, and standard deviation concentrations were 1.07, 0.6, and 2.6 mg/L for nitrate and 2.06, 1.4, and 1.9 mg/L for TKN, respectively. The difference between the mean and median indicates that the concentration distribution was skewed toward higher concentrations and the large standard deviation indicates that the distribution was relatively broad. Kayhanian *et al.* (2012) reviewed 15 highway stormwater quality studies around the world where nitrate and TKN were reported, with a mean, median, and standard deviation in nitrate concentration, $[NO_3^-]$, of 2.13, 1.07, and 2.29 mg/L, respectively. These observations indicate that $[NO_3^-]$ in runoff from highways varies substantially, both between storms and between locations. $[NO_3^-]$ in runoff from agricultural practices is also variable, but it is generally higher than that from highways (Stuntebeck et al. 2011).

Removing nitrogen from impacted waters requires an understanding of biotic and abiotic nitrogen cycling. Nitrogen cycling in the environment is dominated by biologically mediated redox processes (Brezonik and Arnold 2011). Nitrification is the chemoautotrophic oxidation of ammonium (NH^+) to nitrite (NO^-) through *Nitrosomanas* and to nitrate (NO_3^-) through *Nitrobacter* (Stumm and Morgan 1981). Denitrification is the anaerobic biodegradation of nitrate to nitrogen gas (N_2) by bacterial species such as *Pseudomonas* and *Clostridium* (Smil 2000). Such processes are commonly used to remove nitrogen from wastewater, but the short residence time and limited water storage volume provided by stormwater treatment practices are often not sufficient to allow adequate removal of nitrate by denitrification alone, unless significant design changes are incorporated (Kim *et al.* 2003, Hsieh and Davis 2005). Although sorption and ion exchange

are not among the well-known nitrogen removal processes, recent research (Figure 30) has shown that materials capture nitrogen, particularly as nitrate, through these abiotic processes.

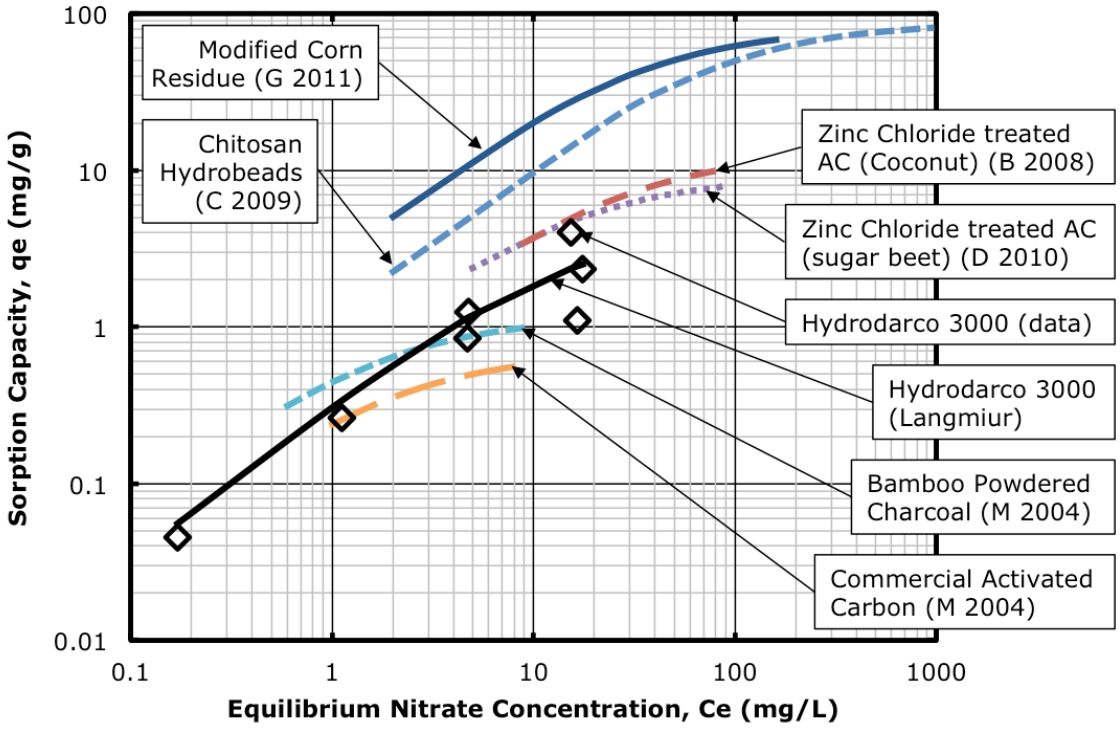

Figure 30. Literature values for nitrate adsorption (Langmuir) isotherms compared with Hydrodarco 3000 data and isotherm fit (a = 4.44 mg $NO3^-$ -N/g GAC; b = 0.07 L water/mg $NO3^-$ -N; R^2 = 0.57) at 20 – 25 °C. (C 2009 = Chatterjee and Woo 2009; G 2011=Gao et al. 2011; M 2004= Mizuta et al. 2004; D 2010 = Demiral and Gunduzoglu 2010; B 2008 = Bhatnagar et al. 2008).

Chatterjee and Woo (2009) found that adsorption of nitrate to chitosan hydrogel beads in a synthetic stock solution at equilibrium was described by the Langmuir isotherm, with the sorption being both temperature and pH dependent. The sorption capacity increased by 14 – 27% when temperature was decreased from 50 °C to 20 °C. When pH was decreased from pH 5 to pH 3, the sorption capacity increased by 4 – 20%, and when pH was increased from pH 5 to pH 8, the sorption capacity decreased by 43 – 56%.

Reported sorption capacities were 90 mg/g for pH 3, initial [NO_3^-] = 1000 mg/L, at 20 °C; but as low as 15 mg/g for pH 8, initial [NO_3^-] = 50 mg/L, at 30 °C. They also found that nitrate could be desorbed after 24 h of mixing under high pH conditions (~87% desorption at pH 11 and 12) and suggest that electrostatic interactions dominate the removal process (Chatterjee and Woo 2009). Stormwater runoff is typically between a pH of 7 and 8 and a temperature of 5 °C and 25 °C, so these results are marginally helpful for stormwater.

Modified corn residue adsorbed nitrate from a synthetic stock solution according to the Langmuir isotherm with a maximum capacity of 81 mg/g at 20 °C and 73 mg/g at 40 °C (Gao *et al.* 2011). They found that lower pH resulted in less sorption, which is contrary to the findings of Chatterjee and Woo (2009). Zhang *et al.* (2007) found that a zeolite sourced from Gongyi, Henan Province, removed 70% of total nitrogen and nearly 90% of NH_4^+ from lake water and raw wastewater in a simulation of a vertical flow constructed wetland with a hydraulic loading rate of 1000 – 2500 mm/day (41.7 – 104.2 mm/h). The authors attribute removal to the high ion-exchange capacity of the zeolite (Zhang *et al.* 2007).

Granular activated carbon (GAC) made from bamboo residue adsorbed nitrate from a synthetic stock solution with a Langmuir isotherm sorption capacity of 1.25 mg/g for initial [NO_3^-] = 10 mg/L at 10 °C (Mizuta *et al.* 2004). When the temperature was increased from 10 °C to 20 °C, the nitrate sorption capacity decreased to 1 mg/g.

Demiral and Gunduzoglu (2010) found that the Langmuir isotherm sorption capacity for nitrate adsorption to GAC was affected by temperature (9 mg/g at 25 °C to 28 mg/g at 45 °C) but was not dependent on pH in a synthetic stock solution. When a commercial GAC (coconut shells) was chemically treated with zinc chloride ($ZnCl_2$), the nitrate capture in a synthetic stock solution increased from 1.7 mg/g to 10.2 mg/g (initial [NO_3^-] = 200 mg/L, 25 ± 2 °C, pH 5.5, time = 2 h), and nitrate capture was described by the Langmuir isotherm (Bhatnagar *et al.* 2008). Bhatnagar *et al.* (2008) also showed that nitrate capture increased as temperature decreased (similar to Chatterjee and Woo 2009; contrary to Demiral and Gunduzoglu 2010) and that nitrate capture was relatively constant for pH 4 – 11 but decreased for pH 3 because of competition with Cl^- (HCl used to adjust pH) and also at pH 12 because of electrostatic repulsion with negatively charged GAC surface.

Clark (1997) found that only GAC mixed with sand, out of nine materials tested, could capture > 90% nitrate from natural stormwater. Clark (2000) reports a nitrate removal capacity for GAC of 6 mg/g from batch studies in natural stormwater, but only 0.3 mg/g in long-term breakthrough column studies, and concludes that batch studies are not appropriate for estimating removal capacity for field applications. From these studies, the authors concluded that GAC removes pollutants through sorption and ion exchange (with sulfates) (Clark 1997, 2000). Additional experiments on natural stormwater found that coconut-based GAC removed nitrate but could export phosphorus (Clark and Pitt 2011) and that nitrate removal coincides with release of phosphorus initially and chlorides toward the end of the experiments, suggesting ion exchange (Pitt *et al.* 2010a, 2010b).

Previous studies indicate that although nitrate capture by various sorbents is possible, the following must be considered: 1) the capacity of sorbents varies substantially (0.3 – 90 mg/g), 2) capacity is affected by temperature and pH, and 3) the removal mechanism is hypothesized to be ion exchange or adsorption. It is possible that the variability in capacity and temperature and pH dependence is because of the variability in sorbent material and manufacturing process, as well as the experimental conditions (primarily $[NO_3^-]$ range). In this chapter, abiotic capture of nitrate by GAC is explored. The capacity of two carbon sources is evaluated, and the experimental flow conditions and the effects of competition with other dissolved species are investigated. Finally, the potential use of GAC in stormwater treatment practices for nitrate removal is illustrated.

2 Experimental Protocols

Two GACs were studied rigorously: Hydrodarco 3000 (HD) and CR830A Low Density Sub-Bituminous (SB). HD (Norit 2012) is manufactured by high-temperature steam activation of lignite coal and has a bulk density of ~344.4 kg/m^3. SB (Carbon Resources 2010) is a low-density sub-bituminous carbon produced by high-temperature steam activation of sub-bituminous coal and has a bulk density of approximately 352.4 – 384.4 kg/m^3. Both HD and SB have less than 5% by weight passing #30 sieve (0.600 mm) and less than 5% by weight retained on the #8 sieve (2.36 mm).

Experiments described in the following sections focus on ranges of [NO_3^-], temperature, and pH that are typical for urban and agricultural stormwater runoff, although the capacity measured in this study will be compared with results in the literature. Two sets of batch studies and four sets of upflow column studies were performed as follows:

1. Media selection batch studies: Experiments were performed to determine which of several materials captured the most dissolved nitrate while also capturing at least some dissolved phosphorus and metals (cadmium, copper, lead, and zinc). HD and SB were chosen as the best at nitrate and metals removal while not releasing phosphate. The experimental protocols, results, and discussion are provided in section 6.1 of the Supplementary Data.
2. Isotherm batch studies: Experiments were performed to measure nitrate removal kinetics and capacity at equilibrium under controlled experimental conditions for the two GACs.
3. Upflow column studies: Experiments were performed to understand the breakthrough of nitrate in a nearly saturated flow-through system, at near-constant vertically upward flow rate, for the two GACs. The purpose of these experiments was to identify and quantify specific treatment processes and capacities, when possible. Synthetic stormwater mixed without nitrate was passed through GAC columns to determine how much, if any, nitrate is released from GAC. The GACs used in the column experiments did not release nitrate (data not shown) and thus no correction to the observed [NO_3^-] in other experiments was needed. Four sets of upflow experiments were performed and each experiment was performed continuously (no dry periods) until equilibrium (inflow concentration = outflow concentration).
    3.1 Dispersion and contact time experiments: Sodium chloride (NaCl) was passed through the columns as a conservative tracer (Crittenden *et al.* 2005) to estimate the dispersion and contact time of flow through the column experiments. Results are provided in section 6.2 of the Supplementary Data.
    3.2 Capture experiments: Deionized (DI) water was passed through the columns at a near-constant flow rate (15 – 25 mL/min) for ~1 h to remove any fine

GAC particles, fully saturate the pore space in the GAC, desorb any loosely bound ions on the GAC, and to adjust the pumps before introducing synthetic stormwater. To determine the capture capacity of the GAC to remove nitrate, the supply was immediately switched to synthetic stormwater, which was passed through the columns until equilibrium with the influent synthetic stormwater (10 – 14 h) was achieved.

3.3 Competition experiments: Each pollutant (e.g., PO_4^{3-} -P) in the synthetic stormwater was mixed separately with nitrate (NO_3^- -N) and passed through a previously unused column of GAC to determine whether other ions in the synthetic stormwater competed with nitrate for capture sites on the GAC.

3.4 Release experiments: To determine how much previously captured nitrate could be released, DI or potable (tap) water was passed through columns previously tested in the capture experiments (i.e., at equilibrium with synthetic stormwater) until effluent concentrations were at equilibrium (10 – 12 h).

2.1 Isotherm batch studies

For each batch experiment, 500 mL borosilicate glass bottles were acid washed with 10% HCl, rinsed with ultrapure water (Milli-Q, 18.2 MΩ•cm), acid washed with 10% oxalic acid, and rinsed again with ultrapure water (Milli-Q, 18.2 MΩ•cm). After drying, 500 mL of ultrapure water and inorganic salts were added and mixed to represent typical values for natural stormwater, as listed in Table 12. The inorganic salts used were KNO_3 (≥ 99%; Fisher Scientific), KH_2PO_4 (99.9%, J.T. Baker), $NaHCO_3$ (99.7 – 100.3%; Sigma Aldrich), $CaCO_3$ (99.5%, J.T. Baker), Na_2CO_3 (100.1%; Fisher Scientific), $MgCO_3$ (40.0 – 43.5%; Fisher Scientific), and $MgCl_2$ (99.0 – 102.0%, J.T. Baker, 99.4%; Fisher Scientific).

Table 12. Synthetic stormwater characteristics for batch and column studies. Batch and Constant Flow Column Studies comprising ultrapure water (Milli-Q, 18.2 MΩ•cm) and inorganic salts. "-" = Not Applicable.

Component	Batch Studies	Constant Flow Column Studies
Nitrate (NO_3^-)	0.27 – 58.9 mg/L (0.019 – 4.20 mM) as NO_3^- -N	5 mg/L (0.357 mM) as NO_3^- -N
Phosphate (PO_4^{3-})	-	0.25 mg/L (0.008 mM) as PO_4^{3-} -P
Alkalinity	150 – 170 mg/L (1.499 – 1.699 mM) as $CaCO_3$	39 mg/L (0.390 mM) as $CaCO_3$
Hardness	39 mg/L (0.390 mM) as $CaCO_3$	135 mg/L (1.349 mM) as $CaCO_3$
pH	7.4	7.8 – 8.1
Conductivity	270 µS/cm	-
Temperature	Room Temperature	21 ± 2 °C

Hydrochloric acid (0.06 M HCl, 37%; Sigma Aldrich) was added to adjust the pH to the median stormwater pH of 7.4 (Maestre and Pitt, 2005). Although the median value for conductivity in natural stormwater is 121 µS/cm with a 1.75 coefficient of variation (Maestre and Pitt, 2005), the measured conductivity of the synthetic stormwater was ~270 µS/cm because of the salts used to create the pollutant concentrations. Thus, the conductivity was not adjusted. Other parameters of natural stormwater such as suspended sediment, bacteria and pathogens, and organic material were not added to the synthetic stormwater to minimize biological activity, limit particle interaction with dissolved compounds to the media, and reduce the number of experimental variables.

Initial samples were collected in acid-washed glass vials and analyzed before adding media to ensure accurate initial pollutant concentrations. Batch test bottles (with media) and blanks (no media) were placed on a Labline Orbital Shaker table at 250 RPM. Samples were collected at several time intervals up to 96 h of mixing, filtered through a 0.45-micron filter to remove particulates, and frozen until analyzed for ion concentrations. Samples were analyzed for [NO_3^-], [Cl^-], and [SO_4^{2-}] using a Dionex ICS-1100 IC System with a Thermo Scientific AS22 Ionpac exchange column and an AS- DV autosampler.

2.2 Upflow column studies

Vertical columns were constructed from a 31-cm long, 5-cm diameter clear PVC and each column was filled with 19 – 23 cm (150 g) of GAC (typically five replicates of either HD or SB) or 20 cm (~780 g) of C-33 sand (one replicate) (Paus *et al.* 2014a, 2014b). Sampling occurred immediately before and after each column through a Luer Lock fitting.

A peristaltic pump was connected to each column to ensure near-constant upward flow through each column. Flow rate varied from 15 to 25 mL/min (0.74 to 1.23 cm/min linear velocity) in these experiments. The peristaltic pumps collected supply water from a 150-L supply tank. Synthetic stormwater was mixed to represent typical stormwater concentrations (Table 12). Nitrate and phosphate concentrations for the column studies were intentionally set higher than typical urban stormwater to also represent agricultural runoff (Kato *et al.* 2009, Stuntebeck *et al.* 2011).

Samples were collected at regular time intervals, filtered through 0.45-µm PTFE filters, and stored in sampling vials until analysis. Nitrate was analyzed colorimetrically (Pritzlaff 2003). Alkalinity was measured through titration with Bromcresol green indicator and hydrochloric acid (APHA 1998, method 2320B). For dispersion and contact time experiments using NaCl as a tracer, the effluent conductivity was measured continuously with an Engineered Systems & Design model 72 conductivity meter.

2.3 Data analysis

2.3.1 Isotherm batch studies.

Equilibrium concentration (C_e) was measured and capture capacity (q_e) was calculated as the ratio of the mass of nitrate captured to the mass of GAC in each bottle. The Langmuir isotherm model, Equation (9) was used:

$$\frac{x}{m} = q_e = \frac{abC_e}{1 + bC_e} \tag{9}$$

where:

x = mass of nitrate adsorbed (mg NO_3^- -N),

m = mass of activated carbon (g GAC),

q_e = sorption capacity (mg NO_3^- -N /g GAC),

a = empirical constant (mg NO_3^- -N / g GAC),

b = empirical constant (L water/mg NO_3^- -N),

C_e = equilibrium concentration of nitrate (mg/L)

2.3.2 Upflow column studies.

From the flow rate and [NO_3^-], the mass of nitrate removed by GAC was calculated and plotted as a function of pore volume (Supplementary Data Figures S8 and S9). Note that when the mass of nitrate captured by GAC was normalized by the mass of GAC in each column, the result is the capture capacity (mg NO_3^- -N/g GAC). Similarly, the mass of nitrate released from GAC was calculated from the flow rate and [NO_3^-] and plotted as a function of pore volume (see Figures 41 and 42 in Supplementary Data). The mass of nitrate released was normalized by the mass of nitrate captured in the capture experiments (Figure 33) to illustrate the fraction of previously captured nitrate that is released.

3 Results and Discussion

3.1 Abiotic removal

Although no antibiological agents were used, biological removal or transformation of nitrate is unlikely and thus the removal process is believed to be abiotic for several reasons:

1. Batch experiments were mixed for 1 h (Media Selection) or up to 96h (Isotherm). Although no anti-biological agents were used, biological activity is assumed to be negligible because (1) ultrapure (Milli-Q, 18.2 MΩ•cm) water and inorganic salts were used for the experiments, (2) the experiments were contained in acid-washed glassware and sealed between sample collection, and (3) the GAC was not exposed to any obvious source of waterborne denitrifying bacteria before or during the experiment.

2. The upflow column experiments used the same water, materials, and media as the batch experiments. Flow through the experiments occurred continuously for 10 – 16 h, although the contact time with the media was approximately 11 min (HD, Table 13 and Supplementary Data Table 16), 19.1 min (SB, Supplementary Data Table 16), and 5.4 min (Sand, Table 13 and Supplementary Data Table 16).
3. The 100% sand replicates in all experiments removed minimal, if any, nitrate.

3.2 Isotherm batch studies

The Langmuir isotherm model in Equation (9) was fit to data collected for HD and compared with Langmuir isotherm parameters and range of equilibrium concentrations reported in the literature (discussed previously), as shown in Figure 30. The results from HD extend to smaller equilibrium concentrations compared with literature values, and better represent concentrations found in urban and agricultural stormwater. The literature did not provide data below ~0.6 mg/L NO_3^--N. Literature values for sorption capacity vary substantially, ranging across approximately one order of magnitude for any given equilibrium [NO_3^-]. The capture capacity for HD is similar to that of bamboo powdered charcoal and commercial activated carbon studied by Mizuta *et al.* (2004), but is generally less than that of other GACs shown in Figure 30. This is likely because the other GACs were modified (modified corn residue; Gao *et al.* 2011), treated to improve performance (Bhatnagar *et al.* 2008, zinc chloride treated by Demiral and Gunduzoglu 2010), or specifically fabricated (chitosan hydrobeads; Chatterjee and Woo 2009). HD, as tested, is commercially available and does not require any additional treatment or modification.

3.3 Upflow column studies

3.3.1 Capture experiments.

Five replicates of 100% GAC are shown in Figure 31 for HD (see Supplementary Data Figure 41 for SB data). The experiments indicate that 100% of the nitrate ($C/C_0 = 0$) was captured until ~10 pore volumes had passed through the columns. After 10 pore

volumes, the effluent [NO_3^-] increased and exceeded the influent concentration ($C/C_0 > 1$) at between 20 and 30 pore volumes. The effluent concentrations peaked at 120% of the influent and then gradually decreased to equilibrium ($C/C_0 = 1$) after ~60 pore volumes. Similar results were obtained for SB, as shown in Supplementary Data Figure 41. Note as shown in Figure 31, the effluent nitrate concentration of 100% sand column [Sand (1)] quickly reached equilibrium with the influent ($C/C_0 = 1$), suggesting that sand has little, if any, capacity to remove nitrate from synthetic stormwater. In general, all five replicates of HD produced similar results with slight variations (Table 14 and Supplementary Data Table 17, Figure 31). The differences could be because of variations in flow rate (Table 13) or trapped air pockets (or lack thereof). Although the capture capacity peaked, the capture capacity at equilibrium is more representative of the capture capacity that could be expected in field applications.

Table 13. Upflow Column Study Overview (See Supplementary Data Table 16 for Sub-Bituminous Data)

					Adsorption Experiments		**Desorption Experiments**		
Column	**Media Mass (g)**	**Media Height (cm)**	**Pore Volume (mL)**	**Pore Volume (%)**	**Water Supplied**	**Average Flow Rate (mL/min)**	**Water Supplied**	**Average Flow Rate (mL/min)**	**Drained Between Experiments?**
HD (1)	150	19.5	243	63.4%	SS	21	DI	21	Yes
HD (2)	150	19	233	62.5%	SS	21	DI	21	No
HD (3)	150	19.5	233	60.8%	SS	23	TW	22	No
HD (4)	150	20.5	273	67.7%	SS	25	TW	25	Yes
HD (5)	150	19	243	65.2%	SS	22	-	-	-
Sand (1)	698	19.5	133	34.7%	SS	24	-	-	-
HD (6)	150	21.5	272	64.5%	-	-	SS w/o NO_3-N	21	-
HD (7)	150	20	263	66.9%	-	-	SS w/o NO_3-N	27	-

DI = deionized water; HD = Hydrodarco; "-" = not applicable; SS = synthetic stormwater; TW = tap (potable) water.

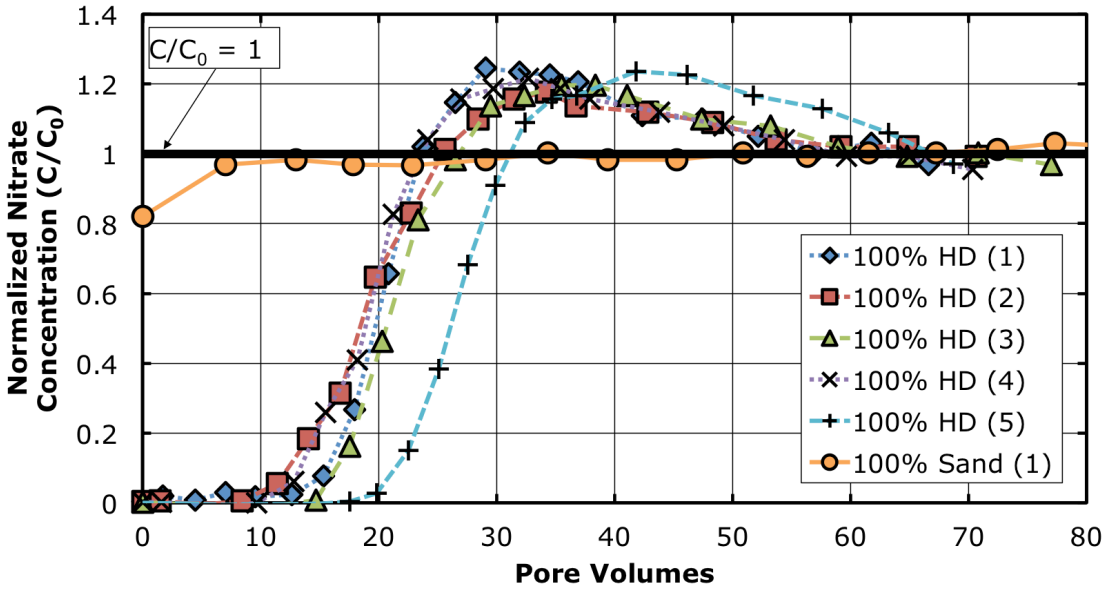

Figure 31. Upflow column experiments: breakthrough curves for nitrate sorption experiments for five Hydrodarco (HD) columns and one C-33 sand column. (see Supplementary Data Figure 41 for Sub-Bituminous data).

Table 14. Column Experiments (Average of All Replicates – Standard Deviation, Where Applicable) of Hydrodarco (See Supplementary Data Table 17 for Sub-Bituminous data)

	Replicates	Media Mass (g)	Flow Rate (mL/min)	Pore Volume (mL)	Pore Volumes Treated	Influent Conc. (mg/L NO_3-N)	Nitrate Captured (mg)	Sorption Capacity (mg NO_3-N/g Media)
Hydrodarco (constant flow)	5	150	22.23	245.4	70.7	5.14	19.01	0.127
C-33 Sand (constant flow)	2	778.7	22.73	122.8	147.3	4.94	0.27	0.005

The equilibrium capture capacity for four of the five HD replicates is approximately 0.12 mg NO_3^- -N/g GAC. The other replicate [HD (5)] was identified as possibly having

better contact between the GAC and the synthetic stormwater, resulting in a larger capture capacity (~0.17 mg NO_3^- -N/g GAC).

3.3.2 *Competition experiment.*

The effluent [NO_3^-] exceeded the influent ($C/C_0 > 1$) after 20–30 pore volumes (Figure 2, Supplementary Data Figure 8). A possible explanation is competition of ions on the GAC. At the beginning of an experiment, the GAC has many sites available for the attachment of ions. Initially, most ions attach to the GAC but as the capacity is approached, the ions begin to compete for sites. Some ions will bond more strongly than nitrate to GAC, resulting in release of nitrate ions. These released nitrate ions in addition to the nitrate ion already present from the influent may explain why the [NO_3^-] in the effluent exceeded that of the influent.

Additional experiments were performed to test this hypothesis, which involved separating each of the source compounds (e.g., KH_2PO_4) used to represent pollutants (e.g., PO_4^{3-} -P) or water chemistry (e.g., alkalinity) in the synthetic stormwater (Table 12) and dosing a previously unused single column of GAC with a single source compound and nitrate (NO_3^- -N), as shown in Figure 32. One column experienced no competition because only nitrate was added to the synthetic stormwater (KNO_3 only). Three pollutant combinations (KNO_3 only, $KNO_3 + KH_2PO_4$, and $KNO_3 + CaCO_3$) behaved similarly and the GAC captured 1.076 mg NO_3^- -N/g GAC (n = 3, standard deviation = 0.021 mg NO_3^- -N/g GAC). For the pollutant combination of $KNO_3 + Na_2CO_3$, the GAC captured 0.444 mg NO_3^- -N/g GAC whereas for $KNO_3 + MgCl_2$, the GAC captured 0.639 mg NO_3^- -N/g GAC. Thus, the order of capture capacity (mg NO_3^- -N/g GAC) is as follows: $KNO_3 + Na_2CO_3 = 0.444 < KNO_3 + MgCl_2 = 0.639 < KNO_3$ only = $KNO_3 + KH_2PO_4 = KNO_3 + CaCO_3 = 1.076$ mg NO_3^- -N/g GAC.

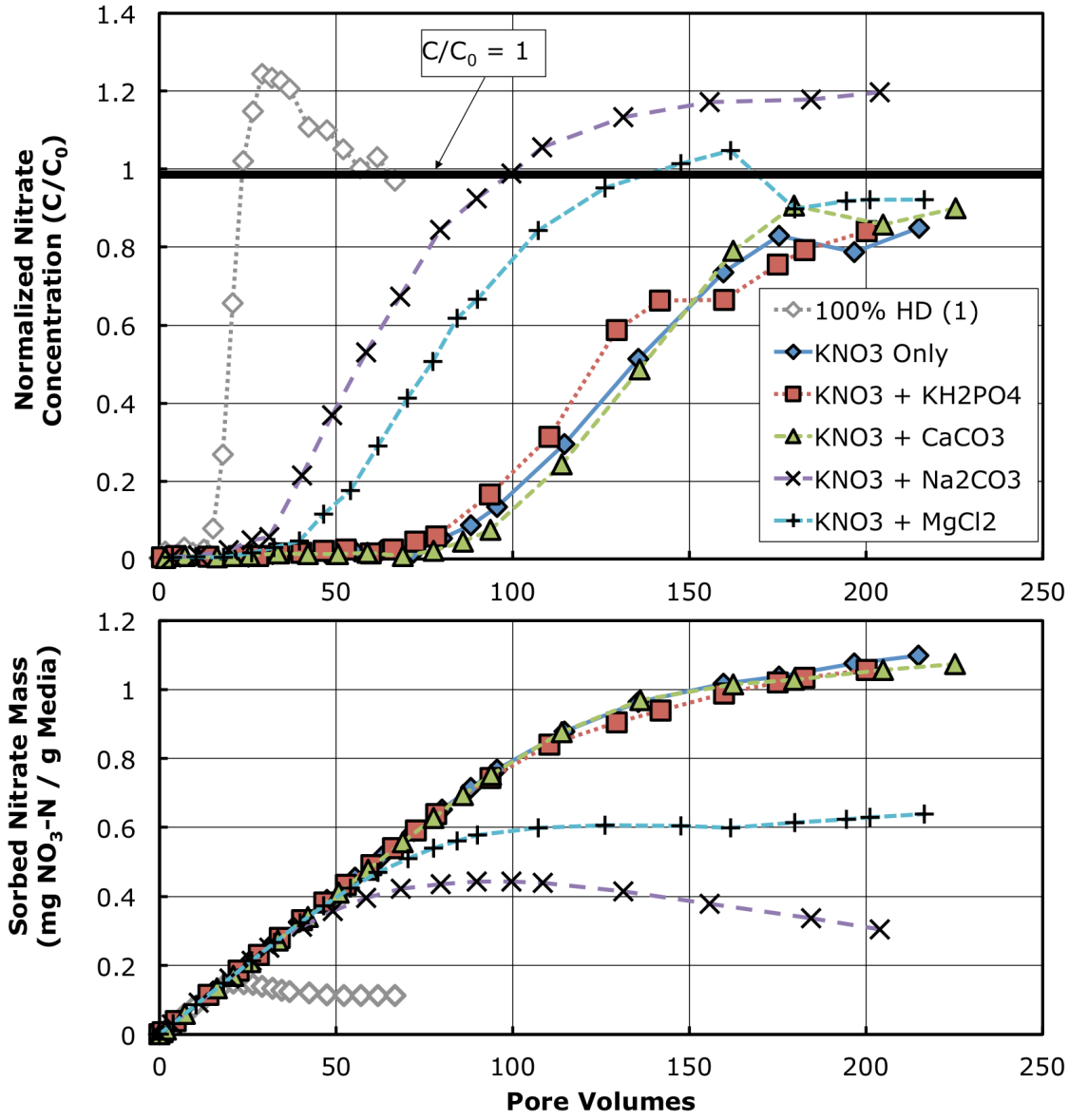

Figure 32. Upflow Column Experiments: Normalized nitrate concentration (top) and sorption capacity (bottom) for competition experiments with separated source compounds and activated carbon (Hydrodarco) (see Table 12 for pollutants concentrations). For comparison, one replicate (HD (1), Figure 31) of nitrate breakthrough with mixed synthetic stormwater is also shown.

First, it is important to note that the columns dosed with NO_3^- -N only [5 mg/L (0.357 mM) KNO_3 -N], NO_3^- -N with KH_2PO_4 [0.25 mg/L (0.008 mM) KH_2PO_4 -P], and NO_3^- -N with $CaCO_3$ [5 mg/L (0.05 mM) as $CaCO_3$] perform similar to each other and do

not exceed the influent [NO_3^-]. The column dosed with NO_3^- -N and $MgCl_2$ [130mg/L (1.299 mM) as $CaCO_3$] appears to slightly exceed the influent ($C/C_0 \sim 1.05$), but this may be within the measurement error. The column dosed with NO_3^- -N and Na_2CO_3 [34 mg/L (0.340 mM) as $CaCO_3$] is the only column that appears to increase to a $C/C_0 = 1.2$, similar to the columns shown in Figure 31. This suggests that either sodium (Na^+) or (bi)carbonate (HCO_3^-/CO_3^{2-}) is competing with nitrate, where (bi)carbonate is more likely than sodium because (bi)carbonate and nitrate are both negatively charged.

It is also important to note that breakthrough required substantially more pore volumes in this experiment (~200 pore volumes, Figure 32) than previous experiments (~30 pore volumes, Figure 31), resulting in a substantially larger capture capacity (~1.1 mg NO_3^- -N/g GAC, Figure 32) than previous experiments (~0.12 mg NO_3^- -N/g GAC). The columns dosed with NO_3^- -N (KNO_3) only, KH_2PO_4, and $CaCO_3$ reached equilibrium (100% breakthrough) at ~200 pore volumes and the column dosed with Na_2CO_3 required approximately 100 pore volumes before the effluent [NO_3^-] exceeded the influent [NO_3^-]. This supports the hypothesis that nitrate competes with other ions, particularly bi(carbonate), for capture by GAC. The increase in capture capacity also suggests that competition of ions in previous experiments is significant, because the GAC captures more nitrate when the pollutants are separated than mixed synthetic stormwater. Also, because the columns dosed with KH_2PO_4 and $CaCO_3$ perform similarly to the column dosed with KNO_3 only, it is assumed that KH_2PO_4 and $CaCO_3$ do not provide noticeable competition with nitrate on GAC at concentrations typical of agricultural stormwater runoff.

The data shown in Figure 32 and Table 15 suggest that nitrate and (bi)carbonate are captured by GAC before any breakthrough occurs. As capacity is approached, the (bi)carbonate begins to outcompete the nitrate, causing the effluent [NO_3^-] to exceed the influent [NO_3^-]. The reason that competition is not evident in the column dosed with CaCO3 could be because the total carbonate concentration is a factor of ~7 less than the column dosed with Na_2CO_3 [5 mg/L (0.05 mM) of $CaCO_3$ vs. 34 mg/L (0.340 mM) Na_2CO_3 as $CaCO_3$].

Table 15. Comparison of Column Experiment Capture Capacity, Competition, and Source Water (Note: Competition = Capture Capacity (KNO_3 Only) – Capture Capacity). The competition and KNO_3 Only experiments utilized Hydrodarco media. "-" = Not Available.

	Capture Capacity (mg NO_3-N/g GAC)	Competition (mg NO_3-N/g GAC)	Flow Rate (mL/min)	Influent Nitrate (mM)	Influent Phosphate (mM)	Alkalinity (mM as $CaCO_3$)	Hardness (mM as $CaCO_3$)	pH	Conductivity (µS/cm)	Temperature (°C)
Upflow Experiments										
Hydrodarco	0.127	0.972	22.33	0.357	0.008	0.390	1.349	7.8–8.1	~270	21 ± 2
Sub-Bituminous	0.158	0.941	15.49	0.357	0.008	0.390	1.349	7.8–8.1	~270	21 ± 2
Competition Experiments (Hydrodarco)										
$KNO_3 + Na_2CO_3$	0.444	0.655	31.87	0.364	0	0.34	0	-	-	21 ± 2
$KNO_3 + MgCl_2$	0.639	0.460	23.63	0.362	0	0	1.30	-	-	21 ± 2
$KNO_3 + KH_2PO_4$	1.056	0.043	21.81	0.363	0.008	0	0	-	-	21 ± 2
$KNO_3 + CaCO_3$	1.074	0.025	28.25	0.358	0	0.05	0.05	-	-	21 ± 2
KNO_3 Only (no competition)	1.099	0.000	26.98	0.362	0	0	0	-	-	21 ± 2

3.3.3 Release experiments

The capture experiments provide columns in equilibrium (i.e., saturated) with a $[NO_3^-]$ = 5.14 mg/L NO_3^- -N. Release experiments were performed ~2.5 days after the capture experiments to determine how much, if any, nitrate would be released in the presence of nitrate-free water by pumping DI water and potable (tap) water through the saturated columns. The results from the release experiments are shown in Figure 33 (see Supplementary Data Figure 41 for SB data). Note that the effluent $[NO_3^-]$ was normalized by the influent $[NO_3^-]$ from Figure 31 (5.14 mg/L NO_3^- -N). As shown in Table 13, two additional columns [HD (6) & HD (7)] were constructed with unused GAC and dosed with synthetic stormwater without nitrate. These columns did not release any background nitrate, suggesting no adjustment to the capture experiments is required.

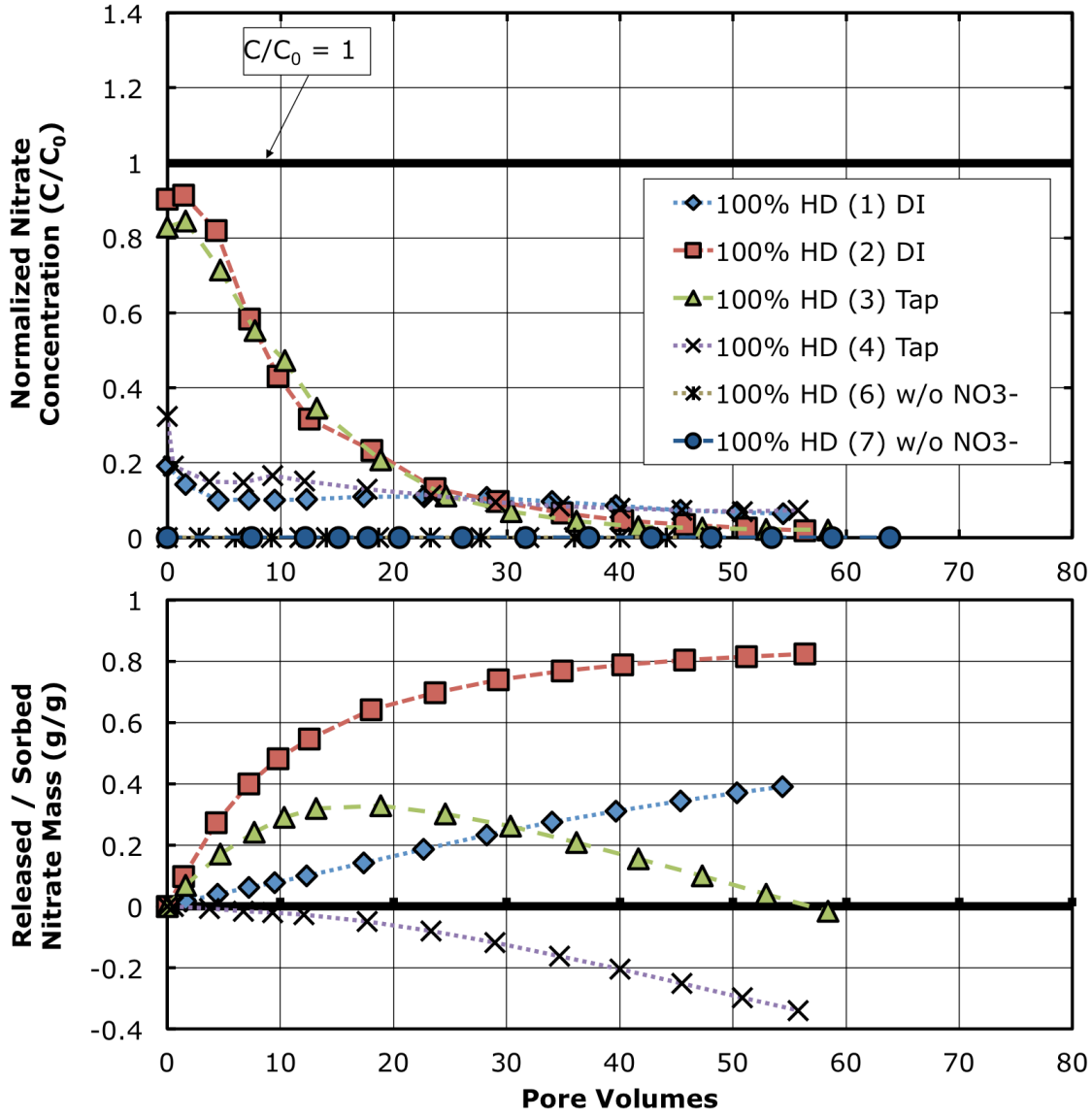

Figure 33. Upflow column experiments: nitrate concentration normalized by the influent nitrate concentration from Figure 31 (top) and fraction of nitrate mass released from Hydrodarco (bottom) in desorption experiments with deionized (DI), potable (tap), and nitrate-free synthetic stormwater (w/o NO_3^- -N). (see Supplementary Data Figure 41 for Sub-Bituminous data)

During the capture experiments, the columns were filled with synthetic stormwater containing $[NO_3^-]$ =5.14 mg/L NO_3^- -N, which is $C/C_0 = 1$. Between the capture and release experiments, this water is stored within the pore volume of the columns so the initial normalized $[NO_3^-]$ at the beginning of the release experiments is expected to be close to

one ($C/C_0 \sim 1$). The effluent concentration in the columns with HD was initially 80–90% of the influent concentration from the capture experiments (Figure 33), which approximates expectations. Within 30 – 40 pore volumes, the effluent concentration was less than 10% of the capture experiment influent and close to equilibrium because the normalized concentration is nearly constant.

As shown in Figure 33, both HD replicates initially released previously captured nitrate. HD (2) released ~80% after ~50 pore volumes, whereas HD (3) released ~30% after 15 pore volumes, but then removed nitrate from the influent tap water. The background [NO_3^-] in tap water was measured as ~0.9 mg/L NO_3^- -N (0.2 C/C_0), which partially explains the difference between HD (2) and HD (3). The release experiments show that a filter with the HD or SB GACs has the potential to release previously captured nitrate when clean water passes through. This is a concern for stormwater treatment because the [NO_3^-] in stormwater can vary substantially over time, although tap water may be more representative of low [NO_3^-] stormwater than ultrapure water.

4 Estimate of Field Performance

It is important to note that the experiments already described were conducted in a laboratory setting with synthetic stormwater. The response of a GAC filter while treating actual stormwater will likely be different because of several reasons, including media clogging, biological activity in field applications, and water quality parameters present in actual stormwater that were not included in these experiments, among others. Water quality characteristics of urban and agricultural stormwater also vary substantially (Kayhanian *et al.* 2007, 2012; Stuntebeck *et al.* 2011), depending on land use, rainfall characteristics, soil types, and stormwater management systems. The results of these experiments may not predict the actual field performance, but can be used to approximate what may be observed in the field.

Practical application of this technology for treating stormwater runoff requires understanding of capacity, lifespan, and maintenance. The expected lifespan of a field application depends on the rainfall, contributing area, and pollutant concentration, which vary. An estimate, however, of field performance can be made for a hypothetic rainfall,

watershed, and filter design. For example, assume a 5-cm rainfall event occurs over a 1-ha parking area with 90% impermeable surface area, which generates 430 m^3 of runoff according to Equation (10) (Schueler 1987).

$$WQV = 0.01 P A (0.009 I + 0.05) \quad (10)$$

where:

WQV = water quality volume (m^3)

P = rainfall (cm)

A = watershed area (m^2)

I = percentage of impervious cover (%)

The WQV is the amount of runoff that a stormwater treatment practice captures and treats without overflow. Assuming the average $[NO_3^-]$ = 0.6 mg/L, the total NO_3^--N mass in the surface runoff from this storm is 258 g (430 m^3 x 0.6 mg NO_3^--N/L = 258 g).

If this runoff and nitrate load are routed to a stormwater filter composed of GAC with a capture capacity similar to that of the upflow column experiments (0.12 mg NO_3^--N/g GAC), then the amount of GAC required to capture the nitrate load from one storm is 2,150 kg (258 g NO_3^--N / 0.12 mg NO_3^--N/g GAC = 2150 kg). This amount of GAC would cost ~$14,220 (2015 USD), but additional cost would be required to install the filter (labor, equipment, materials other than GAC, etc.). If the nitrate captured by the GAC could be removed through denitrification after each rainfall event, the filter could be sized to treat a single storm. Denitrification requires an anoxic environment and in situ denitrification has been observed in some filter designs used for surface runoff treatment (Passeport *et al.* 2009, Brown and Hunt 2011, Luell *et al.* 2011). If practical, denitrification could regenerate the activated carbon between rainfall events and a GAC filter will provide sustainable nitrate treatment of urban and agricultural runoff, although this topic would require more research to understand the minimum requirements and limitations.

5 Summary

Two GACs were tested and found to capture dissolved nitrate abiotically. The short contact time and inorganic characteristics of the influent synthetic stormwater suggest that the nitrate is captured by ion exchange, but (bi)carbonate may compete with nitrate for capture by GAC. The results of this study have the potential to improve stormwater treatment practices and water quality by providing an understanding of the capacity and application of a GAC filter to stormwater treatment. Although using GAC to treat urban or agricultural stormwater runoff can quantifiably and reliably remove dissolved nitrate, additional research is needed to determine whether a filter that combines denitrification with nitrate removal by GAC will sustainably regenerate removal capacity, which could reduce the typical size of the filter.

6 Supplementary Data

6.1 Media Selection Batch Studies

6.1.1 Experimental Protocols

Precisely as described in Chapter 4, Section 2.1, bottles were washed and filled with ultrapure water (Milli-Q, 18.2 MΩ·cm) and inorganic salts to represent stormwater pollutants, as follows:

- 0.5 µg/L (0.0044 µM) $CdCl_2$ as Cd;
- 8 µg/L (0.126 µM) $CuSO_4$ as Cu;
- 3 µg/L (0.0145 µM) $Pb(NO_3)_2$ as N;
- 112 µg/L (1.17 µM) $ZnCl_2$ as Zn;
- 600 µg/L (42.8 µM) KNO_3 as N;
- 120 µg/L (3.87 µM) K_2HPO_4 as P;
- 39 mg/L (0.39 mM) $MgCO_3$ as $CaCO_3$;
- 300 mg/L (3 mM) $NaHCO_3$ as $CaCO_3$.

Triplicate bottles were used for each type of media, and 5 g of each of the following were added to bottles: 6 different activated carbons, 1 activated alumina, C-33 sand, 2 organic (peat) materials, 5 ferrous oxides, 4 commercial sorption materials, and 3 steel products (raw & rusted). These materials were chosen because activated carbons (Corapcioglu and Huang 1987) and organic materials (Paus *et al.* 2014a, 2014c) have been shown to capture metals; aluminum (O'Neill and Davis 2012a, 2012b) and iron materials (Erickson *et al.* 2007, 2012) have been shown to capture phosphorus; and commercial sorption materials are marketed to remove various pollutants. Batch test bottles (with each type of media) and blanks (no media) were placed on a Labline Orbital Shaker table at 250 RPM. Samples were collected after mixing for 1 h and filtered through a 0.45-micron filter to remove particulates. Nitrate was analyzed colorimetrically (Pritzlaff 2003).

6.1.2 Results and Discussion

Of the 22 different media tested, most activated carbons, organic materials, and commercial enhancing materials were found to capture dissolved metals (cadmium, copper, lead, and zinc) at typical stormwater concentrations (Figures 34 – 37). Four activated carbons captured a significant (> 60%) fraction of nitrate (Figure 38), but two of these increased the dissolved phosphorus concentration by at least 100%, likely due to release of phosphorus from the activated carbon (Figure 39). Thus, only two activated carbons captured a significant fraction of dissolved nitrate while also capturing or not releasing metals and phosphorus. These two activated carbons were Hydrodarco 3000 and Sub-bituminous CR830A and were selected for additional investigation.

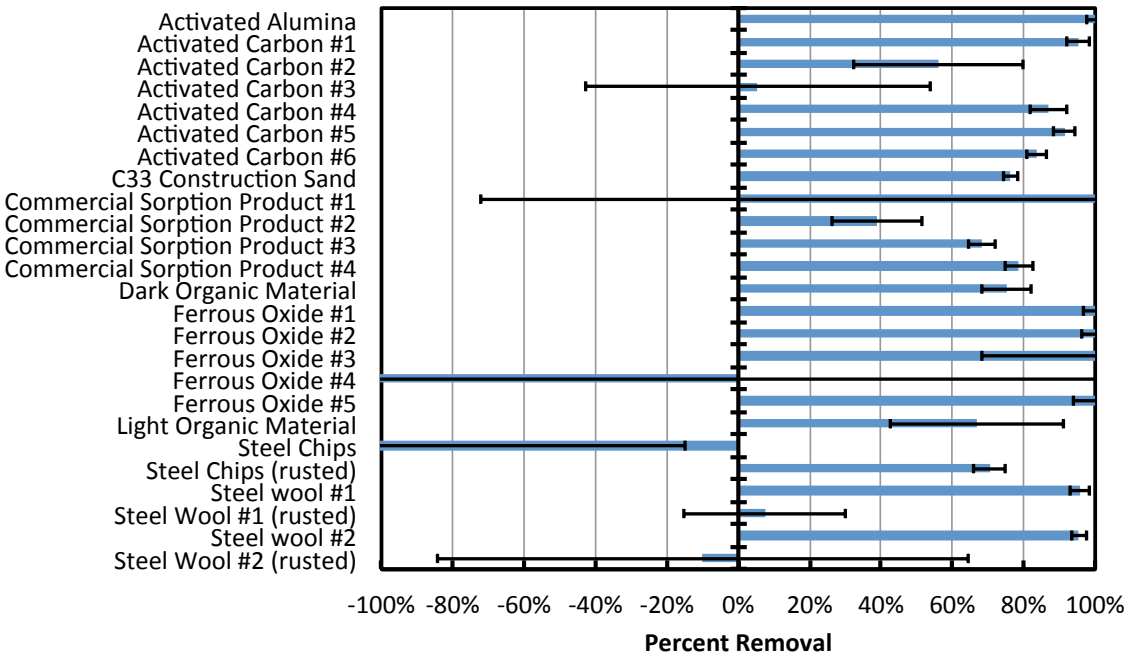

Figure 34. Effectiveness of various enhancing materials for removing dissolved cadmium from synthetic stormwater

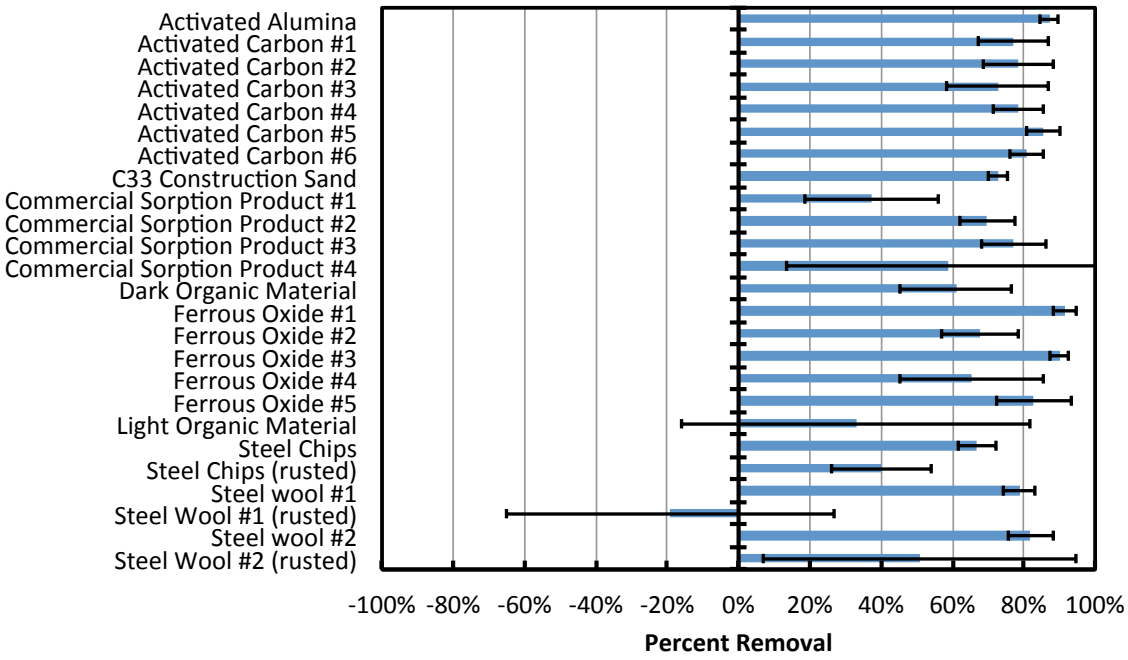

Figure 35. Effectiveness of various enhancing materials for removing dissolved copper from synthetic stormwater

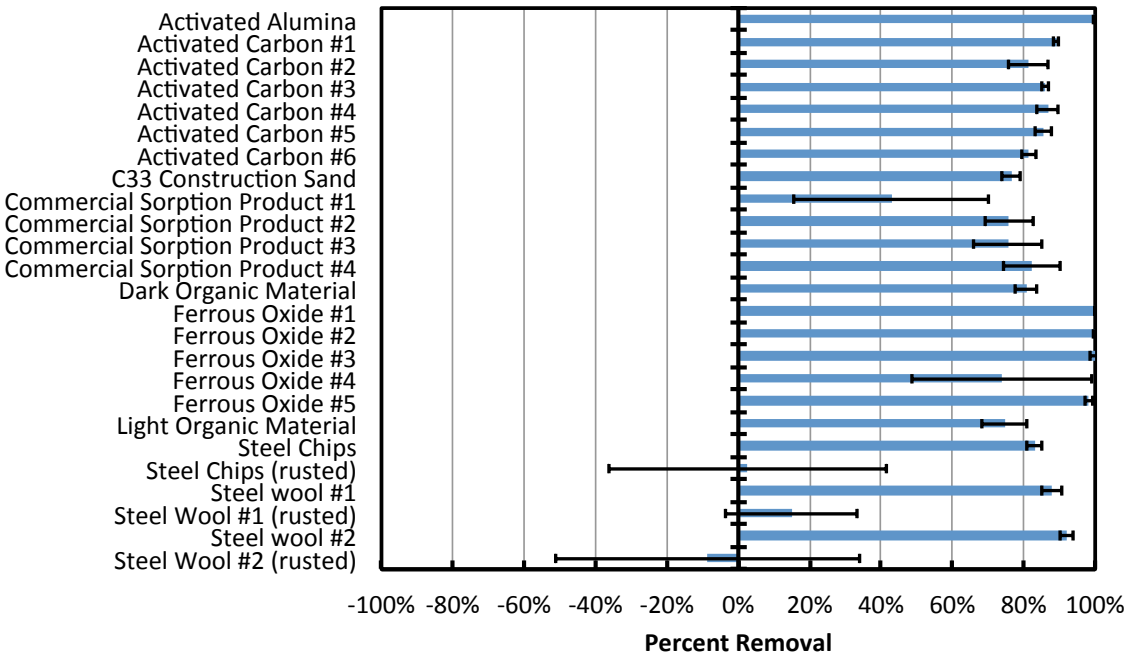

Figure 36. Effectiveness of various enhancing materials for removing dissolved lead from synthetic stormwater

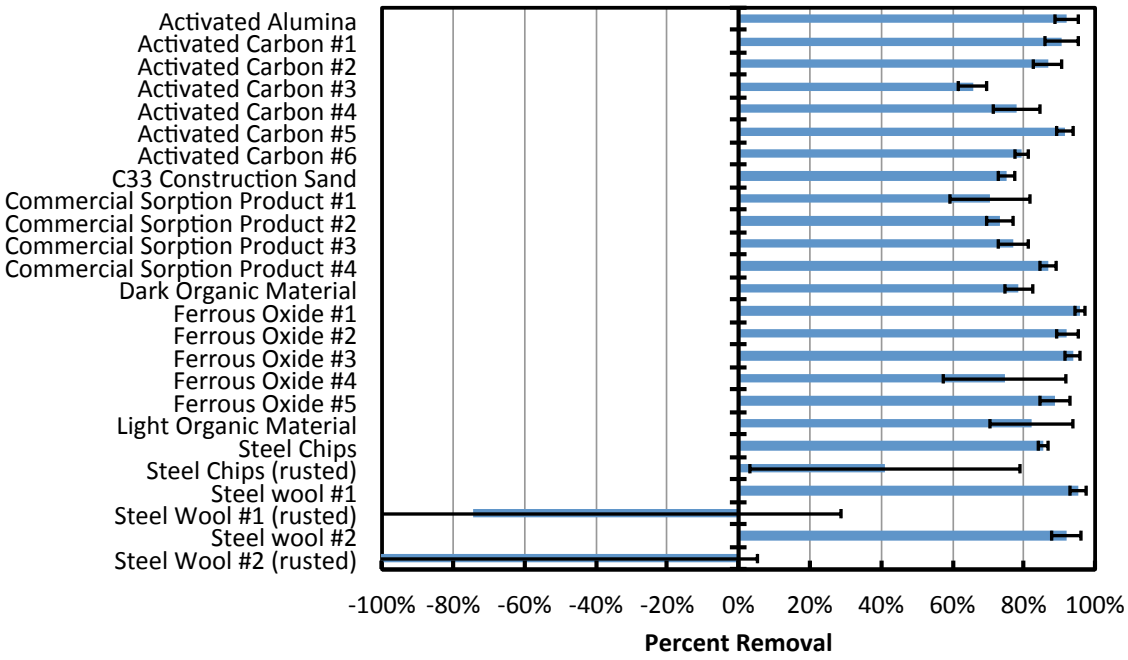

Figure 37. Effectiveness of various enhancing materials for removing dissolved zinc from synthetic stormwater

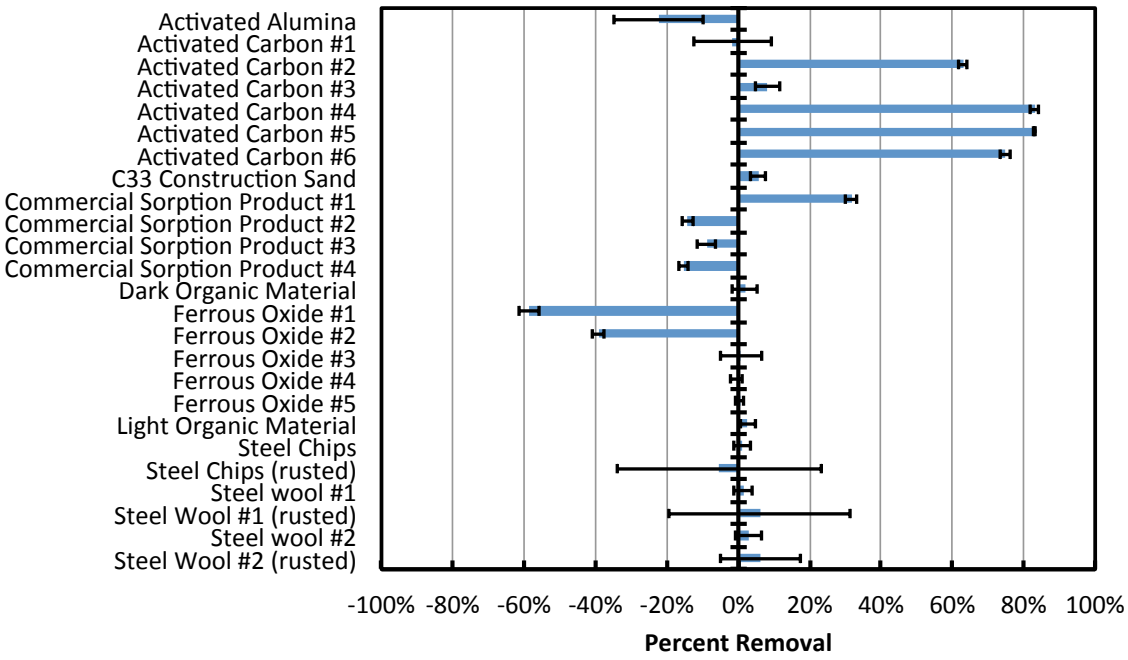

Figure 38. Effectiveness of various sorbent materials for removing dissolved nitrate/nitrite from synthetic stormwater

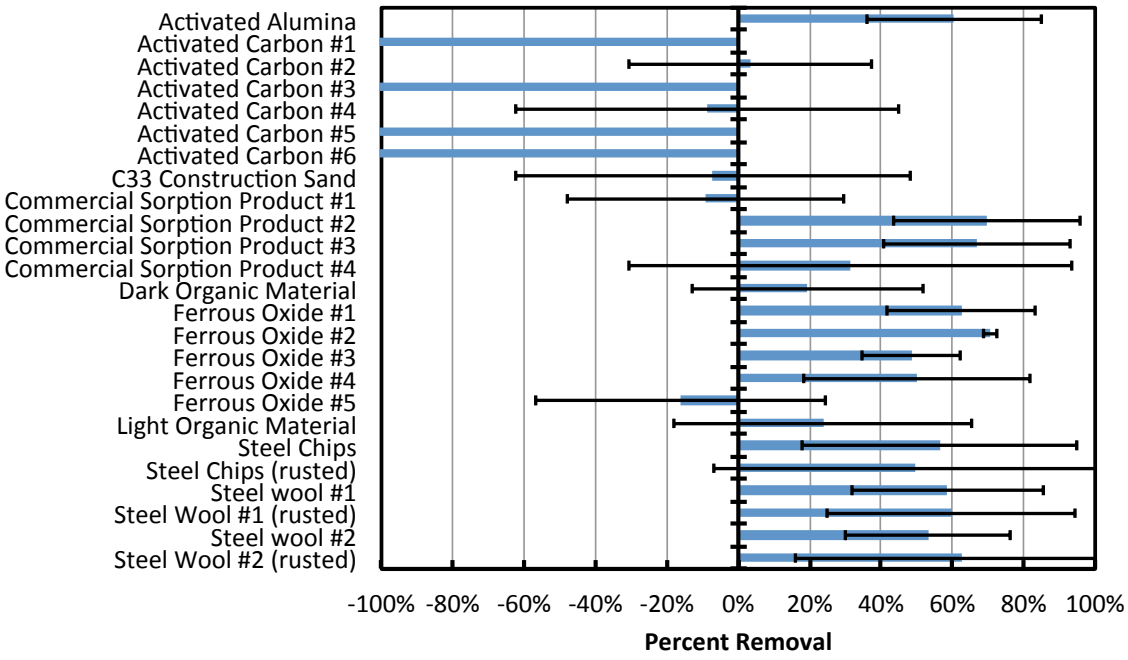

Figure 39. Effectiveness of various enhancing materials for removing dissolved phosphorus from synthetic stormwater

6.2 Dispersion and Contact Time

6.2.1 Results and Discussion

The dispersion of dissolved ions and contact time of flow through the columns were measured using NaCl as a conservative tracer (Figure 40). Less than 15 minutes elapsed from the beginning of the experiment until NaCl concentration (measured as conductivity) began to increase in the effluent for most columns (excluding HD (1) and HD (2)), which substantiates contact time estimates calculated from the pore volumes and flow rates (contact time = pore volume / flow rate), as shown in Tables 13 and 16. The flow rate for both replicates HD (1) and HD (2) during the dispersion experiments was approximately 35% less than the flow for the rest of the replicates shown in Figure 40, and thus required more time for conductivity to increase in the effluent and reach equilibrium with the influent.

Within 15 – 25 additional minutes (30 – 40 minutes total elapsed time) the NaCl concentration had increased to equilibrium (influent = effluent), which indicates that the dispersion of NaCl in the columns is approximately 20 minutes. Capture of nitrate by activated carbon (discussed below) required approximately 3 hours from the start of breakthrough until equilibrium, so dispersion (20 minutes) is relatively minor (~10%). An overview of the column experiments is provided in Tables 13 and 16.

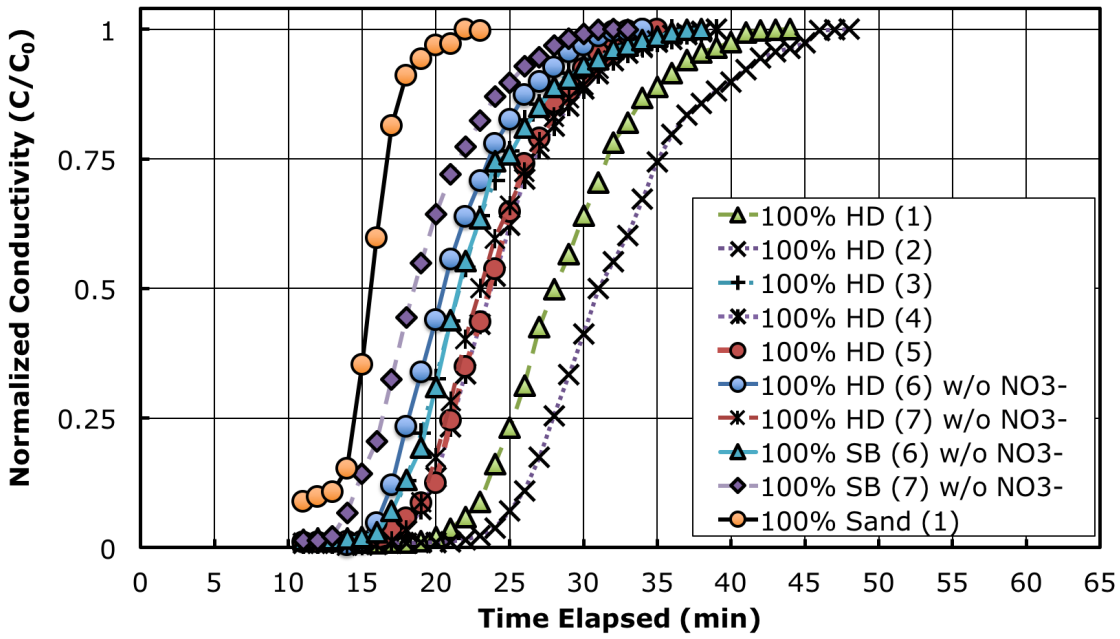

Figure 40. NaCl (conductivity) breakthrough curves for two Sub-bituminous (SB), five Hydrodarco (HD), and one sand column

6.3 Upflow Column Experiments

6.3.1 Results

Table 16. Upflow column study overview (SB = Sub-bituminous, HD = Hydrodarco, SS = Synthetic Stormwater, DI = Deionized water, TW = Tap (potable) Water, "-" = Not Applicable)

					Adsorption Experiments		**Desorption Experiments**	
Column	**Media Mass (g)**	**Media Height (cm)**	**Pore Volume (mL)**	**Pore Volume (%)**	**Water Supplied**	**Average Flow Rate (mL/min)**	**Water Supplied**	**Average Flow Rate (mL/min)**
SB (1)	150	21.5	272	64.5%	SS	18	DI	23
SB (2)	150	21.5	282	66.8%	SS	19	DI	22
SB (3)	150	23	312	69.0%	SS	16	TW	19
SB (4)	150	22.5	322	72.8%	SS	12	-	-
SB (5)	150	21	292	70.9%	SS	12	TW	25
Sand (2)	778	20	113	28.7%	SS	21	-	-
SB (6)	150	22.5	342	77.4%	-	-	SS w/o NO_3-N	-
SB (7)	150	21	302	73.3%	-	-	SS w/o NO_3-N	-
HD (1)	150	19.5	243	63.4%	SS	21	DI	21
HD (2)	150	19	233	62.5%	SS	21	DI	21
HD (3)	150	19.5	233	60.8%	SS	23	TW	22
HD (4)	150	20.5	273	67.7%	SS	25	TW	25
HD (5)	150	19	243	65.2%	SS	22	-	-
Sand (1)	698	19.5	133	34.7%	SS	24	-	-
HD (6)	150	21.5	272	64.5%	-	-	SS w/o NO_3-N	21
HD (7)	150	20	263	66.9%	-	-	SS w/o NO_3-N	27

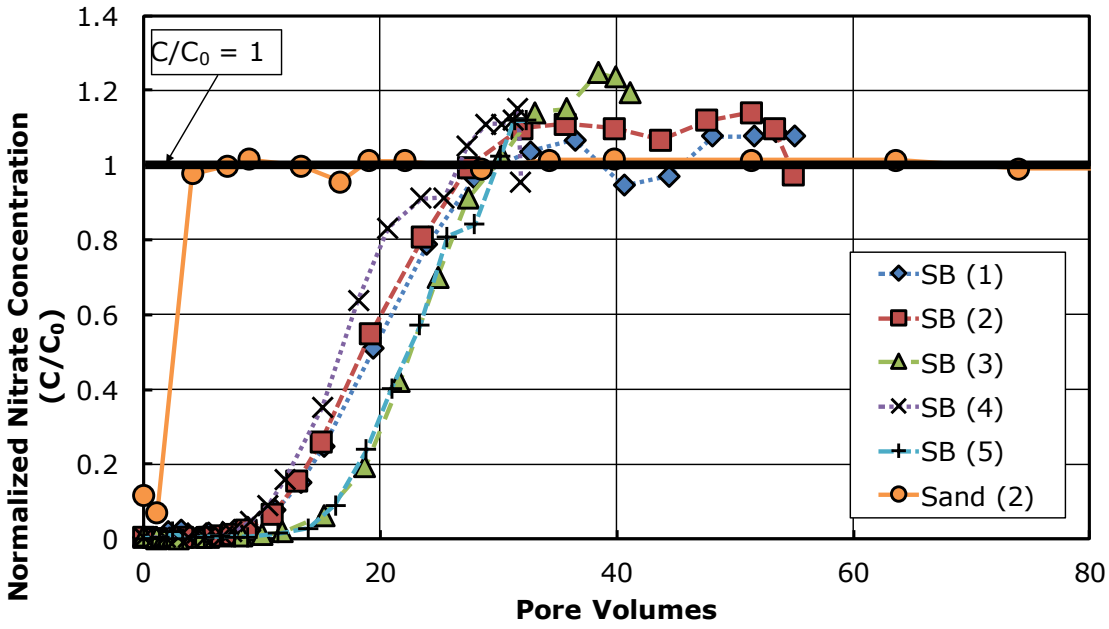

Figure 41. Upflow Column Experiments: Breakthrough curves for nitrate sorption experiments for five Sub-bituminous (SB) columns and one C-33 sand column. (see Figure 31 for Hydrodarco data)

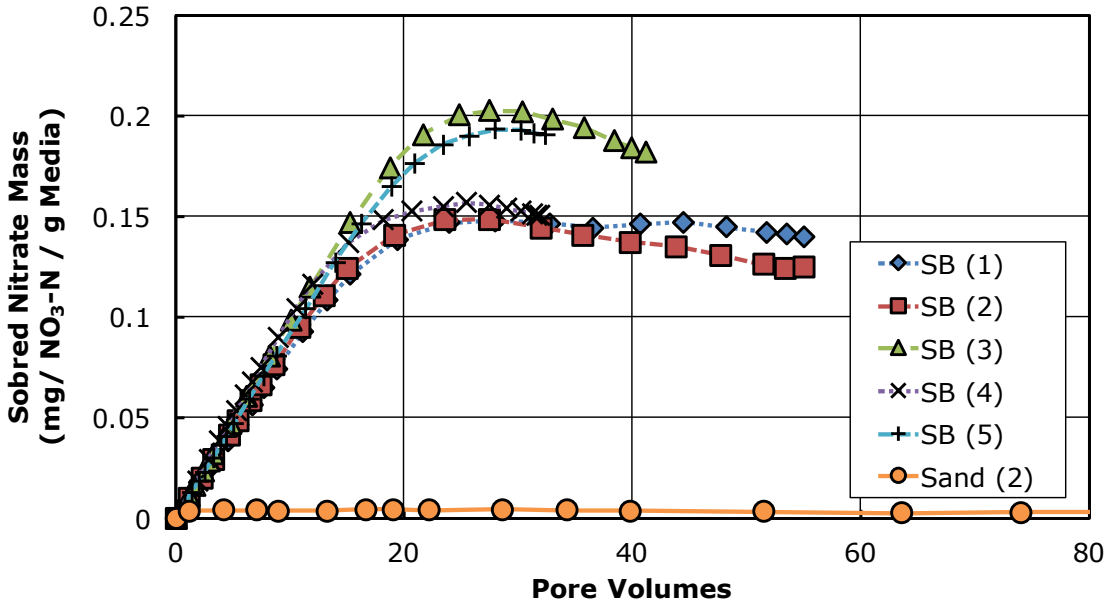

Figure 42: Normalized sorption of nitrate to five replicates of Sub-bituminous activated carbon compared to 100% sand

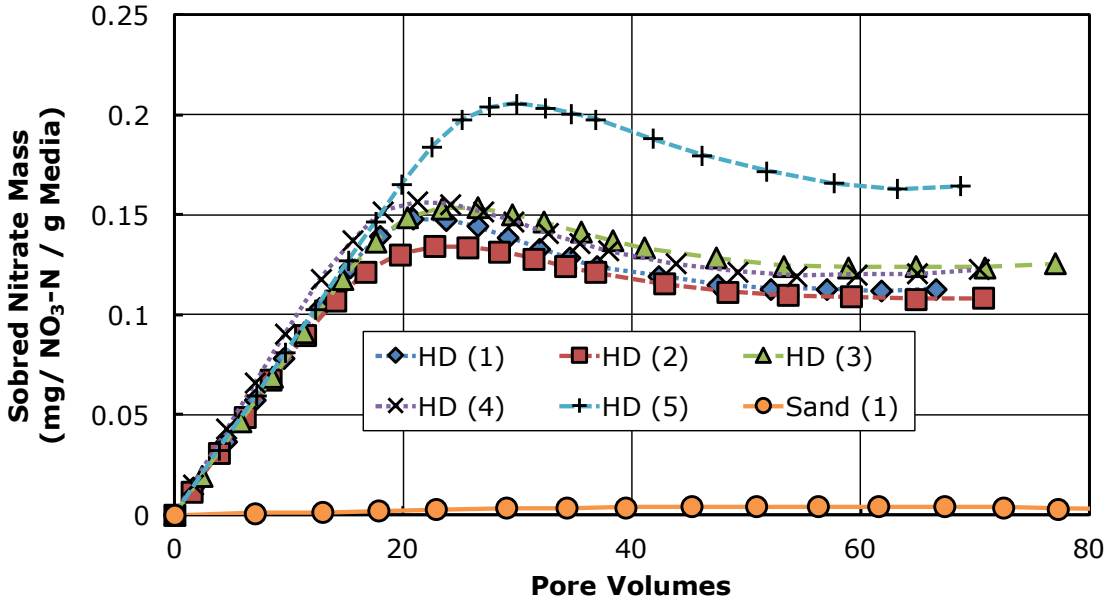

Figure 43: Normalized sorption of nitrate to five replicates of Hydrodarco activated carbon compared to 100% sand

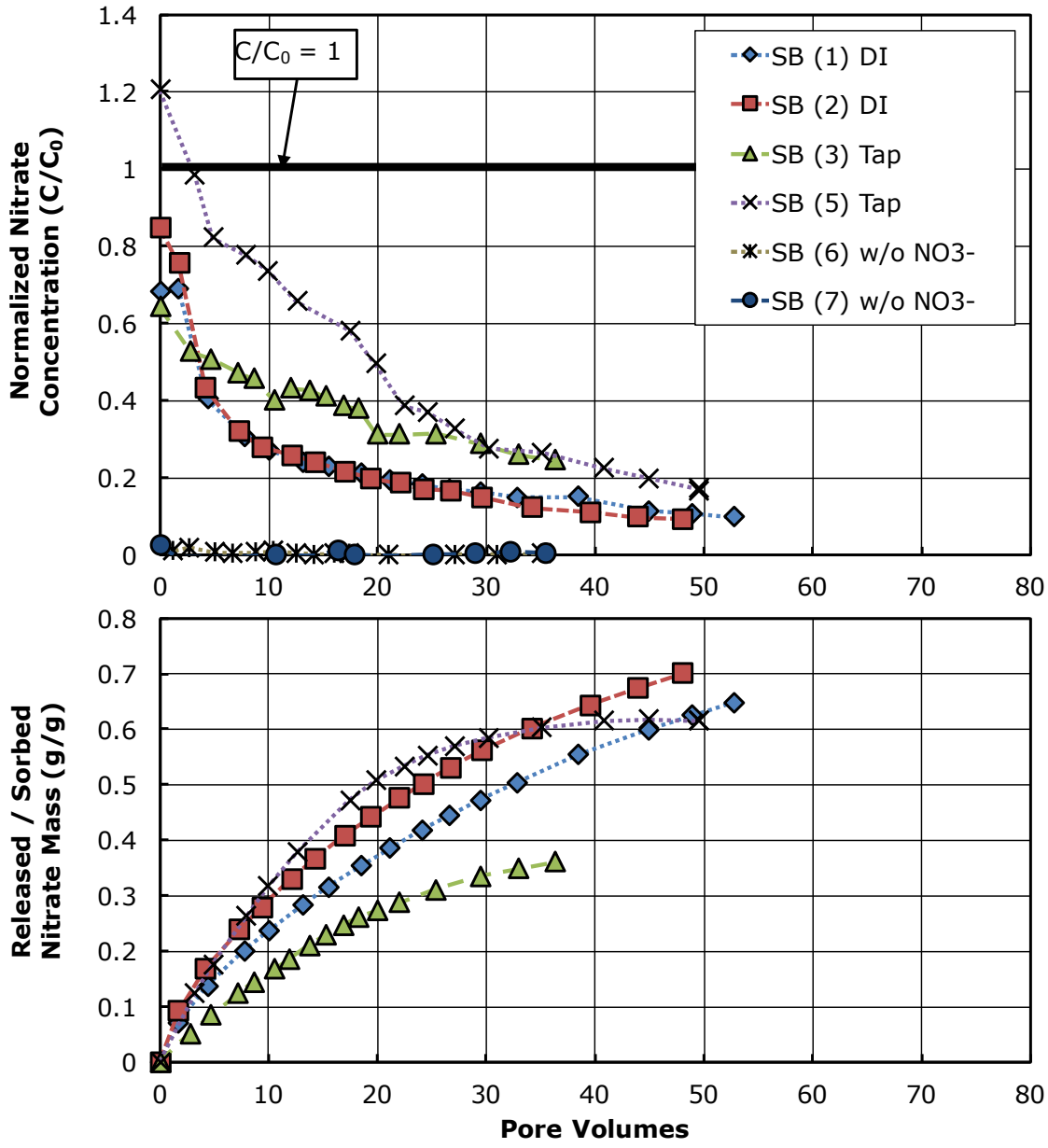

Figure 44: Upflow Column Experiments: Nitrate concentration normalized by the influent nitrate concentration from Figure 41 (top) and fraction of nitrate mass released from Sub-bituminous (bottom) in desorption experiments with deionized (DI), potable (Tap), and nitrate-free synthetic stormwater (w/o NO_3^-). (see Figure 33 for Hydrodarco data)

Table 17. Column Experiments (average of all replicates ± Standard Deviation, where applicable)

	Replicates	Media Mass (g)	Flow Rate (mL/min)	Pore Volume (mL)	Pore Volumes Treated	Influent Conc. (mg/L NO_3^--N)	Nitrate Captured (mg)	Sorption Capacity (mg NO_3^--N/g Media)
Sub-bituminous	5	150	15.49 ± 4.26	296.0 ± 20.5	43.1 ± 11.5	4.73 ± 0.09	23.64 ± 4.17	0.158 ± 0.028
Hydrodarco	5	150	22.33 ± 2.52	244.9 ± 16.2	70.7 ± 3.9	5.14 ± 0.08	19.01 ± 3.31	0.127 ± 0.22
C-33 Sand	2	778.7	22.71 ± 2.82	122.8	147.3	4.94	0.27	0.005

Chapter 6: Conclusions

While nutrients such as phosphate and nitrate are vital to sustain life in Earth's aquatic ecosystems, nutrients in excess result in eutrophication in both freshwater (typically phosphate-limited) and marine (typically nitrate-limited) systems. In addition, nitrate poses a public health risk at elevated concentrations in drinking water. The soluble phase of phosphate and nitrate are bioavailable, and thus have a higher potential of impacted natural water resources compared to particulate forms. Urban stormwater and agricultural treatment systems are typically designed to capture particulate matter by filtration, sedimentation, or both, but these mechanisms cannot capture the soluble phase.

This research has shown that sand filtration, when enhanced with iron, captures phosphate from stormwater runoff in laboratory and field applications. Sand filters mixed with 5% iron filings by weight captured, on average, 88% of the influent phosphate for 200 m of treated depth in laboratory experiments. Neither incorporation of iron filings into a sand filter nor capture of phosphate onto iron filings had a significant effect on the hydraulic conductivity of the filter at mixtures of 5% or less iron by weight. Field applications of IESF with up to 10.7% iron were operated over 1 year without detrimental effects upon hydraulic conductivity. A model was applied and fit to column study data to predict the field performance of IESFs.

The capabilities of IESF was further demonstrated with two different full-scale field applications, which were monitored over two or more rainy seasons to determine their performance with respect to phosphate retention. One application, a pond perimeter IESF in a developing suburban watershed, retained 26% of the influent phosphate over three rainy seasons. The retention rate of the pond perimeter IESF was higher for larger filtered volume events and negative removal (i.e., release) was observed for smaller filtered volume events, especially events with low influent phosphate concentration. In addition, a layer of filamentous algae was transported onto the surface of the pond-perimeter IESF and created a source of phosphate while decomposing that was not quantified. The pond perimeter IESF also treated a relatively large volume of water for its size, resulting in substantial total volume treated within 5 years of operation. Non-routine maintenance improved the

hydraulic performance of the pond perimeter IESF and, after a rinsing event, also improved phosphate retention rates to an average of 45%.

The second application, a traditional surface IESF was installed to treat agricultural tile drainage and reduce soluble (phosphate) and total phosphorus loads received by nearby lakes. For this study, grab samples were collected from 2012 through 2017 and monitoring equipment was installed to collect flow-weighted composite samples for analysis of total phosphorus and phosphate capture performance during rainfall-induced tile drainage flow events of 2015 and 2016. The total phosphorus load reduction varied from 42% to 95% with a flow-weighted mean reduction of 66.3% ± 6.7% ($\alpha = 0.05$) for 20 events in 2016. The phosphate load reduction varied from 9% to 87% with a flow-weighted mean reduction of 63.9% ± 7.7% ($\alpha = 0.05$) for 31 events in 2015 and 2016. In addition, the influent soluble fraction for monitored rainfall events varied from approximately 5% to 90% with an average of 43.2% ± 12.6% ($\alpha = 0.05$) and effluent soluble fraction varied from approximately 15% to 75% with an average of 43.5% ± 10.0% ($\alpha = 0.05$).

In addition, this research has shown that nitrate can be captured abiotically by granular activated carbon (GAC) in laboratory experiments designed to mimic urban and agricultural stormwater runoff. The short contact time and inorganic characteristics of the influent synthetic stormwater suggest that the nitrate was captured by ion exchange, but (bi)carbonate may have competed with nitrate for capture by GAC. In addition, 30 – 80% of the previously captured nitrate was released (i.e., desorbed) when rinsed with potable or ultrapure. The current state-of-the-science stormwater treatment design relies on denitrification to capture nitrate in stormwater treatment practices, requiring storage of captured stormwater, anaerobic conditions, and enough residence time for the bacteria to convert nitrate to nitrogen gas. Abiotic capture of nitrate as demonstrated by this research, requires less stormwater storage volume and less residence time to remove nitrate, which could be used to design smaller treatment practices for nitrate removal.

Additional lessons learned from this research is that IESF must be allowed to oxidize so phosphate capture performance is optimal. This is commonly achieved by keeping the underdrain system below IESFs above the high-water level of any downstream conveyance or waterbody such that atmospheric oxygen can penetrate the bottom of the

IESF media. In addition, intermittent flow onto the IESF surface is recommended to periodically allow atmospheric oxygen to penetrate the surface of the media. The iron used in the IESF should be high purity (90%+ elemental iron) with little or no toxic impurities (e.g., copper, cadmium, lead, etc.), and also be reactive with phosphate. The IESF should be designed with 8% or less of iron by weight to prevent iron oxide from filling in the pore spaces with iron oxide accumulation. In addition, the iron should be mixed thoroughly with clean washed sand to prevent areas within the IESF media that have more than 8% iron by weight. Though not reported in this research, the cost to build an IESF is approximately 5 – 20% more than a standard, non-iron sand filter. Maintenance is also needed to optimize IESF performance for phosphate capture and hydraulic flow. Maintenance includes inspections at least annually, removing accumulated sediment and vegetation as needed, raking the surface to break up oxidized iron clumps or crust, and removing duckweed, algae, and other organic material as buildup occurs for pond-perimeter trenches.

This research has created several opportunities for potential future research. As discussed in Chapters 2 – 4, capture of phosphate with iron-enhanced sand filtration (IESF) has been studied with laboratory experiments and field monitoring, but there is a need to better understand the limitations, interferences, and further enhancements to the technology. For example, additional research is needed to understand the relationship between phosphate concentration (specifically low concentrations), oxic state (specifically anoxic and near-anoxic), and capture of phosphate with IESF. As demonstrated in Chapter 3, pond-perimeter IESF trenches appear to capture less phosphate than other IESFs (Chapter 2, Chapter 4), which was attributed to low influent phosphate concentration, periods on inundation (leading to anoxic conditions and gleyed sand), and organic material decomposition. Additional research is needed to understand which of these possible explanations, and the relative importance of each, contributed to the poor performance. This could be completed with column experiments in the laboratory in which phosphate and oxic state are controlled and the phosphate capture performance is measured; or this could be completed in the field with additional measurement of field oxic state within the IESF media. Perhaps the best approach would be a controlled mesocosm study in the

natural environment under controlled conditions such that phosphate, oxygen, and other important water quality parameters could be accurately measured.

Another possibility for future research of IESF is a study of the interferences to performance and subsequent lifespan of the IESF media. Other studies have shown that iron can be used to remove arsenic and other ions from water. Capture of these ions could compete with capture of phosphate, thus reducing the effectiveness of IESF for phosphate capture. In addition, other water quality parameters found in stormwater may impact phosphate capture performance, such as temperature, soluble fraction, and positive ions such as calcium and magnesium. Studying the performance of IESF in response to known competing ions and other water quality parameters would yield a more accurate estimate of long-term lifespan of IESF installations. These factors could be tested with simple bench-top batch studies (i.e., jar tests) to quickly evaluate the primary competitors and interactions between iron, phosphate, and other ions. Then, more elaborate column studies in the laboratory, or larger pilot-scale mesocosms in the field, could be used to verify laboratory findings with natural stormwater runoff. Through these experiments, the lifespan and sorption capacity of IESF media may be better understood and thus used to improve design of IESFs.

IESF design could be enhanced by understanding the relationships between iron percent in the media, size of iron particles, and relative mixing of iron in the media. Current research has been limited to 5%, 2%, 0.3% iron in the laboratory and 5%, 6%, 7.2%, and 10.7% in the field (though 7.2% and 10.7% have limited data). A comprehensive set of experiments are needed to understand how iron percentage affects performance and lifespan of IESFs, both for phosphate capture and hydraulic conductivity. In addition, more research is needed on the effect of iron particle size on phosphate capture performance and hydraulic performance over time. Larger particles have less surface area per mass than smaller particles, but smaller particles restrict hydraulic conductivity and allow iron oxides to ‘bridge’ the pore spaces, sometimes resulting in solidified iron-sand complexes (Chapter 3). More research is needed to determine the optimal iron (and sand) particle size to the best possible combination of phosphate capture, particulate capture, and hydraulic

conductivity. Replicate column studies could be used to test side-by-side combinations of iron and sand at different iron fractions and various iron particle sizes.

Additional research is needed on iron alternatives. To date, only one supplier provides iron particles that are reactive with phosphate, of the grain size suitable for mixing with clean washed concrete sand, and has minimal impurities that could potentially pollute downstream waterbodies. Many possible alternatives have been suggested, but few have been through rigorous testing to determine whether they are less, equivalent, and more suitable for use in IESF. In addition, waste products could potentially be used that would reduce costs and waste production. Some have been proposed and tested, but found to be unreactive with phosphate, likely due to the crystalline structure of the iron (e.g., hematite vs. magnetite). Thorough testing with bench-top batch studies would quickly eliminate alternatives that do not react with phosphate as well as those that release potentially harmful compounds. Additional testing on the raw iron materials for elemental and crystalline structure, when coupled with phosphate capture performance, would reveal which products are best suited for IESF systems.

A question on the minds of stormwater professionals who have, or who are interested in IESFs is: what can be done with the iron-sand media after it is exhausted? Additional research could evaluate different remediation methods that could potentially remove phosphate from the iron, and allow it to be re-used in another IESF. Perhaps the exhausted iron media could be returned to a refinery to be ‘re-cast’ as cast iron. The waste reclamation industry may have interest in this material for harvesting phosphate, iron, and other valuable resources. If these options are cost-prohibitive, then studies on the exhausted iron media could determine whether it can be re-used as fill material for construction projects or disposed in an environmentally-safe manner.

There is also a significant amount of potential future research on nitrate removal from stormwater runoff. The findings presented in Chapter 5 illustrate that abiotic capture of nitrate is possible, but the capture capacity is minimal and thus large granular activated carbon (GAC) filters would be needed to treatment stormwater for more than a few rainfall events. The first potential area of research is coupling abiotic capture of nitrate by GAC with denitrification to rejuvenate the GAC filter, providing additional sorption sites for

capture of nitrate during future rainfall events. To allow for denitrification, a GAC filter would need to be designed such that the filter media remains continuously saturated, which would promote anoxia between events. Careful closed-system column experiments could be used to determine whether denitrifying bacteria can 1) grow within a GAC filter used to treat stormwater, 2) access nitrate captured by the GAC filter, and 3) consistently denitrify between rainfall events efficiently enough to regenerate the GAC filter before the next event. It is likely that a 'clean' carbon source would need to be added to the columns to support a biological community large enough to efficiently convert the nitrate, because the GAC itself is unlikely suitable.

If denitrification can be viably integrated with abiotic capture of nitrate, then pilot-scale mesocosm studies would likely be needed to determine the appropriate sizing of a GAC filter for urban stormwater treatment, and separately for agricultural tile drainage treatment. Urban systems are often quick, intense rainfall-induced flow systems that produce a large volume of water. Runoff is then routed downstream and stormwater treatment systems are often limited to treating stormwater for 24 or 48 hours. This allows for several days or weeks to elapse before the next rain event. Can a denitrifying bacterial community survive during these extended periods? Studies on the antecedent 'dry' time and impacts on bacteria communities for denitrification would be needed to determine 1) how quickly can denitrification convert nitrate, and 2) how long can a system be 'dry' before the community is no longer efficient for the next event. Perhaps enough denitrifying bacteria are already present in stormwater to re-populate the GAC filter during each event. Conversely, agricultural tile drainage systems often have continuous or near-continuous flow patterns, resulting in dry periods that are few, short, or both. Mesocosm studies would be needed to determine the appropriate size of a GAC filter for agricultural tile drainage that would be not 'flushed out' by the near-continuous flow. Relationships between contact time and nitrate removal performance (abiotic and biotic) could be used to determine the appropriate size to balance abiotic capture and denitrification.

Once an adequate system design in developed, then additional testing would be needed to better understand competition of ions with nitrate for capture by GAC. Many studies have shown removal of metals, organic compounds, and other ions by GAC. Some

of these ions and compounds may compete with nitrate for sorption to GAC, as was observed with sodium or (bi)carbonate (Chapter 5). Most of the ions that will compete with nitrate, will likely outcompete nitrate and either prevent nitrate capture or cause nitrate to be released from the GAC. Batch studies, column studies, or both could be used to test competition and determine a hierarchy of sorption for compounds commonly found in urban and agricultural stormwater. With this information, a realistic lifespan of a GAC filter with denitrification could be estimated.

Finally, pilot-scale or full-scale GAC filters could be installed in the field, in both urban and agricultural watersheds, to verify laboratory measured removal, sorption capacity, and expected lifespan. These experiments would give stormwater decision-makers proof-of-concept results they could use to convince their governing boards to allocate funds towards installed GAC filters for removal of nitrate.

References

Aldridge, K.T. and Ganf, G.G. (2003). Modification of sediment redox potential by three contrasting macrophytes: implications for phosphorus adsorption/desorption. Marine & Freshwater Research 54(1), 87 – 94.

APHA (American Public Health Association, American Water Works Association, and Water Environment Federation). (1998). "4500-P phosphorus." In *Standard methods for the examination of water and wastewater*, 20 ed., L.S. Clesceri, A.E. Greenberg, and A.D. Eaton, eds., APHA, Washington, D.C., 4-139 – 4-155.

ASTM. (2002). C 33-02a: Standard Specification for Concrete Aggregates. In *Annual Book of American Society for Testing and Materials (ASTM) Standards*, vol. 04.02.

Bhatnagar, A., Ji, M., Choi, Y.-H., Jung, W., Lee, S.-H., Kim, S.-J., Lee, G., Suk, H., Kim, H.-S., Min, B., Kim, S.-H., Jeon, B.-H., and Kang, J.-W. (2008). Removal of nitrate from water by adsorption onto zinc chloride treated activated carbon. Separ. Sci. Technol. 43, 886.

Brezonik, P.L., and Arnold, W.A. (2011). Water Chemistry: An Introduction to the Chemistry of Natural and Engineered Aquatic Systems. New York: Oxford University Press.

Brown, R.A., and Hunt, W.F. (2011). Underdrain configuration to enhance bioretention exfiltration to reduce pollutant loads. J. Environ. Eng. 137, 1082.

Carbon Resources. (2011). Technical Specifications: Granular Activated Carbon CR830A. Oceanside, CA: Carbon Resources, Inc. 2535 Jason Court. Available at: www.carbonresources.com. (accessed September 6, 2011).

Chatterjee, S., and Woo, S.H. (2009). The removal of nitrate from aqueous solutions by chitosan hydrogel beads. J. Hazard. Mater. 164, 1012.

Chow, V.T. (1959). Open-Channel Hydraulics. McGraw-Hill, New York.

City of Minneapolis. (2011). Record of Data for the Year 2010 Plant Effluent Water Analysis. Personal Communication, November 28, 2011.

Clark, S.E. (1997). Stormwater Runoff Treatment by Filtration: A Pilot-Scale Study. Dissertation Research Proposal, Birmingham, AL: The University of Alabama at Birmingham.

Clark, S.E. (2000). Urban Stormwater Filtration: Optimization of Design Parameters and a Pilot-Scale Evaluation. Ph.D. Department of Civil and Environmental Engineering. Birmingham, AL: The University of Alabama at Birmingham.

Clark, S.E., and Pitt, R. (2011). Filtered Metals Control in Stormwater using Engineered Media. Palm Springs, CA: World Environmental and Water Resources Congress 2011.

Claytor, R.A., Schueler, T.R., (1996). Design of Stormwater Filtering Systems. Center for Watershed Protection for Chesapeake Research Consortium and U.S. EPA.

Connelly GPM Inc. (2009). Screen Specification, Typical Analysis of Iron Aggregate, and Material Data Safety Sheet. Personal Communication.

Corapcioglu, M.O., and Huang, C.P. (1987). The Adsorption of Heavy-Metals onto Hydrous Activated Carbon. Water Research, 21(9): 1031-1044.

Crittenden, J.C., Trussell, R.R., Hand, D.W., Howe, K.J., and Tchobanoglous, G. (2005). Water Treatment: Principles and Design. Hoboken, N.J: John Wiley, Montgomery Watson Harza.

Davis, A.P., Shokouhian, M., Sharma, H., Minami, C. (2001). Laboratory study of biological retention for urban stormwater management. Water Environment Research 73 (1), 5 – 14.

Demiral, H., and Gunduzoglu, G. (2010). Removal of nitrate from aqueous solutions by activated carbon prepared from sugar beet bagasse. Bioresour. Technol. 101, 1675.

Diamond, D. (2002). Determination of orthophosphate in waters by flow injection analysis. QuikChem® Method 10-115-01-1-M. Loveland, CO: Lachat Instruments.

Discovery Farms Minnesota (DFM). (2017). 2016 Year in Review. Discovery Farms Minnesota, Available online: http://www.discoveryfarmsmn.org/ (Accessed April 2017).

Erickson, A.J. (2005). Enhanced Sand Filtration for Storm Water Phosphorus Removal. M.S. thesis. University of Minnesota, Minneapolis.

Erickson, A.J. and Gulliver, J.S. (2010). Performance Assessment of an Iron-Enhanced Sand Filtration Trench for Capturing Dissolved Phosphorus, St. Anthony Falls Laboratory Project Report #549, Prepared for the City of Prior Lake. University of Minnesota, Minneapolis, MN.

Erickson, A.J., Gulliver J.S., Arnold W.A., Brekke C., and Bredal M. (2016). Abiotic Capture of Stormwater Nitrates with Granular Activated Carbon. Environmental Engineering Science. May 2016, 33(5): 354-363.

Erickson, A.J., Gulliver, J.S. and Weiss, P.T. (2007). Enhanced sand filtration for storm water phosphorus removal. Journal of Environmental Engineering 133(5), 485-497.

Erickson, A.J., Gulliver, J.S. and Weiss, P.T. (2012). Capturing phosphates with iron enhanced sand filtration. Water Research 46(9), 3032-3042.

Erickson, A.J., Gulliver, J.S. and Weiss, P.T. (2015). Monitoring an Iron-Enhanced Sand Filter Trench for the Capture of Phosphate from Stormwater Runoff. St. Anthony Falls Laboratory Project Report #575, University of Minnesota, Minneapolis, MN September 2015.

Erickson, A.J., Gulliver, J.S., and Weiss, P.T. (2017a, submitted). Phosphate Removal from Agricultural Tile Drainage with Iron Enhanced Sand. Water: Special Issue: Additives in Stormwater Filters for Enhanced Pollutant Removal.

Erickson, A.J., Weiss, P.T. and Gulliver, J.S. (2013). Optimizing Stormwater Treatment Practices: A Handbook of Assessment and Maintenance. Springer-Verlag, New York.

Erickson, A.J., Weiss, P.T., and Gulliver, J.S. (2017b, accepted). Monitoring and Maintenance of Phosphate Adsorbing Filters. Journal of Environmental Engineering Special Issue: Environment and Sustainable Systems: A Global Overview.

Franzini, J.B. and Finnemore, E.J. (1997). Fluid mechanics with engineering applications, McGraw Hill, New York.
Gao, B.Y., Wang, Y., Yue, Q.Y., Xu, X., Yue, W.W., and Xu, X.M. (2011). Adsorption kinetics of nitrate from aqueous solutions onto modified corn residue. Int. J. Environ. Poll. 45, 58.
Genc-Fuhrman, H., Wu, P., Zhou, Y., Ledin, A. (2008). Removal of As, Cd, Cr, Cu, Ni and Zn from polluted water using an iron based sorbent. Desalination 226 (1 – 3), 357 – 370.
Hsieh, C.H., and Davis, A.P. (2005). Evaluation and optimization of bioretention media for treatment of urban storm water runoff. J. Environ. Eng. 131, 1521.
Kato, T., Kuroda, H., and Nakasone, H. (2009). Runoff characteristics of nutrients from an agricultural watershed with intensive livestock production. J. Hydrol. 368, 79.
Kayhanian, M., Fruchtman, B.D., Gulliver, J.S., Montanaro, C., Ranieri, E., and Wuertz, S. (2012). Review of highway runoff characteristics: Comparative analysis and universal implications. Water Res. 46, 6609.
Kayhanian, M., Singh, A., and Meyer, S. (2002). Impact of non-detects in water quality data on estimation of constituent mass loading. Water Science and Technology 45 (9), 219 – 225.
Kayhanian, M., Suverkropp, C., Ruby, A. and Tsay, K. (2007). Characterization and prediction of highway runoff constituent event mean concentration. Journal of Environmental Management 85(2), 279-295.
Kim, H., Seagren, E.A., and Davis, A.P. (2003). Engineered bioretention for removal of nitrate from stormwater runoff. Water Environ. Res. 75, 355.
Koerselman, W., Kerkhoven, M.B.V., Verhoeven, J.T.A., (1993). Release of inorganic N, P, and K in peat soils; effect of temperature, water chemistry and water level. Biogeochemistry 20, 63 – 81.
LeFevre, G.H., Hozalski, R.M. and Novak, P.J. (2012). The Role of Biodegradation in Limiting the Accumulation of Petroleum Hydrocarbons in Raingarden Soils. Water Research, 46(20), 6753–6762.
LeFevre, G.H., Paus, K.H., Natarajan, P., Gulliver, J.S., Novak, P.J., and Hozalski, R.M. (2015). "A Review of Dissolved Pollutants in Urban Stormwater and their Removal and Fate in Bioretention Cells." Journal of Environmental Engineering, 141 (1).
Lucas, W.C., Greenway, M. (2008). Nutrient retention in vegetated and nonvegetated bioretention mesocosms. Journal of Irrigation and Drainage Engineering 134 (5), 613 – 623.
Lucas, W.C., Greenway, M. (2011). Phosphorus retention by bioretention mesocosms using media formulated for phosphorus sorption: response to accelerated loads. Journal of Irrigation and Drainage Engineering 137 (3), 144 – 153.
Luell, S.K., Hunt, W.F., and Winston, R.J. (2011). Evaluation of undersized bioretention stormwater control measures for treatment of highway bridge deck runoff. Water Sci. Technol. 64, 974.

Maestre, A., and Pitt, R. (2005). The National Stormwater Quality Database, Version 1.1: A Compilation and Analysis of NPDES Stormwater Monitoring Information. University of Alabama, Center for Watershed Protection: Ellicott City, MA.

MDNR (Minnesota Department of Natural Resources). (2017). "National Wetland Inventory for Minnesota." Available online: http://mndnr.maps.arcgis.com/apps/OnePane/basicviewer/index.html?appid=7132a264fcd449deb8521268c0698046 (Accessed on 10 July 2017).

Mizuta, K., Matsumoto, T., Hatate, Y., Nishihara, K., and Nakanishi, T. (2004). Removal of nitrate-nitrogen from drinking water using bamboo powder charcoal. Bioresour. Technol. 95, 255.

Morgan, J., Hozalski, R.M., Gulliver, J.S., (2010). When Do We Need to Replace Bioretention Media? 9th Annual StormCon. San Antonio, TX.

Morgan, J.G. (2011). Sorption and Release of Dissolved Pollutants Via Bioretention Media. M.S. thesis. University of Minnesota, Minneapolis.

Namasivayam, C., Ranganathan, K., (1995). Removal of Pb(II), Cd(II), Ni(II) and mixture of metal-ions by adsorption onto waste Fe(III)/Cr(III) hydroxide and fixed-bed studies. Environmental Technology 16 (9), 851 – 860.

Norit Americas. (2012). Datasheet: Hydrodarco 3000 Granular Activated Carbon. Marshall, TX: Norit Americas, Inc. 3200 University Avenue. Available at: www.norit-americas.com (accessed July 12, 2012).

O'Neill, S.W., Davis, A.P. (2012a). Water treatment residual as a bioretention amendment for phosphorus. I: Evaluation studies. Journal of Environmental Engineering, 138(3, special issue):318-327.

O'Neill, S.W., Davis, A.P. (2012b). Water treatment residual as a bioretention amendment for phosphorus. II: Long-term column studies. Journal of Environmental Engineering, 138(3, special issue):328-336.

Passeport, E., Hunt, W.F., Line, D.E., Smith, R.A., and Brown, R.A. (2009). Field study of the ability of two grassed bioretention cells to reduce storm-water runoff pollution. J. Irrig Drain Eng. 135, 505.

Paus, K.H., Morgan, J., Gulliver, J.S., and Hozalski, R.M. (2014a). Effects of bioretention media compost volume fraction on toxic metals removal, hydraulic conductivity, and phosphorous release. J. Environ. Eng. 140, 04014033.

Paus, K.H., Morgan, J., Gulliver, J.S., Leiknes, T., and Hozalski, R.M. (2014b). Effects of temperature and NaCl on toxic metal retention in bioretention media. J. Environ. Eng. 140, 04014034.

Paus, K.H., Morgan, J., Gulliver, J.S., Leiknes, T., and Hozalski, R.M. (2014c). Assessment of the Hydraulic and Toxic Removal Capacities of Bioretention Cells after 2 to 8 Years of Service. Water, Soil and Air Pollution, 225 (1803).

Pitt, R., Clark, S.E., and Steets, B. (2010a). Evaluation of the Contaminant Removal Potential of Biofiltration Media. 2010 International Low Impact Development Conference: Re- defining Water in the City. San Francisco, CA.

Pitt, R., Clark, S.E., and Steets, B. (2010b). Laboratory Evaluations to Support the Design of Bioretention Systems in the Southwestern U.S. Providence, RI: World Environmental and Water Resources Congress 2010.

Pitt, R., Maestre, A., Morquecho, R., Brown, T., Schueler, T., Cappiella, K., Sturm, P., (2005). Evaluation of NPDES Phase 1 Municipal Stormwater Monitoring Data. University of Alabama and the Center for Watershed Protection.

Pritzlaff, D. (2003). Determination of nitrate/nitrite in surface and wastewaters by flow injection analysis. QuikChem® Method 10-107-04-1-C. Loveland, CO: Lachat Instruments.

Rosenquist, S.E., Hession, W.C., Eick, M.J., Vaughan, D.H., (2010). Variability in adsorptive phosphorus removal by structural stormwater best management practices. Ecological Engineering 36 (5), 664 – 671.

Ruddy, B.C., Lorenz, D.L., and Mueller, D.K. (2006). County-Level Estimates of Nutrient Inputs to the Land Surface of the Conterminous United States, 1982–2001. Scientific Investigations Report 2006–5012. United States Geological Survey, Reston, Virginia.

Schindler, D.W. (1977). Evolution of phosphorus limitation in lakes: Natural mechanisms compensate for deficiencies of nitrogen and carbon in eutrophied lakes. Science 195(4275), 260 – 262.

Schueler, T.R., (1987). Controlling Urban Runoff; a Practical Manual for Planning and Designing Urban BMP's. Department of Environmental Programs. Washington, D.C: Metropolitan Washington Council of Governments.

Sharpley, A.N., Smith, S.J., Jones, O.R., Berg, W.A. and Coleman, G.A. (1992). The Transport of Bioavailable Phosphorus in Agricultural Runoff. Journal of Environmental Quality 21(1), 30 – 35.

Shumway, R.H., Azari, R.S., Kayhanian, M. (2002). Statistical approaches to estimating mean water quality concentrations with detection limits. Environmental Science and Technology 36 (15), 3345 – 3353.

Smil, V. (2000). Cycles of Life: Civilization and the Biosphere. Henry Holt and Company.

Stewart, B., (1992). Final Report: Compost Storm Water Treatment System. W&H Pacific.

Stumm, W., and Morgan, J.J. (1981). Aquatic Chemistry: An Introduction Emphasizing Chemical Equilibria in Natural Waters. New York: Wiley.

Stuntebeck, T.D., Komiskey, M.J., Peppler, M.C., Owens, D.W., and Frame, D.R. (2011). Precipitation-runoff relations and water-quality characteristics at edge-of-field stations, Discovery Farms and Pioneer Farm, Wisconsin, 2003–2008. U.S. Geological Survey Scientific Investigations Report 2011–5008.

U.S. EPA. (1999). Preliminary Data Summary of Urban Storm Water Best Management Practices. EPA-821-R-99-012. Washington, D.C.: U.S. Environmental Protection Agency.

U.S. EPA. (2000). Storm Water Phase II Final Rule: Fact Sheet 1.0. Washington, D.C.: U.S. Environmental Protection Agency.

U.S. EPA. (2007a). Hypoxia in the Northern Gulf of Mexico. Washington, D.C.: U.S. EPA Science Advisory Board Report EPA-SAB-08-003.

U.S. EPA. (2007b). Total Maximum Daily Loads with Stormwater Sources: A Summary of 17 TMDLs. U.S. Environmental Protection Agency, Office of Wetlands, Oceans and Watersheds, Washington, DC.
U.S. EPA. (2012). Basic Information About Nitrate in Drinking Water. Available at: http://water.epa.gov/drink/contaminants/basicinformation/nitrate.cfm (accessed December 20, 2012).
U.S. EPA. (2016). Specific State Causes of Impairment. Web page: https://iaspub.epa.gov/waters10/attains_nation_cy.cause_detail_303d?p_cause_group_id=792. Accessed on 14 October 2016.
Villemonte, J. (1947). Submerged Weir Discharge Studies. *Engineering News Record,* December 25th, 1947.
Walker Jr., W.W. (1990). P8 Urban Catchment Model: Program Documentation. Concord, Massachusetts.
Weiss, P.T., Gulliver, J.S. and Erickson, A.J. (2007) Cost and pollutant removal of storm-water treatment practices. Journal of Water Resources Planning and Management 133(3), 218 – 229.
Wu, P., Zhou, Y. (2009). Simultaneous removal of coexistent heavy metals from simulated urban stormwater using four sorbents: a porous iron sorbent and its mixtures with zeolite and crystal gravel. Journal of Hazardous Materials 168 (2 – 3), 674 – 680.
Zhang, X.L., Zhang, S., He, F., Cheng, S.P., Liang, W., and Wu, Z.B. (2007). Differentiate performance of eight filter media in vertical flow constructed wetland: Removal of organic matter, nitrogen and phosphorus. Fresen. Environ. Bull. 16, 1468.